

# Measurements of $t\bar{t}W$ differential cross sections and the leptonic charge asymmetry at $\sqrt{s} = 13$ TeV



## The CMS collaboration

Full author list at the end of the paper

E-mail: [cms-publication-committee-chair@cern.ch](mailto:cms-publication-committee-chair@cern.ch)

**ABSTRACT:** Measurements of properties of top quark-antiquark pair production in association with a  $W$  boson in proton-proton collisions at a center-of-mass energy of 13 TeV are presented, using a data sample corresponding to an integrated luminosity of  $138 \text{ fb}^{-1}$ , recorded by the CMS experiment at the CERN LHC. Events are selected based on the presence of either two leptons with the same electric charge or three leptons, and multiple jets and b-tagged jets. We present measurements of differential production cross sections as a function of kinematic variables sensitive to different aspects of the process modeling, using a multivariate discriminator in the two-lepton selection region and a simple selection-based method in the three-lepton region. The normalized cross section measurements are generally consistent with the standard model expectations, while we observe larger values compared to the expectations in the absolute cross section measurements, consistent with previous inclusive cross section measurements. In addition, we measure the leptonic charge asymmetry of this process, obtaining an observed value of  $A_c^\ell = -0.19^{+0.16}_{-0.18}$ , consistent with the expectation of  $-0.085 \pm 0.006$  predicted by next-to-leading order simulations.

**KEYWORDS:** Hadron-Hadron Scattering, Top Physics, Vector Boson Production

ARXIV EPRINT: [2509.13512](https://arxiv.org/abs/2509.13512)

---

**Contents**

<b>1</b>	<b>Introduction</b>	<b>1</b>
<b>2</b>	<b>The CMS detector and event reconstruction</b>	<b>3</b>
<b>3</b>	<b>Data and simulated samples</b>	<b>5</b>
<b>4</b>	<b>Object and event selection</b>	<b>6</b>
<b>5</b>	<b>Background estimation</b>	<b>8</b>
5.1	Nonprompt leptons	8
5.2	Charge-misidentified leptons	10
5.3	Photon conversions	12
5.4	Irreducible backgrounds	12
<b>6</b>	<b>Systematic uncertainties</b>	<b>12</b>
6.1	Experimental uncertainties	12
6.2	Theoretical uncertainties	15
<b>7</b>	<b>Differential cross section measurements</b>	<b>15</b>
7.1	Definition of measured observables	16
7.2	Statistical model	16
7.3	Signal extraction in the $2\ell SS$ region	17
7.4	Consistency checks	20
7.5	Signal extraction in the $3\ell$ region	30
<b>8</b>	<b>Measurement of the charge asymmetry</b>	<b>31</b>
<b>9</b>	<b>Summary</b>	<b>34</b>
<b>A</b>	<b>Results in the <math>2\ell SS</math> region using the counting method</b>	<b>37</b>
	<b>The CMS collaboration</b>	<b>50</b>

---

**1 Introduction**

The production of a top quark pair in association with a W boson ( $t\bar{t}W$ ) is sensitive to the interaction of the top quark with the electroweak bosons, which makes it one of the most intriguing processes studied recently at the LHC in proton-proton (pp) collisions. At leading order (LO), this process is induced by the  $q\bar{q}'$  partonic initial state and receives contributions from the  $gq$  channel only at next-to-LO (NLO), while the  $gg$  contribution is suppressed and only starts to appear at next-to-NLO (NNLO). Because of this, perturbative calculations for the  $t\bar{t}W$  production introduce large corrections at higher orders in the

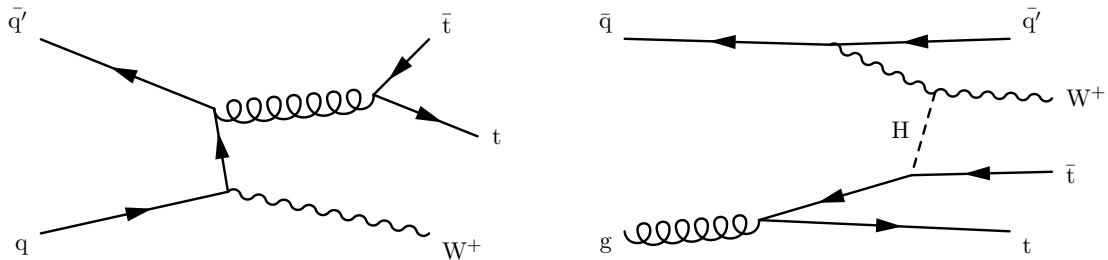


**Figure 1.** Examples of Feynman diagrams for  $t\bar{t}W$  production: at LO (left) and one of the NLO diagrams introducing sizeable electroweak corrections (right).

quantum chromodynamics (QCD) expansion [1, 2] and sizable electroweak corrections [3, 4]. Figure 1 shows representative Feynman diagrams for this process.

In inclusive top quark-antiquark ( $t\bar{t}$ ) production, top quarks are produced with a wider rapidity distribution than top antiquarks due to interference effects present at NLO accuracy, which break the symmetry under charge conjugation, giving rise to an asymmetry in the  $t\bar{t}$  system [5, 6]. In the case of  $t\bar{t}W$  production, this asymmetry is enhanced due to the absence of the gluon-gluon partonic initial state and to the  $W$  boson acting as a polarizer for the incoming quark in LO diagrams, such as the one in figure 1 [7]. This feature can be used as an experimentally robust probe of physics beyond the standard model (BSM) that could modify these asymmetries. In addition, the  $t\bar{t}W$  process is a unique probe of four-quark contact interactions [8], which may introduce a dominant contribution to the production cross section, in contrast to other processes that are dominated by gluon-fusion production, such as the inclusive production of  $t\bar{t}$  pairs. Finally, being one of the few processes that give rise to pairs of leptons (electrons or muons,  $\ell$ ) with the same electric charge (same-sign (SS) lepton pairs), this process constitutes the leading irreducible background to studies that profit from this topology, including measurements of the simultaneous production of four top quarks ( $t\bar{t}t\bar{t}$ ) [9, 10] or the production of a top quark pair in association with a Higgs boson ( $t\bar{t}H$ ) [11].

Considering the production of on-shell top quarks without their subsequent decay, the state-of-the-art in the calculation of the  $t\bar{t}W$  cross section is an NNLO computation [2], which estimates the contribution from two-loop amplitudes by means of approximate methods. Calculations at NLO in QCD and electroweak corrections including resummation at next-to-next-to-leading logarithm [12–14] are also available. In addition, recent advances [15, 16] show that this process receives contributions from off-shell top quark effects in low and high transverse momentum ( $p_T$ ) phase space regions. Finally, several event generators [17–19] are available to simulate this process at NLO matched to parton showers, including up to two extra partons in the matrix element calculation.

One additional motivation for precision studies of  $t\bar{t}W$  production is the continuing tension between previous measurements and the set of standard model (SM) predictions. The inclusive production cross section for this process has been measured 17–29% larger than the SM expectation, by both the ATLAS [20] and CMS [11, 21] Collaborations, in measurements that achieve precisions of the order of 10%. The ATLAS Collaboration has in addition performed a measurement of its differential production cross section [20] and of the

charge asymmetry of the  $t\bar{t}$  system in this process [22]. The measurements of the normalized distributions and the charge asymmetry are in agreement with the SM predictions.

In this paper, we report measurements of the  $t\bar{t}W$  production cross section as a function of several kinematic variables, and a measurement of the leptonic charge asymmetry in the  $t\bar{t}$  system, in events with at least one SS lepton pair and hadronic jets recorded by the CMS experiment. One of the challenges in the differential cross section measurement is the contribution of processes with leptons not produced in the prompt decays of W or Z bosons, that can contaminate the signal selection. Two different strategies are pursued to mitigate the effect of this contribution. In the first method, denoted as “multivariate analysis (MVA)-based method”, we employ a loose lepton selection, and use an MVA discriminator with information on the event kinematic properties to discriminate the signal against the main background processes, which are events with nonprompt or charge misidentified leptons and associated  $t\bar{t}$  production processes. An alternative method, dubbed as “counting method”, that instead relies on a more stringent lepton selection achieving a larger signal purity is also used. Both methods use a likelihood-based unfolding strategy, performing a fit to the signal region (SR) and several control regions (CRs). We use the MVA-based method to measure the differential cross section in events with two leptons. Both measurements attain a similar sensitivity in most bins, but the MVA-based method is more precise in all measured bins, achieving up to a 40% better precision in some bins of this region. The counting method is used to measure the differential cross section and charge asymmetry in events with three leptons. We also provide the results of the counting method in the two-lepton region in the appendix of the paper to complement the results from the MVA-based method. Tabulated results are provided in the HEPData record for this analysis [23].

This manuscript is organized as follows. Section 2 provides an overview of the CMS detector and section 3 describes the collision data and simulated samples used in this study. The object and event selections are described in section 4, the estimation of background events contributing to the measurements in section 5, and the systematic uncertainties affecting the measurements in section 6. In section 7, we discuss the differential cross section measurements performed with the MVA-based and counting methods. The measurement of the charge asymmetry is shown in section 8 and a summary is given in section 9. Finally, the results of the differential cross section measurements are shown in appendix A.

## 2 The CMS detector and event reconstruction

The central feature of the CMS apparatus is a superconducting solenoid of 6 m internal diameter, providing a magnetic field of 3.8 T. Within the solenoid volume are a silicon pixel and strip tracker, a lead tungstate crystal electromagnetic calorimeter (ECAL), and a brass and scintillator hadron calorimeter (HCAL), each composed of a barrel and two endcap sections. Forward calorimeters extend the pseudorapidity ( $\eta$ ) coverage provided by the barrel and endcap detectors. Muons are measured in gas-ionization detectors embedded in the steel flux-return yoke outside the solenoid. More detailed descriptions of the CMS detector, together with a definition of the coordinate system used and the relevant kinematic variables, can be found in refs. [24, 25].

Events of interest are selected using a two-tiered trigger system. The first level, composed of custom hardware processors, uses information from the calorimeters and muon detectors to select events at a rate of around 100 kHz within a fixed latency of about  $4\ \mu\text{s}$  [26]. The second level, known as the high-level trigger, consists of a farm of processors running a version of the full event reconstruction software optimized for fast processing, and reduces the event rate to around 1 kHz before data storage [27, 28].

The CMS particle-flow (PF) algorithm [29] provides a global event description combining optimally the information from all subdetectors, to reconstruct and identify all individual particles in the event. The particles are subsequently classified into five mutually exclusive categories: photons, electrons, muons, and charged and neutral hadrons.

In this work, we consider particles produced at the primary vertex (PV), which is taken to be the vertex corresponding to the hardest scattering in the event, evaluated using tracking information alone, as described in section 9.4.1 of ref. [30]. Photons are identified from clusters in the ECAL not compatible with tracks in the tracker, which are also used to determine the photon energy. Electrons are reconstructed via a combination of tracker and ECAL measurements [31, 32] in the range  $|\eta| < 2.5$ . Their energy is determined from a combination of the electron momentum at the PV as determined by the tracker, the energy of the corresponding ECAL cluster, and the energy sum of all bremsstrahlung photons spatially compatible with originating from the electron track. Muons are reconstructed in the range  $|\eta| < 2.4$  by combining information from the tracker and the muon spectrometers in a global fit [33]. The energy of muons is obtained from the curvature of the corresponding track. The energy of charged hadrons is determined from a combination of their momentum measured in the tracker and the matching ECAL and HCAL energy deposits, corrected for the response function of the calorimeters to hadronic showers. Finally, the energy of neutral hadrons is obtained from the corresponding corrected ECAL and HCAL energies.

Hadronic jets are clustered from the PF objects using the infrared- and collinear-safe anti- $k_T$  algorithm [34, 35] with a distance parameter of 0.4. We only consider in the analysis jets that have a  $p_T > 25\ \text{GeV}$  and  $|\eta| < 2.4$ , and are separated by  $\Delta R = \sqrt{(\Delta\eta)^2 + (\Delta\phi)^2} > 0.4$  from any identified lepton (following the criteria given in section 4), where  $\phi$  is the azimuthal angle with respect to the beam axis. Jet momentum is determined as the vectorial sum of all particle momenta in the jet, and is found from simulation to be, on average, within 5 to 10% of the true momentum over the whole  $p_T$  spectrum and detector acceptance. Additional pp interactions within the same or nearby bunch crossings (pileup) can contribute additional tracks and calorimetric energy depositions, increasing the apparent jet momentum. To mitigate this effect, tracks identified to be originating from vertices in the same bunch crossing but different from the PV are discarded and an offset correction is applied to correct for remaining contributions [36]. Jet energy corrections are derived from simulation studies so that the average measured energy of jets becomes identical to that of particle level jets. In situ measurements of the momentum balance in dijet, photon+jets, Z+jets, and multijet events are used to determine any residual differences between the jet energy scale in data and in simulation, and appropriate corrections are made. The jet energy resolution (JER) amounts typically to 15–20% at 30 GeV, 10% at 100 GeV, and 5% at 1 TeV. A smearing procedure is applied to match the JER in simulation to that in data [37]. Additional selection

criteria are applied to each jet to remove jets potentially dominated by instrumental effects or reconstruction failures [36].

The missing transverse momentum vector  $\vec{p}_T^{\text{miss}}$  is computed as the negative vector sum of the  $p_T$  of all the PF candidates in an event, and its magnitude is denoted as  $p_T^{\text{miss}}$  [38]. The  $\vec{p}_T^{\text{miss}}$  is modified to account for corrections to the energy scale of the reconstructed jets in the event. Anomalous high- $p_T^{\text{miss}}$  events can be due to a variety of reconstruction failures, detector malfunctions or noncollision backgrounds. Such events are rejected by event filters that are designed to identify more than 85–90% of the spurious high- $p_T^{\text{miss}}$  events with a mistagging rate less than 0.1% [38].

Jets originating from b quarks are identified with the DEEPJET algorithm [39–41], with two defined working points (WPs) labeled “loose” and “medium”. The loose (medium) WP has a selection efficiency for b quark jets of about 90 (76)%, and a misidentification rate of about 49 (17)% for c quark jets and 18 (3)% for light quark and gluon jets. Unless specified otherwise, the term “b-tagged jets” is used to refer to jets that pass the loose WP requirements.

### 3 Data and simulated samples

We use pp collision events at  $\sqrt{s} = 13$  TeV recorded at the LHC between 2016 and 2018, with a total integrated luminosity of  $138 \text{ fb}^{-1}$ . The events used in this study were collected using a set of triggers requiring the presence of one, two, or three reconstructed leptons above a certain  $p_T$  threshold, which varies depending on the data-taking era and the lepton flavor and multiplicity.

A suite of simulated samples produced via Monte Carlo (MC) generators are used to train the MVA discriminators and to estimate the efficiency of the reconstruction and identification techniques in signal and background events. These samples use various matrix-element generators, that are described below, and the NNPDF3.1NNLO parton distribution functions (PDFs) [42]. Unless specified otherwise, these generators are interfaced to PYTHIA v8.240 [43] to simulate the parton shower, hadronization, decay, and underlying event using the CP5 tune [44]. We use the MLM [45] (FxFx [46]) matching scheme for MADGRAPH5\_aMC@NLO [47] samples that are produced at LO (NLO) using matrix elements with additional partons. Generated hard-scattering events are overlaid with simulated pileup collisions, with a number of events per bunch crossing matching the distribution inferred from data. The response of the CMS detector is fully simulated using a model of the detector based on the GEANT4 toolkit [48].

The nominal model for the  $t\bar{t}W$  signal is obtained using the MADGRAPH5\_aMC@NLO v.2.6.5 generator, accounting for terms proportional to  $\alpha_S^3\alpha$  (QCD production) and  $\alpha_S\alpha^3$  (electroweak production) and higher order contributions in the QCD expansion, where  $\alpha_S$  and  $\alpha$  are the strong coupling and fine-structure constants, respectively. For the QCD production, we consider NLO corrections to both  $t\bar{t}W$  production with and without an additional parton. In addition to the nominal sample, the results are also compared with an alternative sample produced with MADGRAPH5\_aMC@NLO v3.3.1 interfaced with PYTHIA v8.306, which uses the improved FxFx matching setup described in ref. [17] with a merging scale of 42 GeV.

To assess potential biases in the measurements due to deviations of the signal predictions from the nominal model, we consider a BSM scenario that can be parametrized by an effective

field theory (EFT) that introduces additional terms to the SM Lagrangian. This contribution is modeled using LO signal simulations using MADGRAPH5\_AMC@NLO, introducing the EFT contribution using the `dim6top` model [49], considering non-zero values of 22 different operators. Samples are reweighted according to the method described in ref. [50] and as used in ref. [8].

The contributions from backgrounds such as  $t\bar{t}H$ , the production of a top quark pair in association with a Z boson ( $t\bar{t}Z$ ), the production of a top quark pair in association with a photon ( $t\bar{t}\gamma$ ), the production of a single top quark in association with a Z boson ( $tqZ$ ), the production of a single top quark in association with a photon ( $t\gamma$ ), the production of a single top quark in association with a Z and W ( $tWZ$ ) and  $Z/\gamma^*$  production in association with jets ( $DY$ +jets) are estimated using MADGRAPH5\_AMC@NLO at NLO. We use the diagram-removal scheme [51] to remove the diagrams contributing both to  $t\bar{t}Z$  and  $tWZ$  production. The associated production of a W and Z (WZ) or two Z bosons (ZZ) are both estimated at NLO using the POWHEG generator. We use NLO predictions with electroweak corrections [1] to normalize the  $t\bar{t}H$  samples, and the NLO computations from the generators for  $tqZ$  and  $tWZ$  productions. The normalizations of the  $t\bar{t}Z$  and diboson processes are determined in data, so we do not assume any specific reference cross section. Simulations of  $t\bar{t}$  production,  $DY$ +jets, and  $tW$  production are used to train the multivariate discriminators described later in the paper and for validating the estimation of the nonprompt-lepton background, as described below. We simulate  $t\bar{t}$  and  $tW$  production using the POWHEG generator [52–56]. The  $t\bar{t}\gamma$  process is normalized to the cross section measured by CMS [57]. The grouping of the  $t\bar{t}Z$  and  $t\bar{t}H$  processes is referred to as  $t\bar{t}X$ , while ZZ and WZ are grouped into “Diboson”. Rare top quark related backgrounds and multiboson productions are grouped into “Other”.

We account for differences between data and simulation arising in lepton reconstruction, identification, and triggering efficiencies, the energy scale of jets and JER, the response of the DEEPJET algorithm, and the resolution in  $p_T^{\text{miss}}$ . These corrections are typically at the level of a few percent [37–39, 58] and are measured using as standard candles a variety of SM processes, such as  $Z \rightarrow ee$ ,  $Z \rightarrow \mu\mu$ ,  $t\bar{t}$ +jets, and  $\gamma$ +jets production.

## 4 Object and event selection

Muons and electrons are considered in this analysis if they are within the detector acceptance, removing electrons in the region between the barrel and endcap of the ECAL ( $1.44 < |\eta| < 1.57$ ). Both types of leptons are subjected to a set of loose quality requirements referred to as baseline selection. They must be compatible with originating from the PV and fulfill a set of pre-defined selections [31, 33]. This includes requirements on their relative isolation,  $I_{\text{rel}}$ , which is defined as the scalar  $p_T$  sum of all particles within a certain distance  $\Delta R$  around the lepton, divided by the lepton  $p_T$ . We use a  $p_T$ -dependent distance [59] of  $\Delta R < 0.2$  for leptons with  $p_T < 50$  GeV,  $\Delta R < 10 \text{ GeV}/p_T$  for  $50 < p_T < 200$  GeV, and  $\Delta R < 0.05$  for  $p_T > 200$  GeV, and require all leptons to pass a loose requirement of  $I_{\text{rel}} < 0.4$ . Specifically for electrons, the number of missing hits, defined as the number of positions in the pixel tracker where a hit by the passing electron is expected but not found, is required to be less than two. In addition, those electrons that are identified as likely to come from photons converting in the detector material are rejected [60].

We denote leptons originating from the decays of electroweak bosons or  $\tau$  leptons produced in the primary interaction as prompt leptons, while those originating from other sources, e.g., hadron decays or misidentified jets or hadrons are called nonprompt leptons. The presence of several prompt leptons in the final state is one of the main signatures of our signal, and hence the discrimination between both types of leptons is a crucial part of the analysis. We rely on an MVA classifier, described in more detail in refs. [9, 11, 61], which is denoted as prompt-MVA. This algorithm uses a number of variables, including the relative isolation of the lepton with both fixed and variable cone sizes, transverse and longitudinal impact parameters, and several variables related to the jet with the smallest  $\Delta R$  with respect to the lepton, including its b tagging score. We consider two WPs for the prompt-MVA, one for each of the strategies followed. We define a loose WP with 89 (93)% efficiency for prompt electrons (muons) and 2 (3)% acceptance rate for nonprompt electrons (muons), and a tight WP with 75 (88)% efficiency for prompt electrons (muons) and 1 (2)% acceptance rate for nonprompt electrons (muons). The cross section measurement with the counting strategy and the charge asymmetry measurement use the tighter WP to reduce the contribution from nonprompt leptons to the SR, while the MVA-based approach to measure the cross section instead uses the looser WP, and relies on another MVA to discriminate  $t\bar{t}W$  from background events.

We classify events in two regions, depending on the number of reconstructed leptons and charge. For the SS dilepton ( $2\ell$ SS) SR, we select events with exactly two leptons, with  $p_T$  of at least 25 and 15 GeV for the highest  $p_T$  (leading) and second-highest  $p_T$  (subleading) lepton, respectively. We require that the two leptons have the same electric charge to suppress backgrounds from  $t\bar{t}$  and  $DY$ +jets production, and we reject events with a lepton pair whose invariant mass is below 30 GeV to reduce contributions from low-mass resonances. For electrons in the  $2\ell$ SS SR, we apply additional criteria that demand consistency among three measurements of the charge sign, described as “selective algorithm” in ref. [60]. Two of these measurements are performed using two different parametrizations of the electron track, while the other exploits the relative position between the electron track and the calorimeter energy deposit. This approach further reduces the electron charge mismeasurement rate by a factor of five with an efficiency of about 97%. We also reject the events in which the invariant mass of the two selected electrons is closer than 10 GeV to the Z boson mass,  $m_Z = 91.19$  GeV [62]. In the MVA-based strategy, we additionally require  $p_T^{\text{miss}} > 30$  GeV, allowing us to create one of the CRs enriched in nonprompt leptons with  $p_T^{\text{miss}} < 30$  GeV (described in section 5). Finally, we require events to have at least three jets, of which at least two are b tagged.

For the three lepton ( $3\ell$ ) SR, we select events with exactly three leptons with  $p_T > 25$ , 15, and 15 GeV, respectively, among which there is at least one pair with opposite electric charge. We reject events with a lepton pair whose invariant mass is below 30 GeV or with an opposite-charge same-flavor (OSSF) lepton pair with an invariant mass within 10 GeV of  $m_Z$ . We select only events with at least two jets, two of which are required to be b tagged.

Several event regions, which are discussed in section 5, are defined to validate the modeling of the main background processes. The yields of some of these regions are included in the likelihood fit described in section 7 to constrain the relevant backgrounds. We denote these regions as CRs, while we denote the regions that are not included in the fit as validation regions (VRs). We note that predictions in the VRs are affected by the same sources of

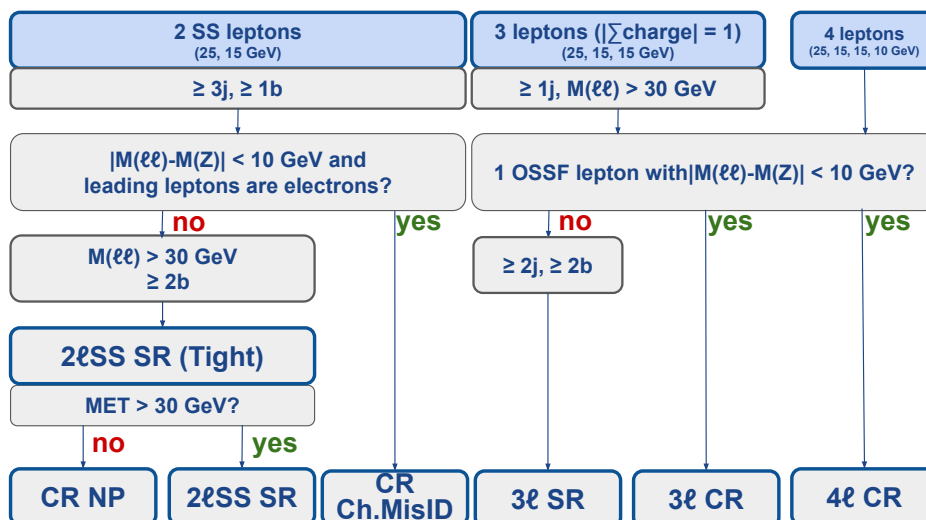


**Figure 2.** An overview of all control regions (CR) and signal regions (SR) used in the analysis.

uncertainties as the SRs and CRs and are therefore modified by the result of the likelihood fit, even if they do not directly affect it. An overview of all analysis regions is shown in figure 2.

## 5 Background estimation

The background contributions to the SRs are divided into four categories: processes with at least one nonprompt lepton, processes with at least one charge-misidentified lepton, processes with one electron produced by a photon conversion, or irreducible backgrounds that contribute to the SR with prompt leptons whose charge has been correctly identified. The latter two categories are estimated from simulated samples (described in section 3) that are normalized according to the measured luminosity and predicted cross sections, while the nonprompt and charge-misidentified lepton backgrounds are estimated from sideband regions in data.

### 5.1 Nonprompt leptons

Events with at least one nonprompt lepton that pass the signal selection are mainly coming from  $t\bar{t}$  and, to a smaller extent,  $DY$ +jets where one of the selected electrons and muons is either a secondary lepton coming from the decay of a  $b$  or a  $c$  hadron, or a light jet wrongly identified as a lepton.

The nonprompt-lepton background is estimated with a “tight-to-loose” ratio method [8, 9, 11, 63], performed separately for electrons and muons passing the tight and loose selection. The main feature of the method is the usage of a sideband region with events that pass the same selection as the SRs, but where one or more of the selected leptons fail the required identification criteria while passing a loosened set of identification criteria specifically designed for this method. This region is enriched in events containing nonprompt leptons. After subtracting the residual contribution from prompt leptons using predictions from simulation, we weight these events by a misidentification rate to estimate the nonprompt-lepton contribution in the SRs. This misidentification rate is measured in a data sample enriched in nonprompt leptons produced in SM events composed uniquely of jets produced

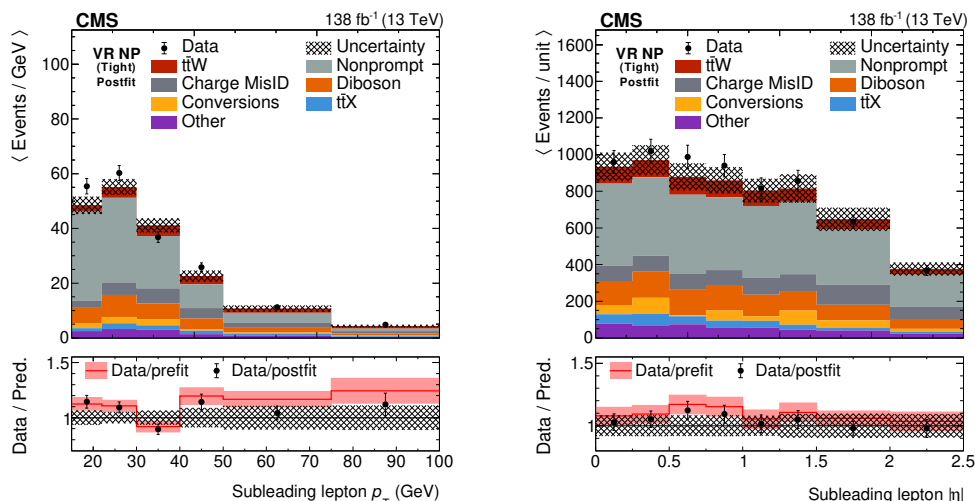


**Figure 3.**  $p_T$  of the sub-leading lepton (left) and  $|\eta|$  of the subleading lepton (right), in a VR enriched with nonprompt leptons by applying requirements on the number of (b-tagged) jets orthogonal to the SR, for data (points) and predictions (filled histograms) after the fit to the data in the SR and CR as described in section 7 for the tight lepton selection. The lower panels show the ratio of the data to the sum of the postfit predictions (points) and the ratio of the data to the prefit predictions (red line). The vertical lines on the data points represent the statistical uncertainty in the data and the hatched (filled) band corresponds to the total uncertainty in the postfit (prefit) prediction. Events that exceeded the range of the plot are included in the last bin. The bin contents are divided by bin width.

through the strong interaction, referred to as multijet events, that is collected by a set of dedicated triggers.

The method is validated in simulation separately with  $t\bar{t}$  and  $DY$ +jets events, which have different sources of nonprompt leptons, and also separately for nonprompt electrons and muons. We compare the event yields predicted by the simulations in the SRs with the predictions from nonprompt leptons that pass the loose but fail the tight ID and are reweighted with the tight-to-loose ratio method. We observe an overall good agreement between the two methods, with the largest deviations being smaller than 30%.

The method is then checked in one data CR and one data VR enriched in the nonprompt-lepton background. For the VR (referred to as VR NP), we select events that pass similar requirements as in the  $2\ell$ SS SR, but modify the jet and b-tagged jet multiplicity requirements: we require events to have exactly two jets, of which one is a b-tagged jet using the medium WP. For the CR (referred to as CR NP and only used with the loose lepton selection), we subdivide events in the  $2\ell$ SS SR in two categories. The region with  $p_T^{\text{miss}} < 30$  GeV, which is a region depleted in signal and rich in nonprompt leptons, is used as the CR NP. The region with  $p_T^{\text{miss}} > 30$  GeV remains as the  $2\ell$ SS SR. The prediction matches the data accurately in both regions within the uncertainties, as shown in figures 3–4 for leptons passing the tight and loose lepton selections, respectively.

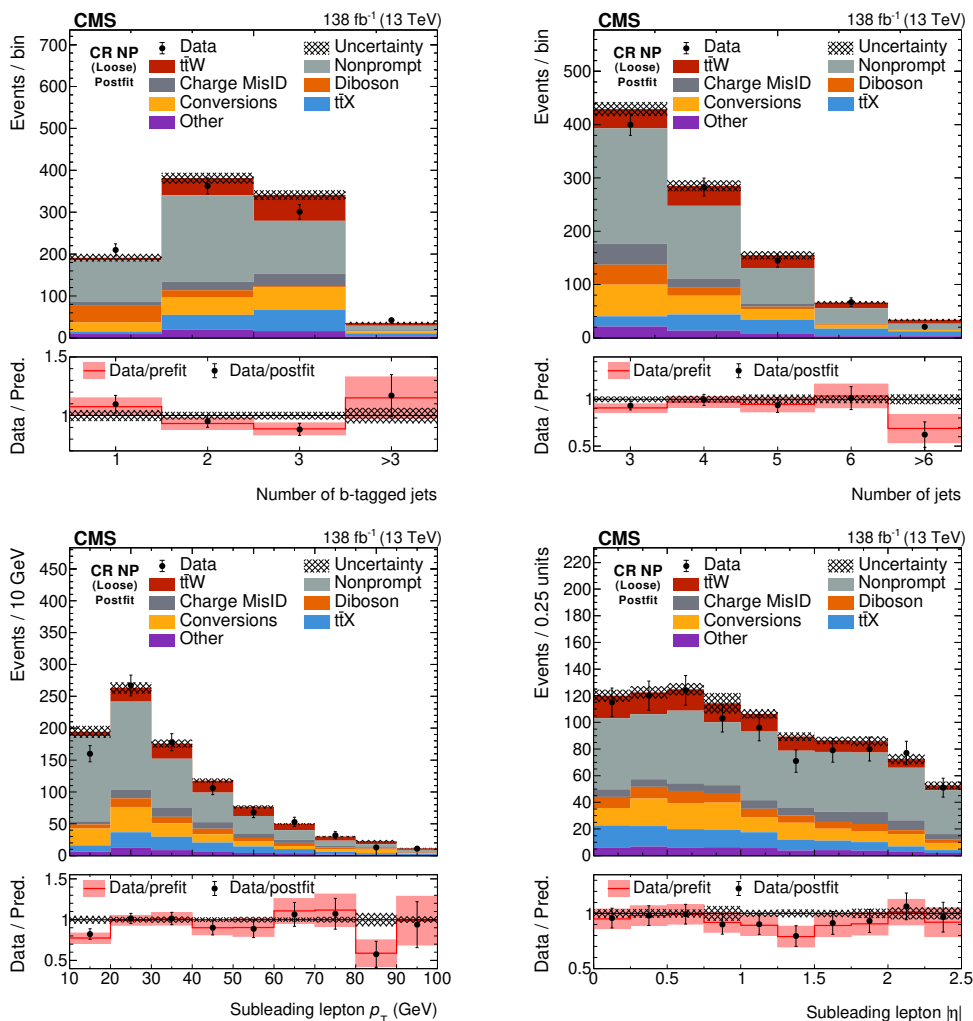


**Figure 4.** Number of selected b-tagged jets in the event (upper left), number of selected jets in the event (upper right),  $p_T$  of the sub-leading lepton (lower left), and  $|\eta|$  of the sub-leading lepton (lower right), in a CR enriched with nonprompt leptons by inverting the  $p_T^{\text{miss}}$  requirement, for data (points) and predictions (filled histograms) after the fit to the data in the SR and CR as described in section 7 for the loose lepton selection. The lower panels show the ratio of the data to the sum of the postfit predictions (points) and the ratio of the data to the prefit predictions (red line). The vertical lines on the data points represent the statistical uncertainty in the data and the hatched (filled) band corresponds to the total uncertainty in the postfit (prefit) prediction. Events that exceed the range of the plot are included in the last bin.

## 5.2 Charge-misidentified leptons

The  $2\ell$ SS SR contains a non-negligible contribution of events where the electric charge of one of the leptons has been wrongly measured. This contribution is dominated by electrons, which undergo Bremsstrahlung as they traverse the detector, making the measurement of the track curvature more challenging. The charge-misidentification probability is negligible for muons.

To determine the charge-misidentified background, which we denote as “Charge MisID”, the electron charge-misidentification probability is determined in simulated  $DY$ +jets samples

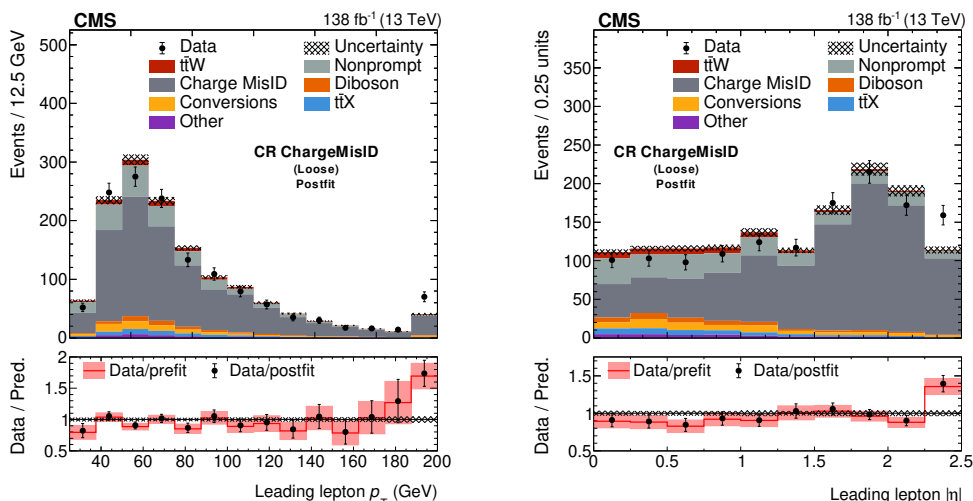


**Figure 5.**  $p_T$  of the leading lepton (left),  $|\eta|$  of the leading lepton (right), in a CR enriched with charge-misidentified leptons and additional jets for data (points) and predictions (filled histograms) after the fit to the data in the SR and CR as described in section 7 for the loose lepton selection. The lower panels show the ratio of the data to the sum of the postfit predictions (points) and the ratio of the data to the prefit predictions (red line). The vertical lines on the data points represent the statistical uncertainty in the data and the hatched (filled) band corresponds to the total uncertainty in the postfit (prefit) prediction. Events that exceed the range of the plot are included in the last bin.

and parameterized as a function of  $p_T$  and  $|\eta|$  of the lepton. We then estimate the contribution from charge-misidentified leptons in the SR by weighting data events in a sideband, defined with the same requirement as the SR but where the electric charges of the two leptons have the opposite sign, by the charge-misidentification probability we estimated.

To account for residual differences of the charge-misidentification probability between data and simulations, we select events with an SS electron pair whose mass is within 10 GeV of  $m_Z$ , which is enriched in events with charge-misidentified leptons. We compare the data yield with the yield predicted by this method. The two agree between 10 and 40%, depending on the data-taking year and the lepton selection, with residual differences due to the complexity of modeling misreconstruction effects. We use this per-year factor to correct the charge-misidentification probability predicted by the simulations. After this correction, data agrees well with the predictions. A CR, labeled as CR ChargeMisId, is defined, requiring in addition the presence of at least three jet and at least one b-tagged jet, which represents more closely the phase space of the SR. The good agreement between data and prediction after applying these scale factors is preserved in this region, as shown in figure 5. Slight deviations can be observed in the high lepton  $p_T$  and lepton  $\eta$  phase space regions, which are related to the binning in which the charge-misidentification probability is determined. These effects however do not influence the measurement as the binning of the differential measurement is much coarser.

### 5.3 Photon conversions

An additional source of events in the SR is the conversion of photons into electrons in their interaction with the detector material, which we refer to as “conversions”, which is also suppressed by means of dedicated identification algorithms. Nevertheless, a significant contribution from  $t\bar{t}\gamma$ ,  $t\gamma$ , or  $Z\gamma$  is present, amounting to roughly 9% of the events in the SRs, which is estimated using samples of simulated events. The simulation of photon conversion is validated in a data sample with three-lepton events where the invariant mass of the three leptons is required to be consistent with the Z boson mass within 15 GeV. Good agreement between data and simulation is observed in this VR.

### 5.4 Irreducible backgrounds

Irreducible backgrounds consist of events in which all selected leptons are prompt leptons with their electric charge correctly identified. The major contributions to this background category are various production modes of top quark pairs in association with bosons, notably  $t\bar{t}H$  and  $t\bar{t}Z$ . Additional contributions are coming from diboson processes such as WZ and ZZ or multiboson processes and the associated production of a single top quark with bosons, e.g.,  $tqZ$ ,  $tWZ$ . These background contributions are estimated from simulated samples, as detailed in section 3.

The modeling of irreducible backgrounds is studied in a number of VRs and two CRs: the three-lepton CR and four-lepton CR. We build the three-lepton CR by selecting events in the  $3\ell$  region, but require that the events contain an OSSF lepton pair with an invariant mass within 10 GeV from  $m_Z$ . We furthermore do not put the same requirements on the jet and b-tagged jet multiplicities described in section 4, selecting instead events with at least one jet. This CR is enriched mainly in WZ and  $t\bar{t}Z$ , showing good agreement between data and prediction. Events in this selection are classified depending on the number of jets and b-tagged jets as shown in figure 6, which helps to discriminate between WZ and  $t\bar{t}Z$  backgrounds.

The four-lepton CR is defined by selecting events with exactly four leptons with  $p_T > 25, 15, 15,$  and 10 GeV, respectively. The presence of an OSSF lepton pair with an invariant mass within 10 GeV from  $m_Z$  is required. This CR is enriched mainly in ZZ and  $t\bar{t}Z$  events, and features a good agreement between data and predictions in all relevant variables.

## 6 Systematic uncertainties

The precision on the differential cross section measurements is limited by various sources of experimental and theoretical uncertainties, the nature and estimation of which is described in this section. The total uncertainty in the measurements is however dominated by the limited statistical precision.

### 6.1 Experimental uncertainties

The integrated luminosity of each data-taking period is used to normalize the predictions obtained from simulation. Its measured value has an associated systematic uncertainty of 1.2–2.5%, partially correlated across the data-taking years [64–66], with an overall uncertainty of 1.6%.

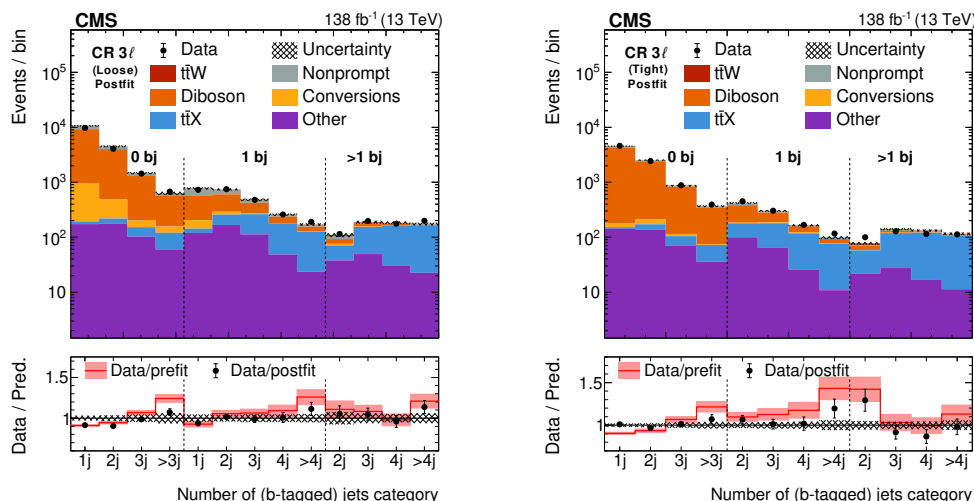


**Figure 6.** Number of selected (b-tagged) jets in the event for events with three leptons passing the loose (left) and tight (right) selection after the fit to the data in the SR and CR as described in section 7. Events with no b-tagged jets are classified in bins 1 to 4, events with one b-tagged jet are classified in bins 5 to 9 (8) and events with more than one b tag are classified in bins 10 (9) to 13 (12) for the loose (tight) lepton selection. The lower panels show the ratio of the data to the sum of the postfit predictions (points) and the ratio of the data to the prefit predictions (red line). The vertical lines on the data points represent the statistical uncertainty in the data and the hatched (filled) band corresponds to the total uncertainty in the postfit (prefit) prediction.

The uncertainty related to the amount of pileup interactions is taken into account by varying the total pp inelastic cross section in all simulated samples by  $\pm 4.6\%$  with respect to its nominal value of 69.2 mb, affecting their distributions as well as their normalization. The pileup uncertainty is fully correlated between all data-taking years and processes.

Uncertainty in the efficiency with which events passing the signal selection are triggered in data is taken into account as well. The trigger efficiency is measured in simulation, as well as in a data sample selected with a set of reference triggers uncorrelated with any of the lepton triggers used in this analysis. Differences in trigger efficiency between simulation and data are taken into account for the SS dilepton selection applying weights to simulated events. For events with three or four leptons, the trigger efficiency is found to be higher than 98% in data at the confidence level of one standard deviation. For these events, an uncertainty of 2% is applied to take into account the limited statistical precision of the efficiency measurement. These uncertainties are considered to be uncorrelated across data-taking years, as they are mainly statistical in nature.

Simulated samples are corrected for the so-called *Level-1 trigger prefireing*, i.e., a time jitter of the trigger signal in the muon [67] and ECAL [26] systems, which led to a loss of events at the level of 0.5% or less.

We take into account the jet energy scale (JES) and JER uncertainties by varying the jet energy scales up and down within their uncertainties [36] for all jets in the event. We consider 14 JES uncertainty sources, some of which are independent per data-taking period, making a total of 29 independent nuisance parameters, and 6 JER sources, all independent

per data-taking period. These variations are propagated to  $\vec{p}_T^{\text{miss}}$  and the b tagging efficiency scale factors [37]. They are considered to be partially correlated across all data-taking years and processes, depending on the origin of the uncertainty. An additional uncertainty in the unclustered energy is taken into account by varying all unclustered contributions to  $\vec{p}_T^{\text{miss}}$  within their respective resolutions and propagating these changes to  $\vec{p}_T^{\text{miss}}$  [38]. This uncertainty is considered to be uncorrelated among the data-taking years.

As the event selection relies on b tagging, the associated uncertainty is taken into account by varying the data-to-simulation scale factors for the b tagging efficiency up and down within their uncertainties. These uncertainties are related to the purity of heavy and light flavor jets in their respective measurement regions and to the statistical fluctuations. They are considered to be fully correlated across the processes and correlated (uncorrelated) across the years for the uncertainty sources of systematic (statistical) origin.

The lepton reconstruction and identification come with a set of scale factors, determined using the tag-and-probe method [58] in  $Z/\gamma^*$  events decaying to two leptons. Uncertainties in the resulting scale factors stem from the limited sizes of the data and simulated samples and from different sources of systematic effects, such as the choice of the dilepton invariant mass line-shape, the dilepton invariant mass window, or the phase space of the measurement. The effect of these uncertainties is evaluated by varying the scale factors up and down within their uncertainties.

For the nonprompt background prediction, we apply different uncertainty sources to account for potential biases introduced by the method. We assign uncertainties based on the non-closure observed in the simulations (between 5 and 30%, depending on the lepton flavor and identification WP), which is found to be independent from the lepton kinematic properties within the statistical uncertainty of the samples. We also assign different sources of uncertainty coming from the limited size of the multijet data samples that were used to measure the nonprompt-lepton rate, from the subtraction of the prompt lepton contamination in the measurement region, and from the differences in the background composition between measurement region (dominated by multijet background) and application region (dominated by  $t\bar{t}$ +jets background). These uncertainties sum up to between 10 and 40% depending on the lepton  $p_T$ ,  $\eta$ , flavor, and data-taking period. These uncertainties are parametrized as several independent sources that vary the integrated nonprompt-lepton rate, as well as its dependence as a function of  $p_T$  and  $|\eta|$ . The uncertainty in the charge misidentification prediction obtained from data is set to 30%, independently from electron kinematics, which is large enough to modify the scale factor used to cover the disagreement between data and simulations that is described in section 5.2, and is considered to be independent in the different data-taking periods.

Two sources of uncertainty are added to account for the mismodeling of the WZ and ZZ processes as a function of number of jets and b-tagged jets, that is observed in the three-lepton and four-lepton CRs, as can be seen in figure 6. The first of these uncertainties adds a 10% uncertainty per selected jet in each event up to a maximum of 50%; the second adds a 10% uncertainty in the event yields for events with zero or one b-tagged jets and 40% for events with two or more b-tagged jets. Both sources of uncertainty are correlated across the data-taking periods.

## 6.2 Theoretical uncertainties

We assign a normalization uncertainty to the background processes estimated with simulation. Dedicated studies have been performed in CMS of WZ, ZZ,  $t\bar{t}Z$ ,  $t\bar{t}H$ ,  $Z\gamma$ , and  $t\bar{t}\gamma$ , measuring their cross sections with a precision between 4 and 8% [11, 68–72]. However, since the phase space of these dedicated measurements does not necessarily correspond to our signal selection, we apply a larger a-priori normalization uncertainty of 30% around their normalizations for the  $Z\gamma$  and  $t\bar{t}\gamma$  [57] processes. The normalization of the WZ, ZZ, and  $t\bar{t}Z$  processes are free parameters in the likelihood fit described in section 7 and are determined by the observed yields. The  $t\bar{t}H$  process takes a 10% normalization uncertainty according to a recent prediction [73]. The remaining processes are of minor importance in the SR, thus we assign conservatively a 50% normalization uncertainty around their latest theory predictions, in agreement with ref. [21].

Imperfect knowledge of the PDFs for the colliding protons yields another source of systematic uncertainty. The PDF uncertainty is taken into account using NNPDF replicas [42] and applying the procedure described in ref. [74], resulting in 100 individual variations that are evaluated simultaneously for all processes, in addition to two variations of the strong coupling constant  $\alpha_S$ .

Uncertainty in the renormalization and factorization scale in the matrix element is taken into account in a similar way. All simulated processes are reweighted using both independent and correlated up and down variations by a factor of 2 of both scales (excluding the two extreme variations). These sources of uncertainty are correlated between the data-taking years but are treated uncorrelated between different processes.

Uncertainties related to the initial-state and final-state radiation (ISR and FSR, respectively) are evaluated similarly by variations in the renormalization scale for emissions in ISR and FSR of a factor two (up and down). These variations are considered to be fully correlated across the data-taking years, while only FSR is correlated between different processes.

Some of these sources of uncertainty can affect both the production cross section and the acceptance of all simulated processes. The systematic effect in the cross section is not taken into account for processes that are assigned a normalization uncertainty based on dedicated measurements or that are left freely floating in the fit. For those processes, only the acceptance effects are considered.

## 7 Differential cross section measurements

We measure the  $t\bar{t}W$  differential cross sections using two complementary methods that share the same statistical model and only differ on the definition of the reconstruction-level bins used in the signal extraction fit. In the  $2\ell SS$  region we use an event-level MVA discriminator and the variable of interest to define the reconstruction-level bins. The other method only uses a reconstruction-level binning in the variable of interest and requires the tighter lepton selection described in section 4. This method is used in the  $3\ell$  region as the main method and in the  $2\ell SS$  region as a complementary measurement to the MVA-based approach.

## 7.1 Definition of measured observables

Particle-level object definitions [75] are used to define the fiducial phase space and to construct the measured observables. We consider particle-level leptons by clustering prompt electrons and muons with photons not arising from hadron decays, using the anti- $k_T$  algorithm with a cone size of  $R = 0.1$ . Only particle-level leptons with  $p_T > 15$  GeV and  $|\eta| < 2.5$  (electrons) or  $|\eta| < 2.4$  (muons) are selected for further processing. Jets are constructed by clustering all stable particles excluding prompt selected leptons and neutrinos using the anti- $k_T$  algorithm with a cone size of  $R = 0.4$ . Only particle-level jets with  $p_T > 25$  GeV and  $|\eta| < 2.4$  are selected in the analysis. To determine the jet flavor, we use the “ghost clustering” procedure described in ref. [75], in which jets are re-clustered including the decayed b hadrons with their momentum scaled to an arbitrary small value (ghosts), in addition to the set of particles included in the jet definition. We define b jets as those that contain a ghost when this reclustering is performed.

Using these objects, we define a fiducial region that aligns with the categories used to perform the measurement. We define a  $2\ell$ SS fiducial region taking events with exactly two leptons with  $p_T > 25$  and 15 GeV that have the same electric charge. Additionally, events are required to have at least 3 jets, out of which at least one is a b jet. For the  $3\ell$  region we select events having at least 3 leptons with  $p_T > 25$ , 15, and 15 GeV respectively, and at least two jets, out of which at least one is a b jet. Signal events that do not pass this fiducial selection are taken into account as background events.

We also use these objects to construct the variables as a function of which the cross section is measured, which are listed in table 1. Many of these distributions, such as the jet multiplicity or the scalar sum of jet  $p_T$ ,  $H_T$ , are useful to assess the  $t\bar{t}W$  modeling as a background to measurements of other processes with larger jet multiplicity, like  $t\bar{t}H$  or  $t\bar{t}t\bar{t}$  production [19]. Other variables, such as the jet and lepton kinematic distributions, are generic probes of the  $t\bar{t}W$  modeling.

## 7.2 Statistical model

We determine the differential cross section as a function of a given variable in  $N_{\text{gen}}$  particle-level bins using the number of observed events  $n_i$  in  $N_{\text{reco}}$  reconstructed-level bins, using a likelihood-based unfolding method. We fit data to a statistical model implemented in the COMBINE software [76] and described by the likelihood function  $\mathcal{L}$ , given by

$$\mathcal{L}(\text{data}; \boldsymbol{\sigma}, \boldsymbol{\theta}) = \prod_i^{N_{\text{reco}}} \mathcal{P}\left(n_i \left| \sum_j^{N_{\text{gen}}} \sigma_j \epsilon_{ij}(\boldsymbol{\theta}) L(\boldsymbol{\theta}) + b_i(\boldsymbol{\theta}) \right.\right) \prod_k p(\tilde{\theta}_k | \theta_k). \quad (7.1)$$

The symbol  $\mathcal{P}$  denotes the Poisson probability for observing  $n_i$  events in a given reconstruction-level bin with an expectation given by the expected background events and signal events outside the fiducial region in that bin  $b_i(\boldsymbol{\theta})$ , the luminosity  $L(\boldsymbol{\theta})$ , the fiducial cross section in each particle-level bin  $\sigma_j$ , which are the parameters of interest in the fit, and the elements of the response matrix  $\epsilon_{ij}(\boldsymbol{\theta})$ . This matrix parametrizes the detector response and is defined by

$$\epsilon_{ij} = \frac{N(\text{signal events generated in bin } j \text{ and reconstructed in bin } i)}{N(\text{signal events generated in bin } j)}. \quad (7.2)$$

Variable	Description
Distances between objects	
$ \Delta\eta(\ell_1, \ell_2) $	Absolute difference in $\eta$ between the two leptons with the highest $p_T$
$\Delta R(\ell_1, \ell_2)$	Separation in $(\eta, \phi)$ space between the two leptons with the highest $p_T$
$\Delta R(\ell_1, \text{jet})_{\min}$	Separation in $(\eta, \phi)$ space between the lepton with the highest $p_T$ and its closest jet
Jet-related variables	
$H_T$	Scalar sum of jet $p_T$
Leading jet $ \eta $	$ \eta $ of the jet with highest $p_T$
Leading jet $p_T$	$p_T$ of the jet with highest $p_T$
Subleading jet $ \eta $	$ \eta $ of the jet with next-to-highest $p_T$
Subleading jet $p_T$	$p_T$ of the jet with next-to-highest $p_T$
Lepton-related variables	
Leading lepton $p_T$	$p_T$ of the lepton with highest $p_T$
Subleading lepton $p_T$	$p_T$ of the lepton with next-to-highest $p_T$
Lepton maximum $ \eta $	Maximum $ \eta $ among the leptons
$\sum$ lepton $p_T$	Sum of the lepton $p_T$ 's
$m(\text{leptons})$	Invariant mass of the system of the two leptons with the highest $p_T$
Object multiplicity	
Number of jets	Jet multiplicity

**Table 1.** Kinematic variables studied in the differential cross section measurement of the signal.

The likelihood model also includes the explicit dependence of the different quantities as a function of the nuisance parameters  $\theta$  that model the impact of the systematic uncertainties and that are constrained by their prior probability density functions,  $p$ .

In this kind of measurement, additional regularization terms are sometimes added to the likelihood to penalize nonphysical fluctuations, effectively reducing the uncertainties at the price of introducing a controlled bias. In our case, we have not included such terms since the response matrices used in this analysis are sufficiently well-conditioned. We quantified that using the condition number, defined as the ratio of the largest to the smallest value in a singular value decomposition of each matrix. The condition of all the matrices is below 4, which indicates that the inverse of the matrix can be computed with high accuracy.

### 7.3 Signal extraction in the $2\ell\text{SS}$ region

The method we use for the differential cross section measurement in the  $2\ell\text{SS}$  region is based on separating the signal and the backgrounds using an MVA discriminator that takes event-level variables as input. This strategy uses the loose lepton identification criterion described in section 4 to ensure a high signal efficiency. In addition, a requirement of  $p_T^{\text{miss}} > 30 \text{ GeV}$  is applied to reject the contribution from nonprompt leptons.

The MVA algorithm of choice is gradient boosted decision tree (gBDT), trained with the XGBOOST library [77]. For the training and validation of the gBDT, 20% of the simulated events are used, and this part of the samples is excluded from the rest of the analysis to avoid potential overtraining biases. In total, 37 variables are selected as input features. It was checked that their distributions are well described by our predictions and their mutual

MVA input variables	Prefit $p$ -value
Leptons	
Leading lepton $p_T$	0.17
Subleading lepton $p_T$	0.33
Leading lepton $\eta$	0.85
Subleading lepton $\eta$	0.29
Leading lepton energy	0.65
Subleading lepton energy	0.82
Jets	
Leading jet $p_T$	0.61
Subleading jet $p_T$	0.29
Leading jet $\eta$	0.37
Subleading jet $\eta$	0.98
Leading jet mass	0.47
Subleading jet mass	0.87
Number of jets	0.36
Maximum $ \eta $ among all jets	0.80
b-tagged jets	
Leading b-tagged jet $p_T$	0.47
Leading b-tagged jet $\eta$	0.75
Highest DEEPJET score among all jets	0.78
DEEPJET score of leading jet	0.26
DEEPJET score of subleading jet	0.98
Number of loose b-tagged jets	0.72
Number of medium b-tagged jets	0.69
Number of tight b-tagged jets	0.59
Angular separation	
Minimum $\Delta R$ between a lepton and a b-tagged jet	0.40
$\Delta R$ between the leading and subleading lepton	0.23
$\Delta \eta$ between the leading and subleading lepton	0.31
Minimum $\Delta R$ between the leading lepton and a jet	0.96
Minimum $\Delta R$ between the leading lepton and a b-tagged jet	0.15
Minimum $\Delta R$ between the leading lepton and a non-b-tagged jet	0.96
Dijet and dilepton properties	
Maximum dijet mass	0.43
Maximum dijet $p_T$	0.81
Invariant mass of the leading and subleading lepton system	0.31
Global variables	
Scalar sum of the $p_T$ of the jets	0.34
Scalar sum of the $p_T$ of the leptons and $p_T^{\text{miss}}$	0.16
Lepton flavor category (ee, e $\mu$ , $\mu$ e, or $\mu\mu$ , with $p_T$ ordering)	0.21
Sum of lepton charges	0.24
$p_T^{\text{miss}}$	0.18
Data-taking year	—

**Table 2.** Overview of input variables to the BDT and their prefit  $p$ -values, obtained in a  $\chi^2$  goodness-of-fit test.

correlation matrix agrees well between simulation and data. The input features include basic kinematic properties of the leptons and jets in the event, the b tagging scores of the jets, the directional separation between various combinations of leptons and jets, the invariant mass and  $p_T$  of various dilepton and dijet systems, and some global event variables such as the scalar  $p_T$  sum of all selected jets, the lepton flavor category, the sum of lepton charges, and the  $p_T^{\text{miss}}$ . The data-taking year is also included as an input variable to allow the algorithm to account for changing experimental conditions. A full overview of the input variables in the  $2\ell\text{SS}$  region is provided in table 2, together with their corresponding prefit  $p$ -values, obtained in a  $\chi^2$  goodness-of-fit test, which show no indication of significant tensions between data and the prediction for these variables. The training was performed in the  $2\ell\text{SS}$  region, including the  $p_T^{\text{miss}} > 30$  GeV requirement. The learning rate, number of estimators, and maximum depth per estimator were optimized simultaneously in a grid search. The good postfit agreement between data and prediction in this selection is shown for a number of variables of interest and the BDT output score in figures 7 and 8, respectively.

The signal extraction is performed by fitting the event yields in reconstruction-level bins defined in a two-dimensional grid between the MVA score and the variable of interest. We use five bins in the MVA score and a number of bins in the variable of interest equal to the number of generator level bins to be measured, as shown in figure 9.

To constrain some of the background processes, the number of observed events in the three- and four-lepton CRs are included in the fit as a function of the jet and b-tagged jet multiplicity in the three-lepton region, and the b-tagged jet multiplicity and number of Z boson candidates for the four-lepton region. In addition, the number of events in the CR NP and the CR ChargeMisId are also included, to constrain the corresponding processes. The differential cross sections measured in the  $2\ell\text{SS}$  signal region as functions of the variables of interest are shown separately for the absolute and normalized differential cross sections in figures 10–16.

In addition to the differential measurements, we also measured the inclusive cross section using the inclusive BDT output distribution in the  $2\ell\text{SS}$  SR, shown in figure 8, the inclusive BDT output distribution in the  $3\ell$  SR, and the same CRs as in the differential measurement. We observe a cross section of  $\sigma_{t\bar{t}W}^{\text{observed}} = 938 \pm 45$  (stat)  $\pm 52$  (syst) fb. This result is well in agreement with the previous measurements by both ATLAS [20] and CMS [11, 21], finding a cross section that is in slight tension with the prediction of  $745 \pm 52$  fb given by the NNLO calculations [2]. This discrepancy in the normalization is also observed in the  $2\ell\text{SS}$  unfolded results. The normalized measured distributions in the  $2\ell\text{SS}$  region are generally however in agreement with respect to any of the reference models described in section 3, which also agree very well with each other for the merging scale chosen.

Across all measured observables and bins, statistical uncertainties are the dominant source of uncertainty, typically ranging from 10 to 25%. Among the systematic uncertainties, the largest contributions arise from background estimation, particularly from the nonprompt sources, which contributes between 3 and 10% in most bins — reaching its highest impact in regions where nonprompt backgrounds are most significant. In bins with higher signal purity, the dominant systematic uncertainties arise from the modeling of key processes such as  $t\bar{t}H$ ,  $t\bar{t}Z$ , and the signal itself, with effects ranging from 0.8 to 1.2%. Among experimental sources, the uncertainty in the integrated luminosity contributes most significantly, at the 2–3% level.

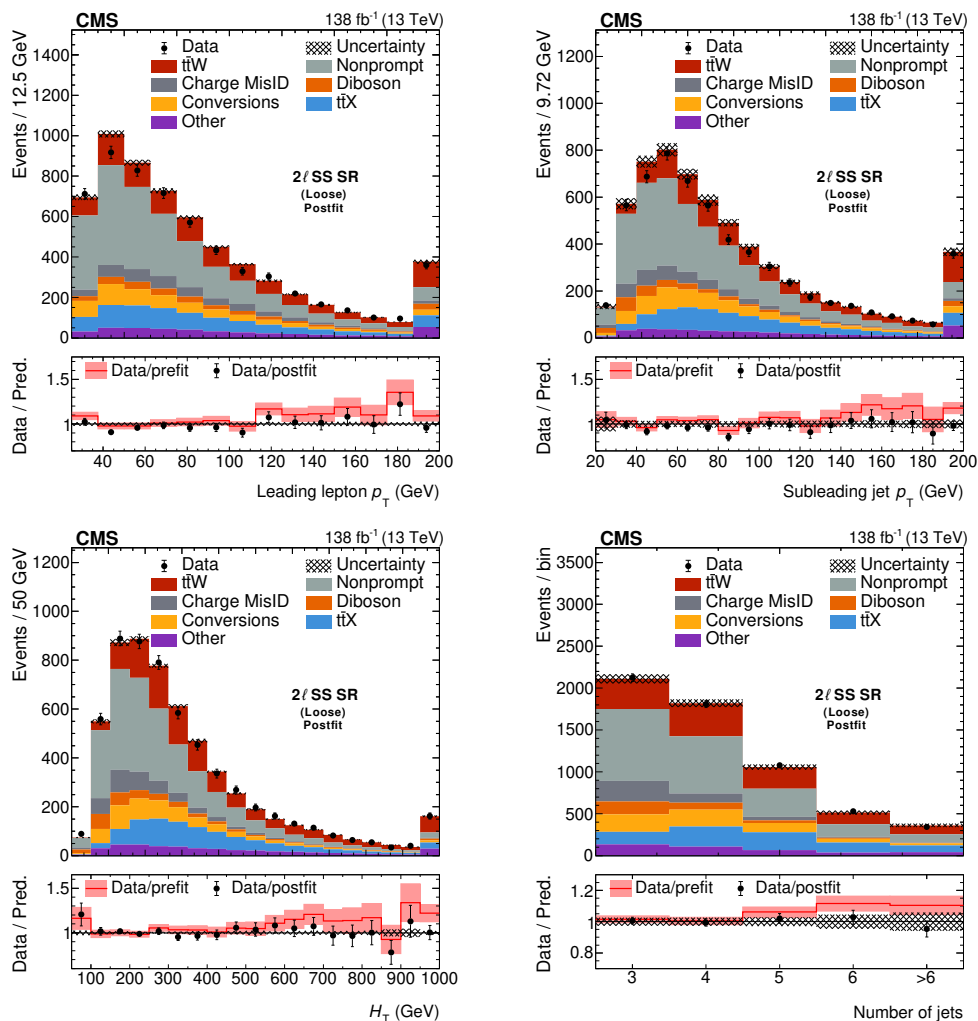


**Figure 7.**  $p_T$  of the leading lepton (upper left),  $p_T$  of the subleading jet (upper right), scalar  $p_T$  sum of selected jets in the event (lower left), and the number of selected jets in the event (lower right), in the two-lepton signal selection for the loose lepton selection for data (points) and predictions (filled histograms) after the fit to the data in the SR and CR. The lower panels show the ratio of the data to the sum of the postfit predictions (points) and the ratio of the data to the prefit predictions (red line). The vertical lines on the data points represent the statistical uncertainty in the data and the hatched (filled) band corresponds to the total uncertainty in the postfit (prefit) prediction. Events that exceed the range of the plot are included in the last bin.

Additional subleading experimental uncertainties, including jet energy calibration, lepton identification, and b tagging, contribute at the 1–3% level, depending on the sensitivity of the observable to the properties of the corresponding reconstructed objects.

### 7.4 Consistency checks

In order to better understand the robustness of our measurement, extensive stress tests have been performed to evaluate our method in terms of its dependence on the signal model. Firstly, we employ the counting method used in the  $3\ell$  region, described in section 7.5, also

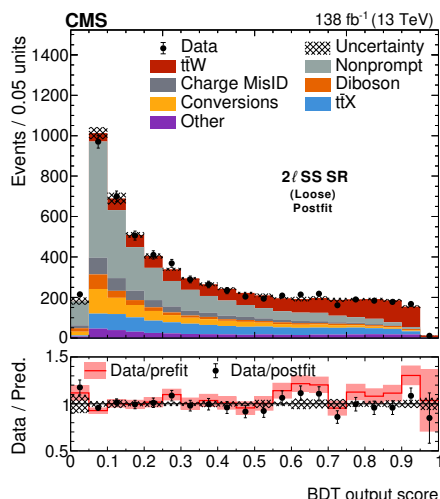


**Figure 8.** Distribution of the BDT output node in the two-lepton signal selection for the loose lepton selection for data (points) and predictions (filled histograms) after the fit to the data in the SR and CR. The lower panels show the ratio of the data to the sum of the postfit predictions (points) and the ratio of the data to the prefit predictions (red line). The vertical lines on the data points represent the statistical uncertainty in the data and the hatched (filled) band corresponds to the total uncertainty in the postfit (prefit) prediction.

in the  $2\ell$ SS region. This allows us to provide a complementary measurement. This strategy profits from the high signal purity achieved by the tighter lepton selection, allowing us not to rely on the BDT discrimination while remaining competitive in terms of sensitivity. This results in a better control over the measured fiducial phase space and, therefore, in a more model-independent measurement. In this region, events are categorized at reconstruction level according to the sum of the lepton charges and their flavor, resulting in six categories. In addition, we consider two reconstruction-level bins per generator-level bin of the variable of interest. The differential cross sections measured by both strategies in the  $2\ell$ SS signal region as functions of the variables of interest are shown separately for the absolute and normalized differential cross sections in the appendix in figures 22–28. We observe an overall good agreement between both methods. In addition, we have computed the inclusive fiducial cross sections by integrating the different measurements independently for each measurement strategy, showing consistent results within uncertainties between the two methods and among the different variables measured. The normalization of backgrounds and behavior of other uncertainties are furthermore found to be consistent within uncertainties between the two methods and among the different variables measured. The agreement between the two different differential measurements and the reference models is quantified with a  $\chi^2$  goodness-of-fit tests done for each variable using the full covariance matrix of the result. These are shown in table 3. The lower values of the normalized  $\chi^2$   $p$ -values for the measured unfolded jet multiplicity, subleading lepton  $p_T$ ,  $H_T$ , and  $\Delta R(\ell_1, \text{jet})_{\min}$  show slight indications of mismodelling. In addition, the counting method also reports slightly lower values for the leading jet  $p_T$  distribution. These trends are however not yet conclusive.

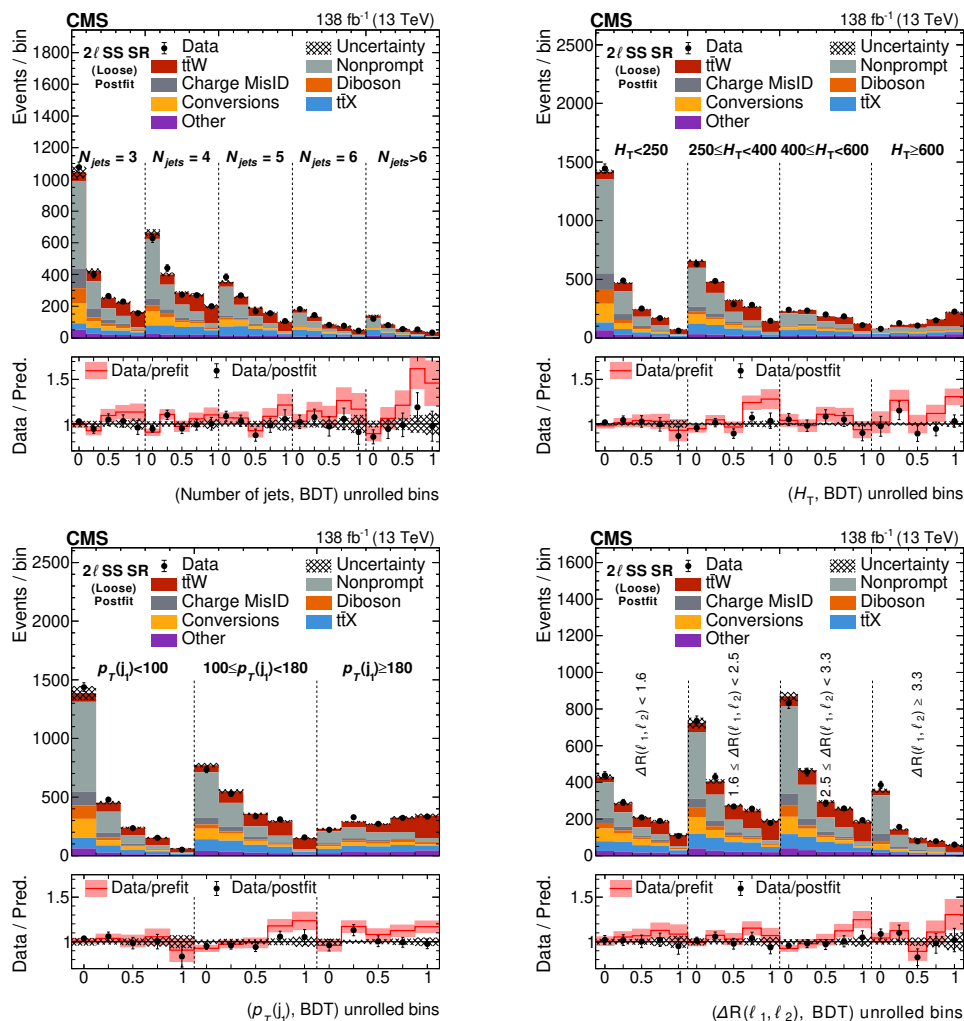


**Figure 9.** Distributions defined in a two-dimensional grid between the MVA score and the variable of interest in the two-lepton signal selection for data (points) and predictions (filled histograms) after the fit to the data in the SR and CR for the loose lepton selection. The lower panels show the ratio of the data to the sum of the postfit predictions (points) and the ratio of the data to the prefit predictions (red line). The vertical lines on the data points represent the statistical uncertainty in the data and the hatched (filled) band corresponds to the total uncertainty in the postfit (prefit) prediction.

As an additional stress test, pseudodata samples were generated by reweighting signal events based on a linear function of each differential variable we want to measure. Each reweighting function was chosen to induce a linear shape difference of 30–40% between the first and last bins of the reweighting variable distribution. The stress test then consisted of trying to capture the reweighted distributions of all other variables based on this linear reweighting function, estimating the sensitivity of the fitting procedure to a mismodelling of this variable. We also perform another signal injection test in which pseudodata are constructed from signal samples incorporating the effect of a number of EFT operators from the  $\text{dim6}_{\text{top}}$  model. We considered the effect of 22 different EFT operators, setting values to their associated Wilson coefficients so that the modification they introduce in the particle-level kinematic

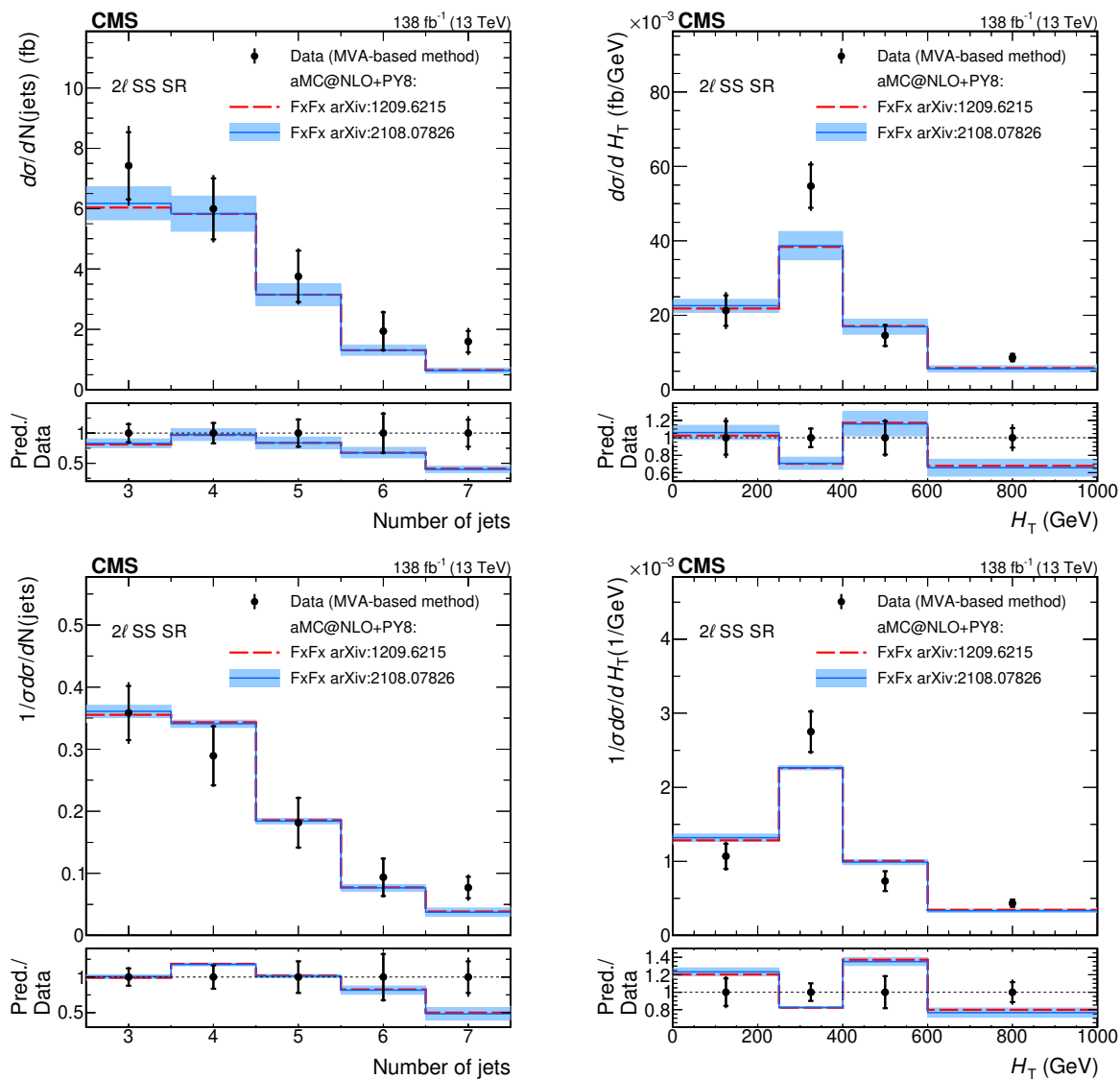


**Figure 10.** Absolute (upper row) and normalized (lower row) differential cross section measured as a function of the jet multiplicity (left) and  $H_T$  (right), using the MVA-based method. The upper panels show the results of the measurement together with the theoretical predictions. The blue band shows the uncertainty of the prediction from ref. [17]. The lower panels show the ratio between the predictions and the measurement. The vertical lines on the unfolded data points represent the total experimental uncertainty of the unfolded cross section, while the horizontal bars show the statistical component of the uncertainty.

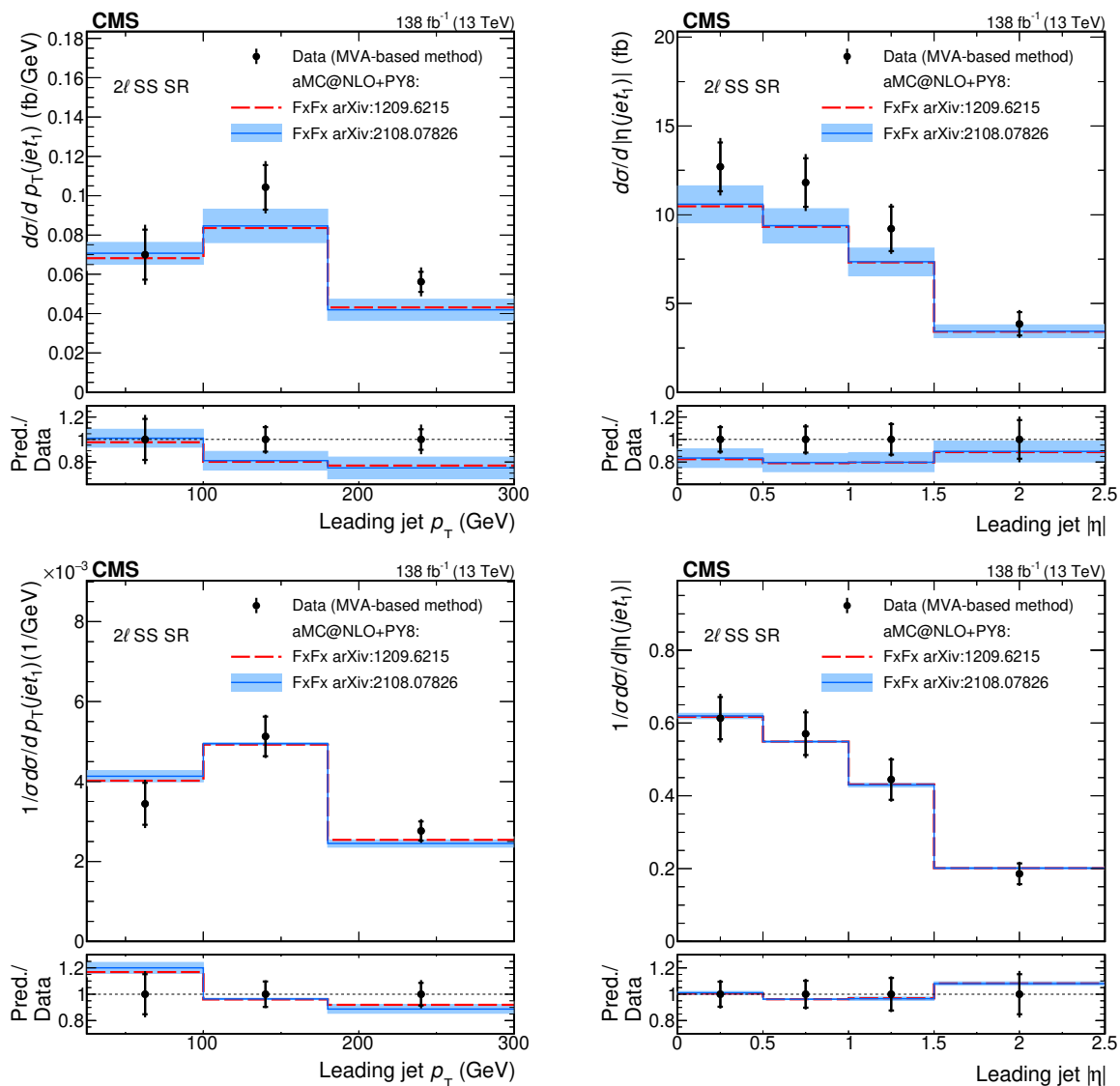


**Figure 11.** Absolute (upper row) and normalized (lower row) differential cross section measured as a function of the leading jet  $p_T$  (left) and leading jet  $|\eta|$  (right), using the MVA-based method. The upper panels show the results of the measurement together with the theoretical predictions. The blue band shows the uncertainty of the prediction from ref. [17]. The lower panels show the ratio between the predictions and the measurement. The vertical lines on the unfolded data points represent the total experimental uncertainty of the unfolded cross section, while the horizontal bars show the statistical component of the uncertainty.

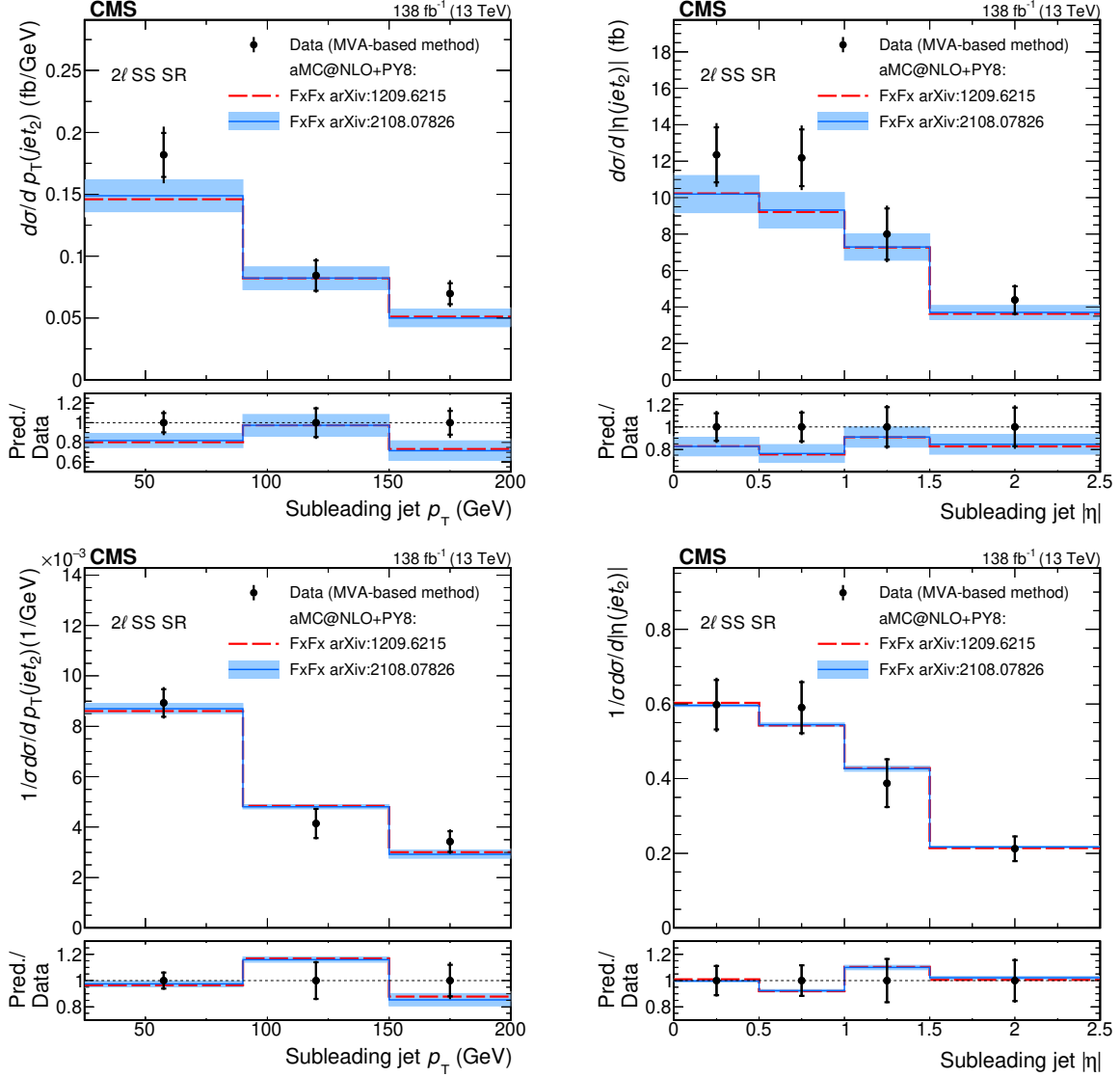


**Figure 12.** Absolute (upper row) and normalized (lower row) differential cross section measured as a function of the subleading jet  $p_T$  (left), and subleading jet  $|\eta|$  (right), using the MVA-based method. The upper panels show the results of the measurement together with the theoretical predictions. The blue band shows the uncertainty of the prediction from ref. [17]. The lower panels show the ratio between the predictions and the measurement. The vertical lines on the unfolded data points represent the total experimental uncertainty of the unfolded cross section, while the horizontal bars show the statistical component of the uncertainty.

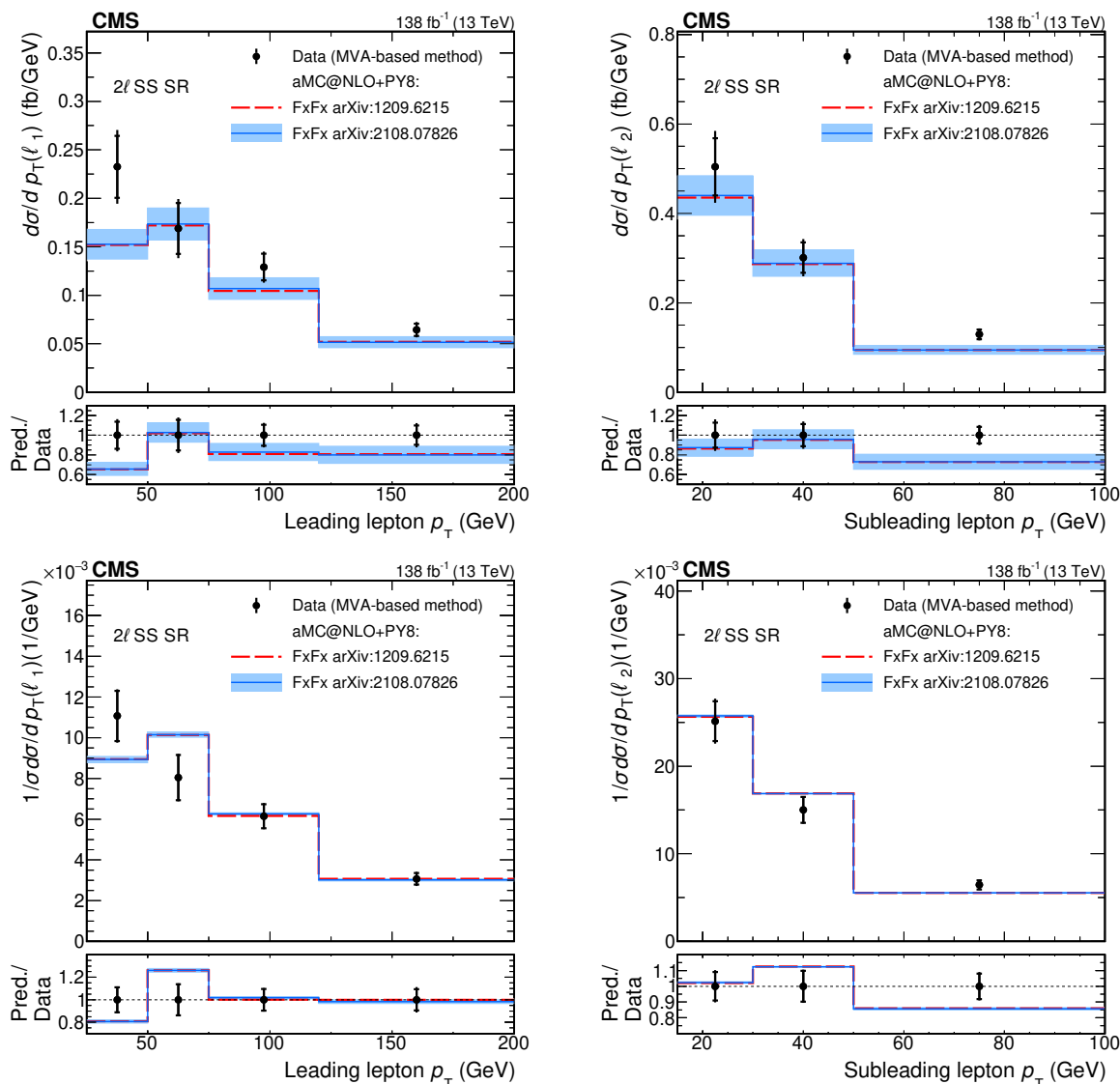


**Figure 13.** Absolute (upper row) and normalized (lower row) differential cross section measured as a function of the leading (left) and subleading (right) lepton  $p_T$ , using the MVA-based method. The upper panels show the results of the measurement together with the theoretical predictions. The blue band shows the uncertainty of the prediction from ref. [17]. The lower panels show the ratio between the predictions and the measurement. The vertical lines on the unfolded data points represent the total experimental uncertainty of the unfolded cross section, while the horizontal bars show the statistical component of the uncertainty.

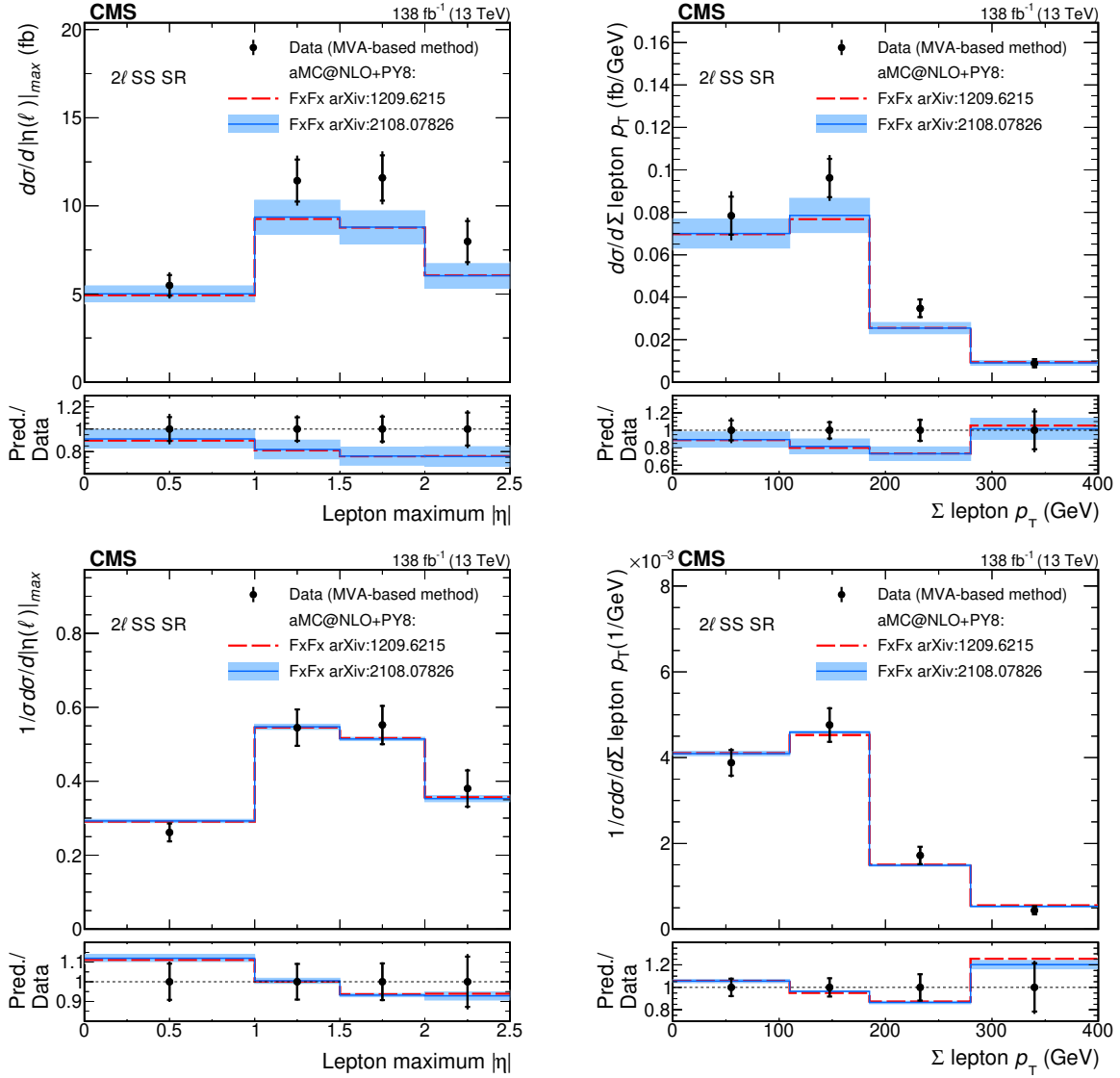


**Figure 14.** Absolute (upper row) and normalized (lower row) differential cross section measured as a function of the maximum  $|\eta|$  of the selected leptons (left) and the sum of their  $p_T$ , using the MVA-based method. The upper panels show the results of the measurement together with the theoretical predictions. The blue band shows the uncertainty of the prediction from ref. [17]. The lower panels show the ratio between the predictions and the measurement. The vertical lines on the unfolded data points represent the total experimental uncertainty of the unfolded cross section, while the horizontal bars show the statistical component of the uncertainty.

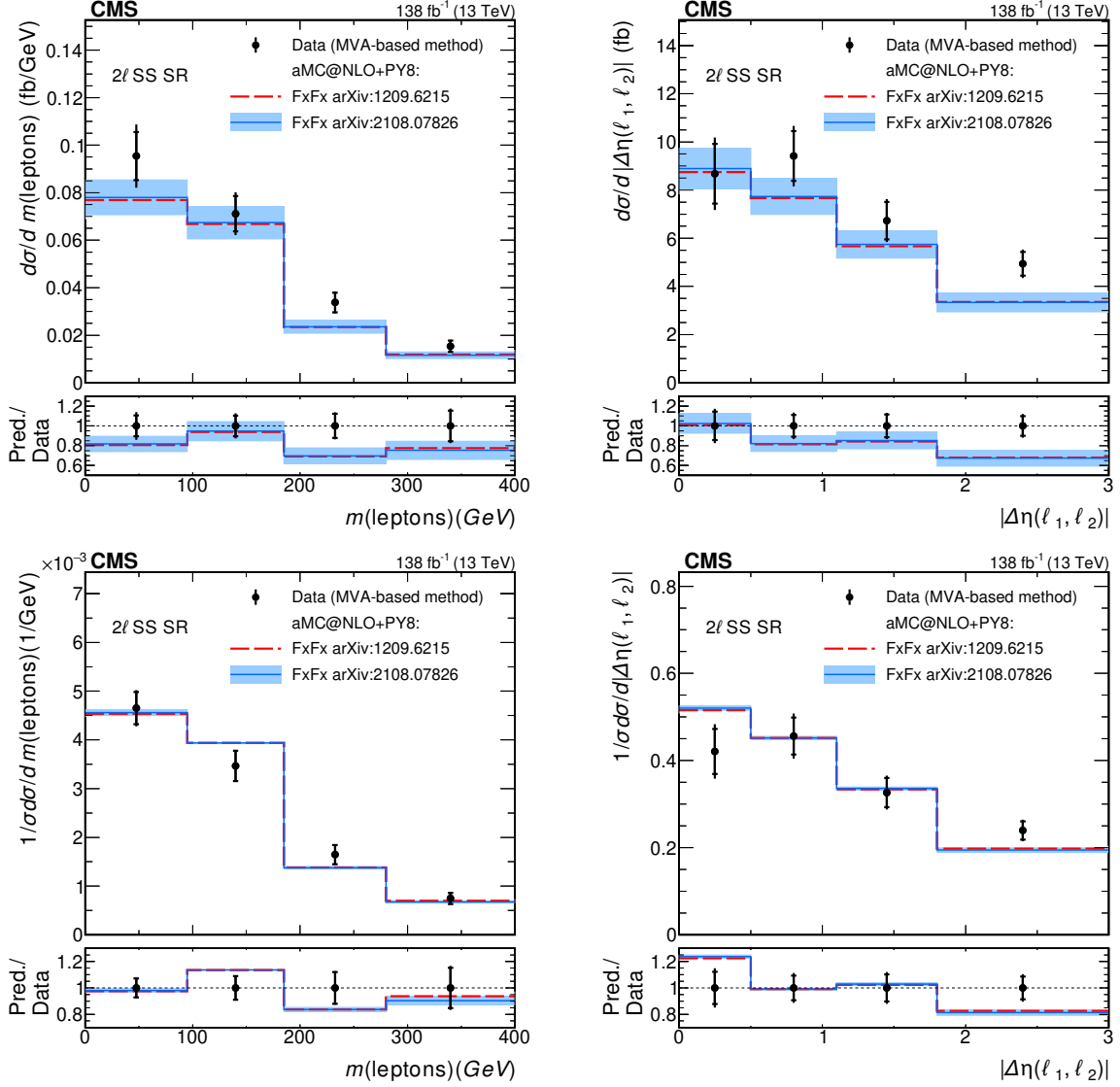


**Figure 15.** Absolute (upper row) and normalized (lower row) differential cross section measured as a function of the invariant mass of the leptons (left) and the  $|\Delta\eta(\ell_1, \ell_2)|$ , using the MVA-based method. The upper panels show the results of the measurement together with the theoretical predictions. The blue band shows the uncertainty of the prediction from ref. [17]. The lower panels show the ratio between the predictions and the measurement. The vertical lines on the unfolded data points represent the total experimental uncertainty of the unfolded cross section, while the horizontal bars show the statistical component of the uncertainty.

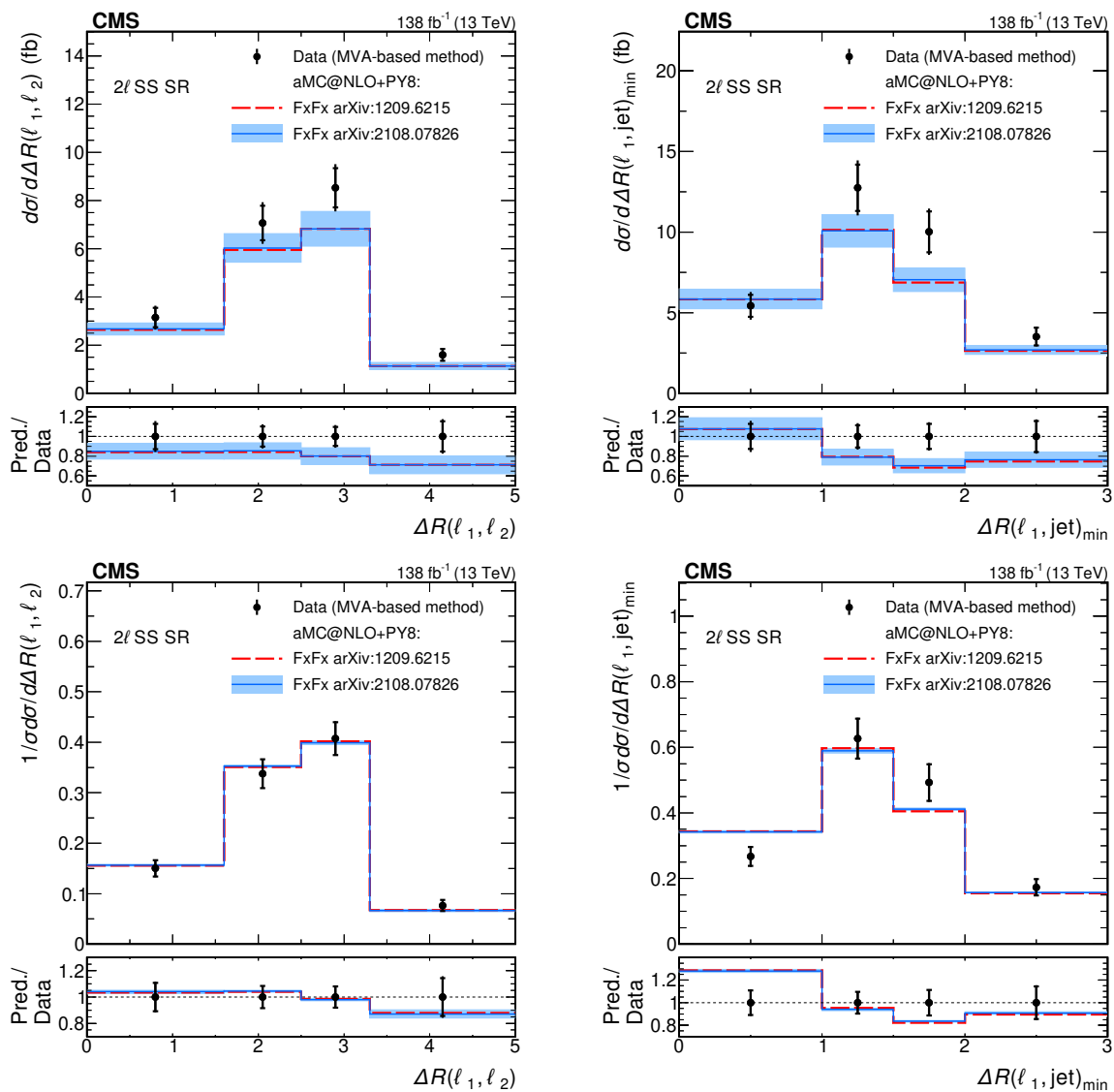


**Figure 16.** Absolute (upper row) and normalized (lower row) differential cross section differential cross section measured as a function of the  $\Delta R(\ell_1, \ell_2)$  and the  $\Delta R(\ell_1, \text{jet})_{\min}$ , using the MVA-based method. The upper panels show the results of the measurement together with the theoretical predictions. The blue band shows the uncertainty of the prediction from ref. [17]. The lower panels show the ratio between the predictions and the measurement. The vertical lines on the unfolded data points represent the total experimental uncertainty of the unfolded cross section, while the horizontal bars show the statistical component of the uncertainty.

Variable	$p$ -value from $\chi^2$ goodness-of-fit			
	Absolute		Normalized	
	MVA-based	Counting	MVA-based	Counting
$ \Delta\eta(\ell_1, \ell_2) $	0.10	0.38	0.24	0.81
$\Delta R(\ell_1, \ell_2)$	0.40	0.60	0.84	0.92
$\Delta R(\ell_1, \text{jet})_{\min}$	0.08	0.08	0.11	0.20
$H_T$	0.05	<0.01	0.05	<0.01
Leading jet $ \eta $	0.40	0.37	0.92	0.32
Leading jet $p_T$	0.24	<0.01	0.49	<0.01
Subleading jet $ \eta $	0.47	0.46	0.91	0.31
Subleading jet $p_T$	0.28	<0.01	0.47	0.01
Leading lepton $p_T$	0.15	0.19	0.31	0.49
Subleading lepton $p_T$	0.11	0.29	0.12	0.89
Lepton maximum $ \eta $	0.35	0.35	0.78	0.46
$\sum$ lepton $p_T$	0.28	0.06	0.39	0.16
$m(\text{leptons})$	0.20	0.19	0.31	0.20
Number of jets	0.18	0.46	0.31	0.64

**Table 3.** The  $p$ -values from the  $\chi^2$  goodness-of-fit tests comparing the absolute (column 1 and 2) and normalized (column 3 and 4) differential cross sections predicted by the new FxFx model [17] with the two measurements in the  $2\ell$ SS region.

distributions is comparable to or higher than the analysis sensitivity. This set-up allows us to study the effect of modifications in multidimensional kinematic distributions of our signal. The results of these studies show that both methods are very robust to such alternate signal models, with the first test showing no bias in both measurement strategies. In the EFT-based injection test, most modified distributions could also be recovered without bias. It is however noted that the counting method is more robust to extreme modifications of more than 100% in the final bin of jet-energy related variables, such as  $H_T$ , but is only biased for models that largely modify the charge asymmetry of  $t\bar{t}W$ . Overall, the counting method is identified as the most resilient and should hence be the preferred result for most BSM interpretations that typically involve large deviations from the SM predictions. As the MVA-based method also shows good robustness and achieves slightly better precision, it is the preferred result only for use-cases where the kinematic distributions of the considered models is close to that of our reference models, such as alternative SM predictions or some BSM scenarios.

### 7.5 Signal extraction in the $3\ell$ region

In the  $3\ell$  region we do not use the event-level MVA as the ML algorithm does not provide a better separability in this region while the signal purity diminishes significantly. Instead, we select events in which the leptons pass the tight selection criteria described in section 4 to

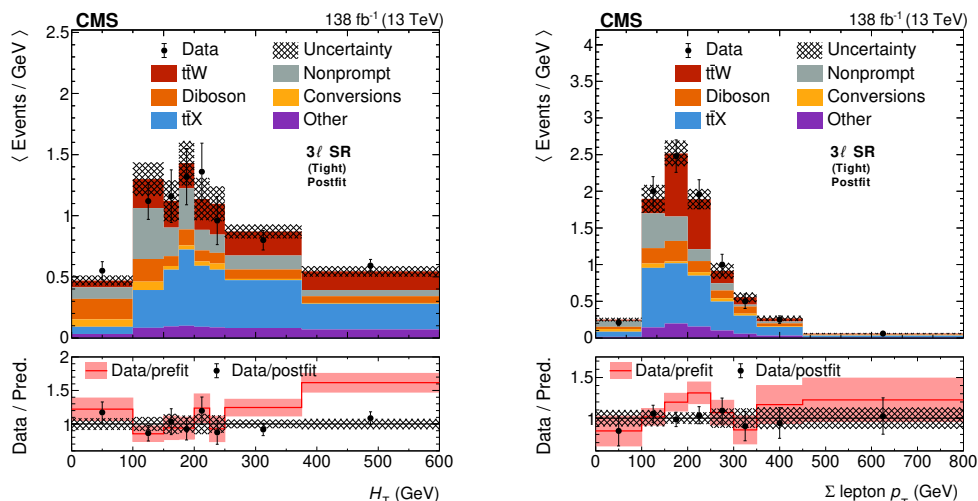


**Figure 17.** Scalar  $p_T$  sum of the jets in the event (left) and scalar  $p_T$  sum of the leptons in the event (right); in the trilepton signal selection for data (points) and predictions (filled histograms) after the fit to the data for the tight lepton selection. The lower panels show the ratio of the data to the sum of the postfit predictions (points) and the ratio of the data to the prefit predictions (red line). The vertical lines on the data points represent the statistical uncertainty in the data and the hatched (filled) band corresponds to the total uncertainty in the postfit (prefit) prediction. Events that exceeded the range of the plot are included in the last bin. The bin contents are divided by bin width.

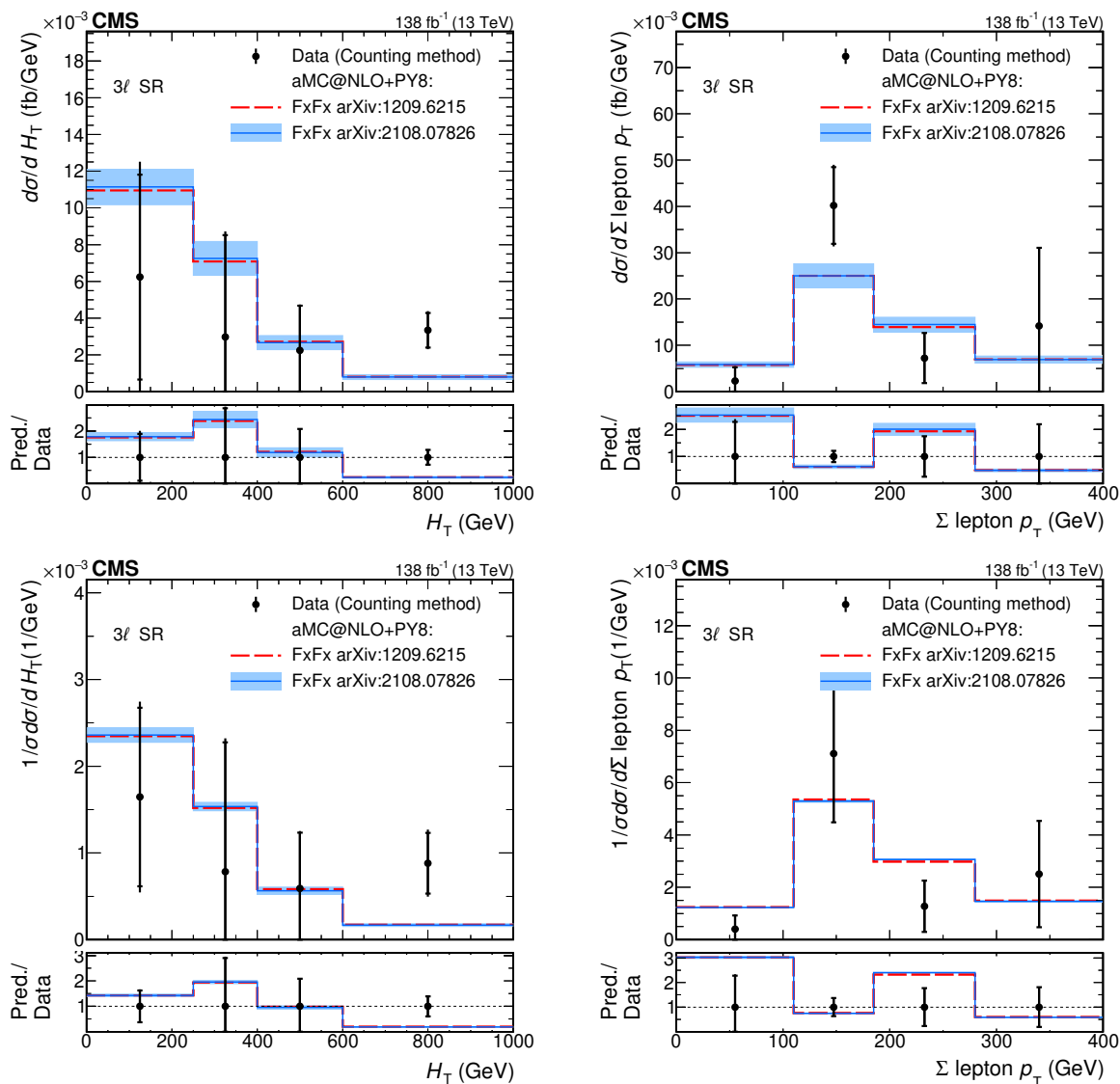
ensure a high-purity selection while relying less on the discrimination between signal and background based on event-level kinematic variables. The  $H_T$  and  $\sum$  lepton  $p_T$  distributions in the  $3\ell$  region are shown in figure 17. To further increase the analysis sensitivity, we categorize events at reconstruction level in four categories according to the flavor of the leptons. To constrain some of the background processes, the number of observed events in the three- and four-lepton CRs are included in the fit as a function of the same variables as in the  $2\ell$ SS region fitting strategy. The VR NP is not included in the fit to guarantee the nonprompt background will not be calibrated in the measurement phase space. The ChargeMisId VR is also not included as the charge-misidentification background is not relevant in the  $3\ell$  region.

Figure 18 shows the absolute and normalized differential cross section measured in the  $3\ell$  SR as a function of  $H_T$  and  $\sum$  lepton  $p_T$ . These two variables were selected as the information contained by the two variables is different from that in the  $2\ell$ SS SR, as  $H_T$  in the  $3\ell$  SR does not contain the two jets in the hadronically decaying W boson present in the  $2\ell$ SS. The  $\sum$  lepton  $p_T$  variable in this region includes three leptons, in contrast to the two that are considered in the  $2\ell$ SS SR.

## 8 Measurement of the charge asymmetry

We measure the leptonic charge asymmetry,  $A_c^\ell$ , in signal events using events with three leptons. The asymmetry  $A_c^\ell$  is defined as

$$A_c^\ell = \frac{N(\Delta y^\ell > 0) - N(\Delta y^\ell < 0)}{N(\Delta y^\ell > 0) + N(\Delta y^\ell < 0)}. \quad (8.1)$$



**Figure 18.** Absolute (upper row) and normalized (lower row) differential cross section measured as a function of the  $H_T$  (left) and the scalar sum of the lepton  $p_T$ 's, using the counting method in the  $3\ell$  SR. The upper panels show the results of the measurement together with the theoretical predictions. The blue band shows the uncertainty of the prediction from ref. [17]. The lower panels show the ratio between the predictions and the measurement. The vertical lines on the unfolded data points represent the total experimental uncertainty of the unfolded cross section, while the horizontal bars show the statistical component of the uncertainty.

$\Delta y^\ell$  denotes  $|y_{\ell^+}| - |y_{\ell^-}|$ , where  $y_{\ell^+}$  ( $y_{\ell^-}$ ) are the rapidity of the lepton produced in the top quark (antiquark) decays. This quantity is only well-defined in the  $3\ell$  region, since for signal events in this region, both top quarks must have produced leptons in their decay.

To reconstruct  $\Delta y^\ell$  we must determine the two leptons that have been produced in the top quark decays out of the three in the event. In a three-lepton  $t\bar{t}W^+$  ( $t\bar{t}W^-$ ) event, there are two leptons with positive (negative) charge and a third one with negative (positive) charge. Since the two top quarks have the opposite electric charge, the negatively (positively) charged lepton must come from a top antiquark (quark) decay. To determine which one of the remaining two is produced in the other top quark decay and which one in the spectator W boson decay, we employ a neural network that assigns to each lepton the probability of belonging to each of the categories. The neural network is trained using PYTORCH [78] considering a sample of positive (negative) leptons from  $t\bar{t}W^+$  ( $t\bar{t}W^-$ ) production, passing the selection of the fiducial region, described in section 7. We define as signal those leptons produced in a top quark decay and as background those produced in the W boson decay. The network, which yields as output a per-lepton quantity, takes as an input a set of variables associated to the given lepton. In addition to the lepton, we consider two jets that are proxies to the b jets produced in the top quark decays, which correspond to the b-tagged jets with the highest  $p_T$ . In case there is only one b-tagged jet in the event, we consider that one and the jet closest in  $\Delta R$  to the lepton. The input variables to the discriminator are

- the lepton  $p_T$ ,  $\eta$ , and  $\phi$ ;
- the invariant mass of the system formed by the lepton and each of the two proxy jets, and
- the  $\Delta R$  distance between the lepton and each of the two proxy jets.

Out of the two SS leptons, we take the one with the largest neural network score. This selection gives the correct pairing in 71% of the cases. We then compute  $\Delta y_{\text{reco}}^\ell$  using the selected lepton and the one with the opposite sign.

In order to measure  $A_c^\ell$ , we consider events in the  $3\ell$  region, with the exception that we replace the requirement that events have two loose b-tagged jets with a requirement of at least one medium b-tagged jet is present in the event. In addition, we require events with an opposite-sign same-flavor lepton pair, less than 4 jets, and less than 2 b-tagged jets to pass a selection of  $p_T^{\text{miss}} > 50$  GeV to reject DY+jets events with nonprompt leptons and photon conversions from  $Z\gamma$  events. Events are then classified based on their kinematic properties with the twofold goal of building regions pure in  $t\bar{t}W$  signal and separating events with  $\Delta y^\ell > 0$  and  $\Delta y^\ell < 0$ . A set of 8 categories is built based on the presence of a pair of opposite-sign same-flavor lepton pair in the event, the jet and b-tagged jet multiplicities, and the invariant mass of the opposite-sign same-flavor lepton pair closest to the Z boson mass. The sequential categorization is shown in figure 19. In addition, we classify events in four bins of  $\Delta y_{\text{reco}}^\ell$  with edges  $(-\infty, -0.5, 0, 0.5, \infty)$ , resulting in a total of 32 analysis bins.

To measure  $A_c^\ell$ , we use a likelihood model similar to the one shown in eq. (7.1), in which the parameters of interest are  $A_c^\ell$  and the signal normalization. The expected signal yield dependence on  $A_c^\ell$  is introduced by means of the MC simulation templates with  $\Delta y^\ell > 0$

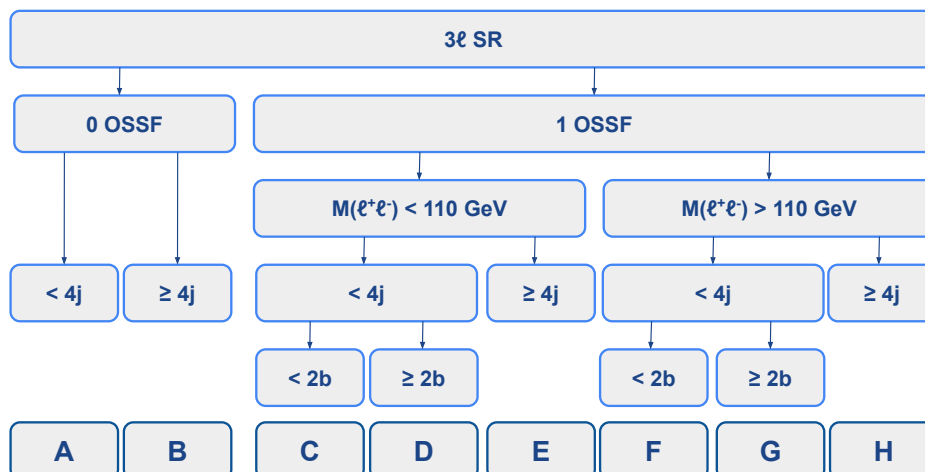


**Figure 19.** Categorization of three-lepton events for the measurement of the leptonic charge asymmetry.

and  $\Delta y^\ell < 0$ . Figure 20 (left) shows the observed number of events in each of these bins, together with the signal and background prediction obtained setting all fit parameters to the values that maximize the likelihood. Figure 20 (right) shows the likelihood as a function of  $A_c^\ell$ , profiling over the systematic uncertainties and the signal normalization. This procedure results in an observed (expected) value of  $A_c^\ell = -0.19_{-0.06}^{+0.05}$  (syst)  $_{-0.16}^{+0.14}$  (stat) ( $-0.09_{-0.05}^{+0.04}$  (syst)  $_{-0.11}^{+0.11}$  (stat)), consistent with the theoretical expectations from next-to-leading order simulations of  $-0.085 \pm 0.006$ , and achieving a better sensitivity than the previous measurement by ATLAS [22]. Additionally, we performed a goodness-of-fit test using the saturated model, obtaining a  $p$ -value of 0.83, showing no indication of significant tensions between data and the fitted model.

## 9 Summary

Measurements of properties of top quark-antiquark pair production in association with a W boson ( $t\bar{t}W$ ) in proton-proton collisions at a center-of-mass energy of 13 TeV are performed using a data sample corresponding to an integrated luminosity of  $138 \text{ fb}^{-1}$ , recorded by the CMS experiment. Events with either two leptons with the same electric charge or three leptons, and multiple jets and b-tagged jets are used. The differential cross sections as a function of kinematic variables sensitive to the modeling of the  $t\bar{t}W$  process are measured, using a multivariate discriminator for events in the two-lepton region and a counting method for events in the three-lepton region. Overall, the normalized differential cross section measurements are generally consistent with the standard model expectations, while the absolute cross sections are above the theoretical predictions by approximately one standard deviation, consistent with previous inclusive cross section measurements. In addition to the differential cross sections, the leptonic charge asymmetry of this process is measured to be  $A_c^\ell = -0.19_{-0.18}^{+0.16}$ , consistent with the expectation of  $-0.085 \pm 0.006$  predicted by next-to-leading order simulations.

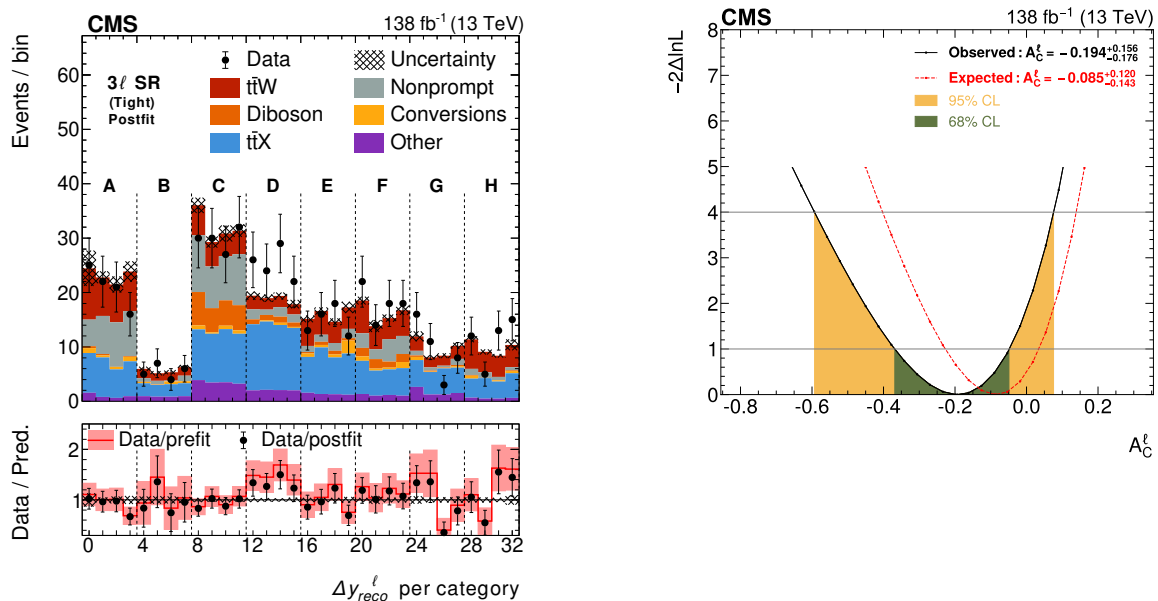


**Figure 20.** Left: Observed yields in the 32 bins used in the analysis for data (points) and predictions (filled histograms) after the fit to the data for the tight lepton selection. The lower panels show the ratio of the data to the sum of the postfit predictions (points) and the ratio of the data to the prefit predictions (red line). The vertical lines on the data points represent the statistical uncertainty in the data and the hatched (filled) band corresponds to the total uncertainty in the postfit (prefit) prediction. Right: the observed (black) and expected (red) likelihood scan as a function of  $A_C^\ell$ . The shaded areas correspond to the 68 and 95% confidence level intervals around the best-fit value, respectively.

### Acknowledgments

We congratulate our colleagues in the CERN accelerator departments for the excellent performance of the LHC and thank the technical and administrative staffs at CERN and at other CMS institutes for their contributions to the success of the CMS effort. In addition, we gratefully acknowledge the computing centers and personnel of the Worldwide LHC Computing Grid and other centers for delivering so effectively the computing infrastructure essential to our analyses. Finally, we acknowledge the enduring support for the construction and operation of the LHC, the CMS detector, and the supporting computing infrastructure provided by the following funding agencies: SC (Armenia), BMBWF and FWF (Austria); FNRS and FWO (Belgium); CNPq, CAPES, FAPERJ, FAPERGS, and FAPESP (Brazil); MES and BNSF (Bulgaria); CERN; CAS, MoST, and NSFC (China); Minciencias (Colombia); MSES and CSF (Croatia); RIF (Cyprus); SENESCYT (Ecuador); ERC PRG, TARISTU24-TK10 and MoER TK202 (Estonia); Academy of Finland, MEC, and HIP (Finland); CEA and CNRS/IN2P3 (France); SRNSF (Georgia); BMFTR, DFG, and HGF (Germany); GSRI (Greece); NKFIH (Hungary); DAE and DST (India); IPM (Iran); SFI (Ireland); INFN (Italy); MSIT and NRF (Republic of Korea); MES (Latvia); LMTLT (Lithuania); MOE and UM (Malaysia); BUAP, CINVESTAV, CONACYT, LNS, SEP, and UASLP-FAI (Mexico); MOS (Montenegro); MBIE (New Zealand); PAEC (Pakistan); MES, NSC, and NAWA (Poland); FCT (Portugal); MESTD (Serbia); MICIU/AEI and PCTI

(Spain); MOSTR (Sri Lanka); Swiss Funding Agencies (Switzerland); MST (Taipei); MHESI and NSTDA (Thailand); TUBITAK and TENMAK (Türkiye); NASU (Ukraine); STFC (United Kingdom); DOE and NSF (U.S.A.).

Individuals have received support from the Marie-Curie program and the European Research Council and Horizon 2020 Grant, contract Nos. 675440, 724704, 752730, 758316, 765710, 824093, 101115353, 101002207, 101001205, and COST Action CA16108 (European Union); the Leventis Foundation; the Alfred P. Sloan Foundation; the Alexander von Humboldt Foundation; the Science Committee, project no. 22rl-037 (Armenia); the Fonds pour la Formation à la Recherche dans l'Industrie et dans l'Agriculture (FRIA-Belgium); the Beijing Municipal Science & Technology Commission, No. Z191100007219010, the Fundamental Research Funds for the Central Universities, the Ministry of Science and Technology of China under Grant No. 2023YFA1605804, and the Natural Science Foundation of China under Grant No. 12061141002 (China); the Ministry of Education, Youth and Sports (MEYS) of the Czech Republic; the Shota Rustaveli National Science Foundation, grant FR-22-985 (Georgia); the Deutsche Forschungsgemeinschaft (DFG), among others, under Germany's Excellence Strategy – EXC 2121 “Quantum Universe” – 390833306, and under project number 400140256 – GRK2497; the Hellenic Foundation for Research and Innovation (HFRI), Project Number 2288 (Greece); the Hungarian Academy of Sciences, the New National Excellence Program – ÚNKP, the NKFIH research grants K 131991, K 133046, K 138136, K 143460, K 143477, K 146913, K 146914, K 147048, 2020-2.2.1-ED-2021-00181, TKP2021-NKTA-64, and 2021-4.1.2-NEMZ\_KI-2024-00036 (Hungary); the Council of Science and Industrial Research, India; ICSC – National Research Center for High Performance Computing, Big Data and Quantum Computing, FAIR – Future Artificial Intelligence Research, and CUP I53D23001070006 (Mission 4 Component 1), funded by the NextGenerationEU program (Italy); the Latvian Council of Science; the Ministry of Education and Science, project no. 2022/WK/14, and the National Science Center, contracts Opus 2021/41/B/ST2/01369, 2021/43/B/ST2/01552, 2023/49/B/ST2/03273, and the NAWA contract BPN/PPO/2021/1/00011 (Poland); the Fundação para a Ciência e a Tecnologia, grant CEECIND/01334/2018 (Portugal); the National Priorities Research Program by Qatar National Research Fund; MICIU/AEI/10.13039/501100011033, ERDF/EU, “European Union NextGenerationEU/PRTR”, and Programa Severo Ochoa del Principado de Asturias (Spain); the Chulalongkorn Academic into Its 2nd Century Project Advancement Project, and the National Science, Research and Innovation Fund via the Program Management Unit for Human Resources & Institutional Development, Research and Innovation, grant B39G680009 (Thailand); the Kavli Foundation; the Nvidia Corporation; the SuperMicro Corporation; the Welch Foundation, contract C-1845; and the Weston Havens Foundation (U.S.A.).

## A Results in the $2\ell$ SS region using the counting method

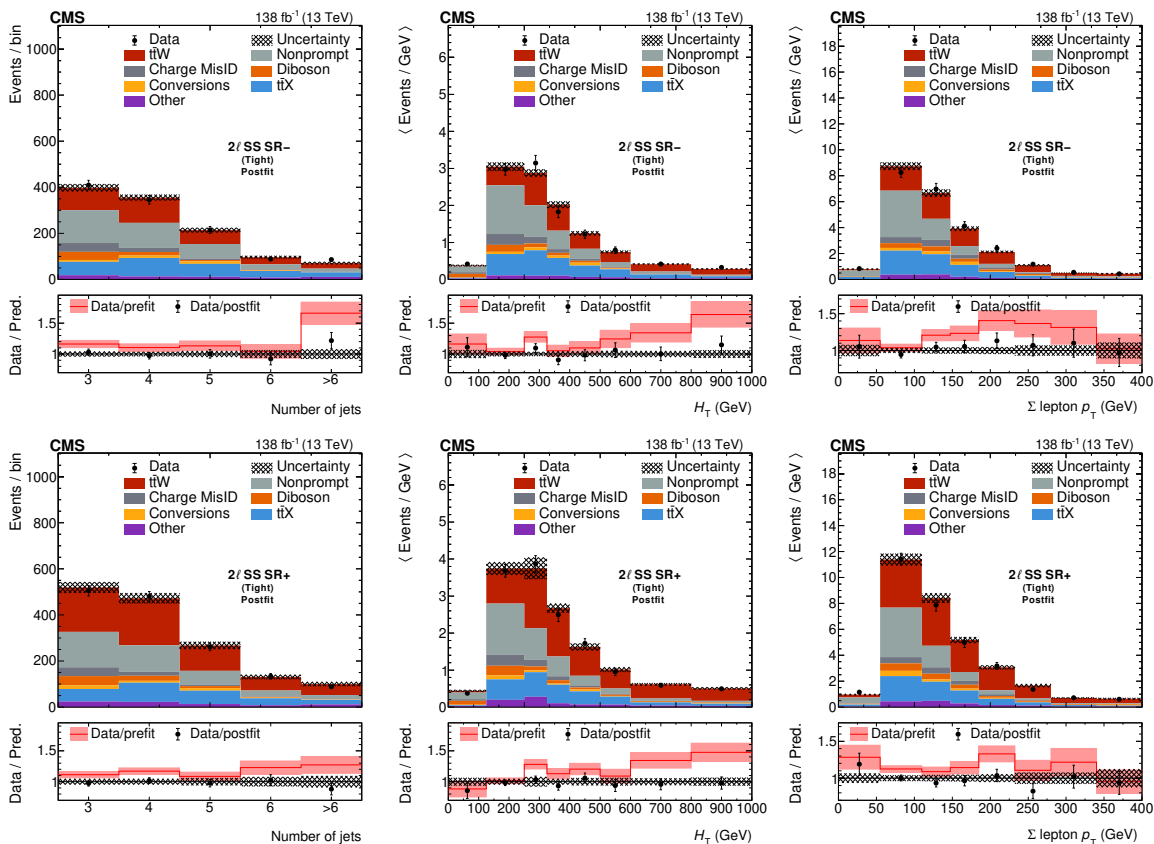


**Figure 21.** Distributions of some variables of interest in the two-lepton signal selection for data (points) and predictions (filled histograms) after the fit to the data for the tight lepton selection. Left: number of selected jets in the event (negative, positive signed leptons SR). Middle: scalar  $p_T$  sum of selected jets in the event (negative, positive signed leptons SR). Right: scalar  $p_T$  sum of the leptons in the event (negative, positive signed leptons SR). The lower panels show the ratio of the data to the sum of the postfit predictions (points) and the ratio of the data to the prefit predictions (red line). The vertical lines on the data points represent the statistical uncertainty in the data and the hatched (filled) band corresponds to the total uncertainty in the postfit (prefit) prediction. Events that exceed the range of the plot are included in the last bin. The bin contents of the middle and right side plots are divided by the width of the bin.

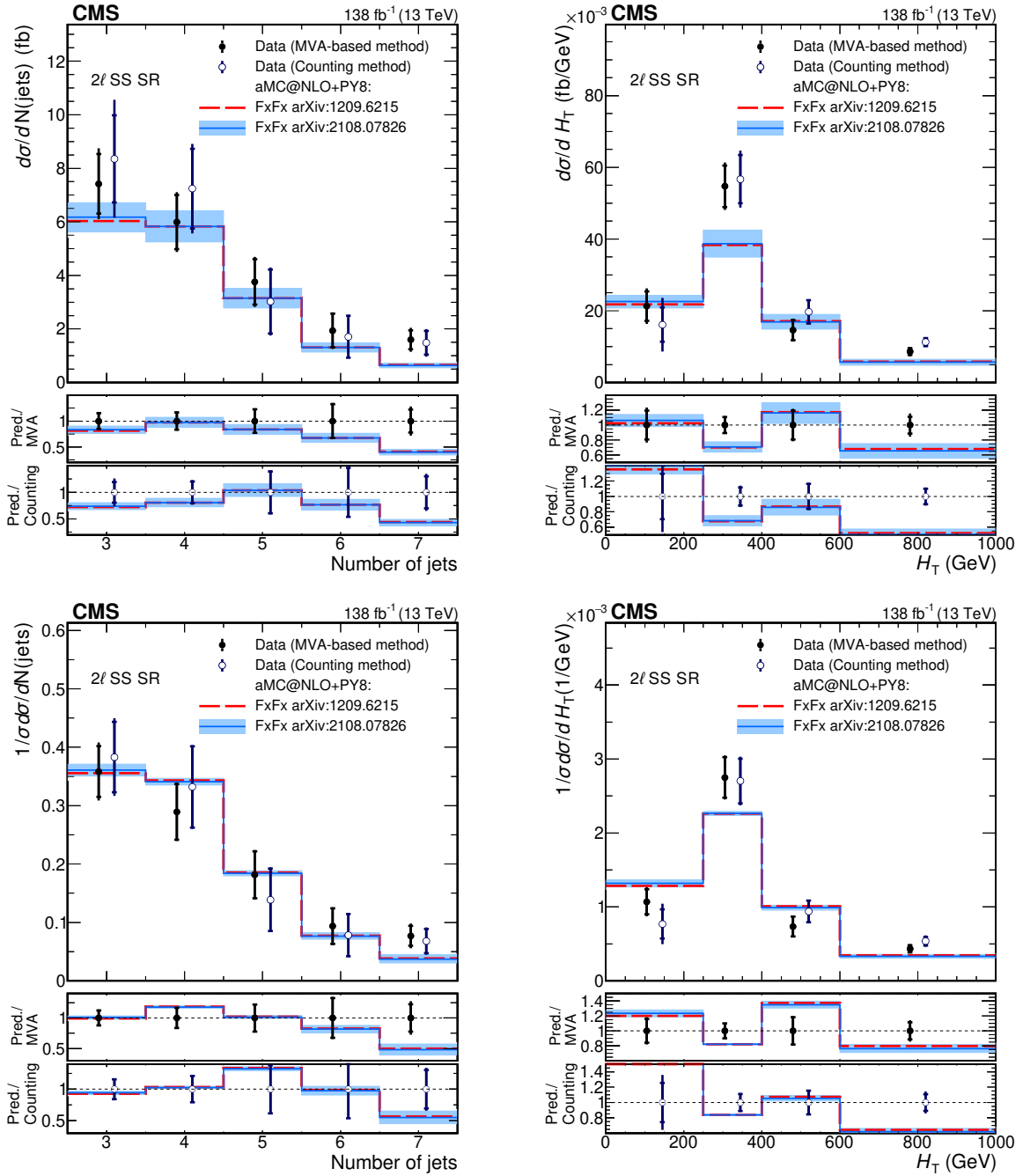


**Figure 22.** Absolute (upper row) and normalized (lower row) differential cross section measured as a function of the jet multiplicity (left) and  $H_T$  (right), using the MVA-based and the counting method. The upper panels show the results of the two measurements together with the theoretical predictions. The blue band shows the uncertainty of the prediction from ref. [17]. Each two lower panels shows the ratio between the predictions and each of the measurements. The vertical lines on the unfolded data points represent the total experimental uncertainty of the unfolded cross section, while the horizontal bars show the statistical component of the uncertainty.

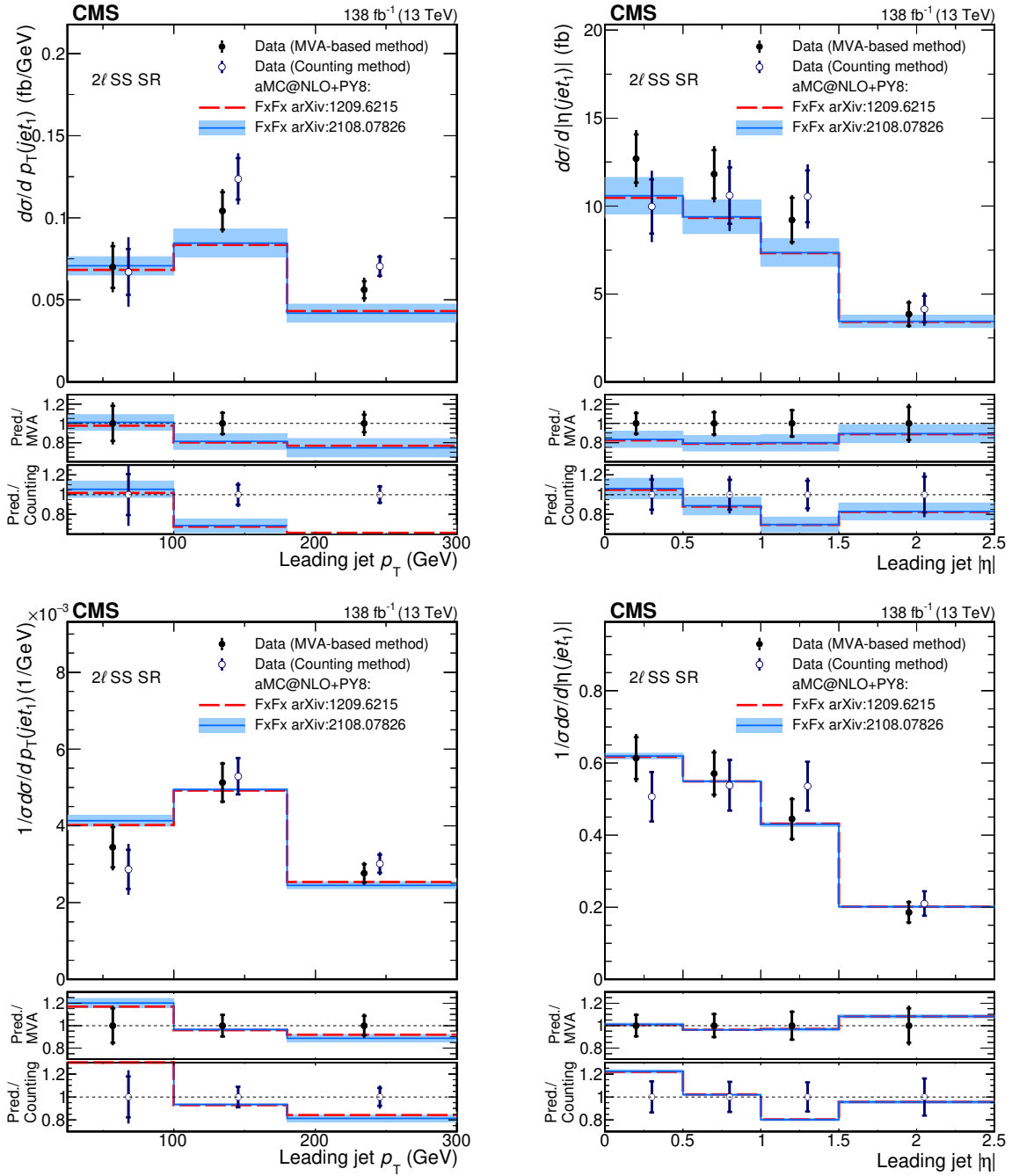


**Figure 23.** Absolute (upper row) and normalized (lower row) differential cross section measured as a function of the leading jet  $p_T$  (left) and leading jet  $|\eta|$  (right), using the MVA-based and the counting method. The upper panels show the results of the two measurements together with the theoretical predictions. The blue band shows the uncertainty of the prediction from ref. [17]. Each two lower panels shows the ratio between the predictions and each of the measurements. The vertical lines on the unfolded data points represent the total experimental uncertainty of the unfolded cross section, while the horizontal bars show the statistical component of the uncertainty.

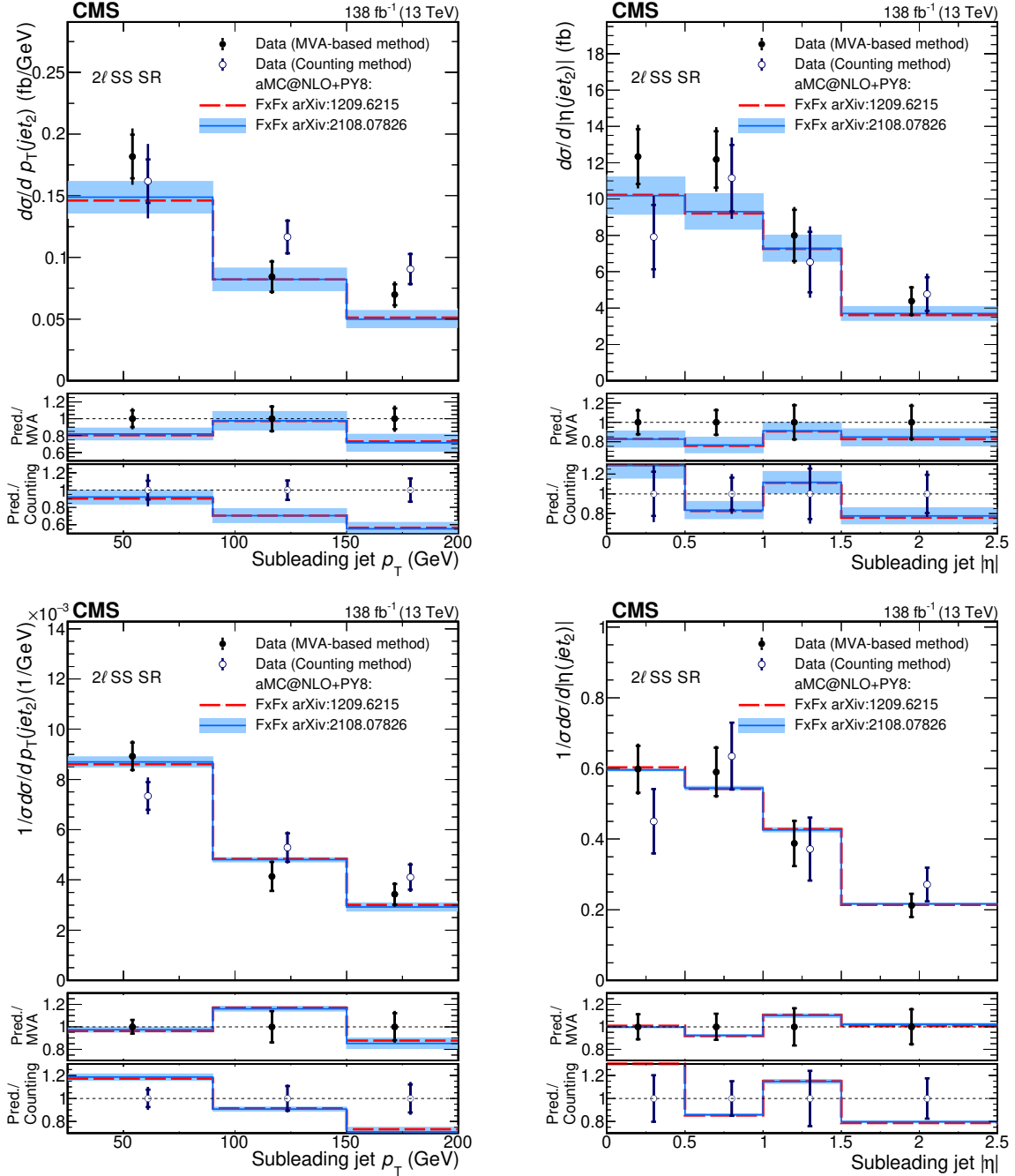


**Figure 24.** Absolute (upper row) and normalized (lower row) differential cross section measured as a function of the subleading jet  $p_T$  (left), and subleading jet  $|\eta|$  (right), using the MVA-based and the counting method. The upper panels show the results of the two measurements together with the theoretical predictions. The blue band shows the uncertainty of the prediction from ref. [17]. Each two lower panels shows the ratio between the predictions and each of the measurements. The vertical lines on the unfolded data points represent the total experimental uncertainty of the unfolded cross section, while the horizontal bars show the statistical component of the uncertainty.

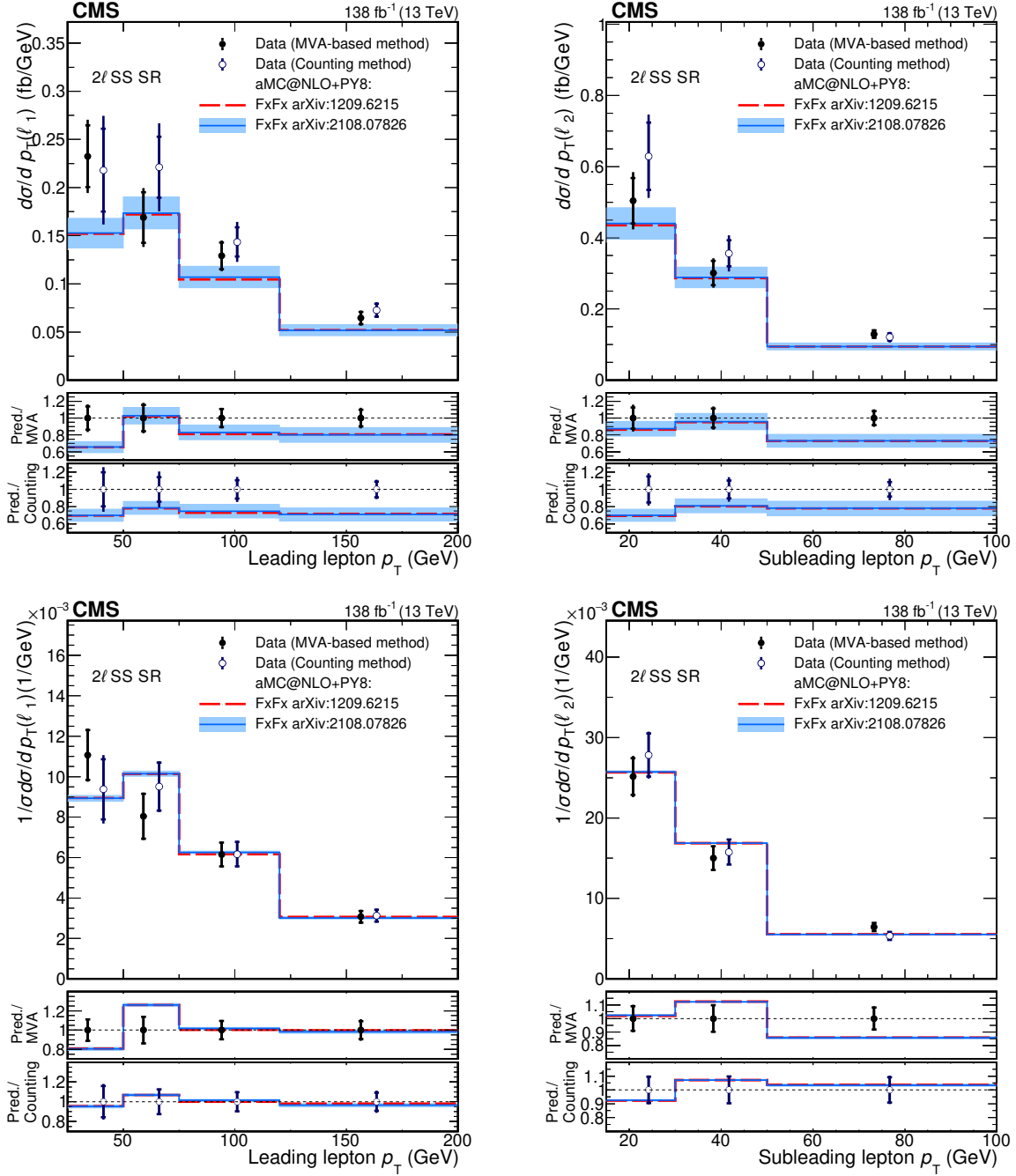


**Figure 25.** Absolute (upper row) and normalized (lower row) differential cross section measured as a function of the leading (left) and subleading (right) lepton  $p_T$ , using the MVA-based and the counting method. The upper panels show the results of the two measurements together with the theoretical predictions. The blue band shows the uncertainty of the prediction from ref. [17]. Each two lower panels shows the ratio between the predictions and each of the measurements. The vertical lines on the unfolded data points represent the total experimental uncertainty of the unfolded cross section, while the horizontal bars show the statistical component of the uncertainty.

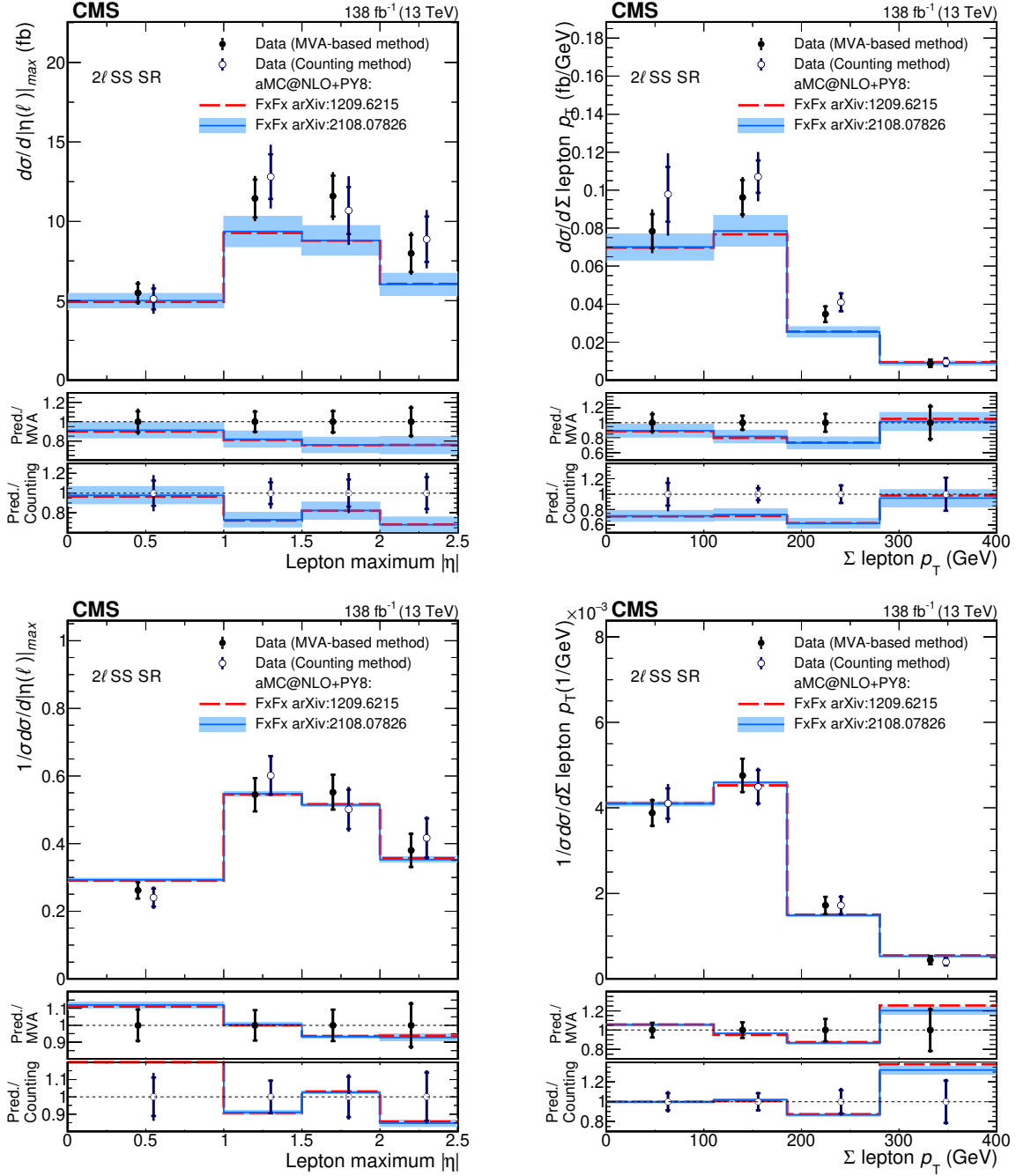


**Figure 26.** Absolute (upper row) and normalized (lower row) differential cross section measured as a function of the maximum  $|\eta|$  of the selected leptons (left) and the sum of their  $p_T$ , using the MVA-based and the counting method. The upper panels show the results of the two measurements together with the theoretical predictions. The blue band shows the uncertainty of the prediction from ref. [17]. Each two lower panels shows the ratio between the predictions and each of the measurements. The vertical lines on the unfolded data points represent the total experimental uncertainty of the unfolded cross section, while the horizontal bars show the statistical component of the uncertainty.

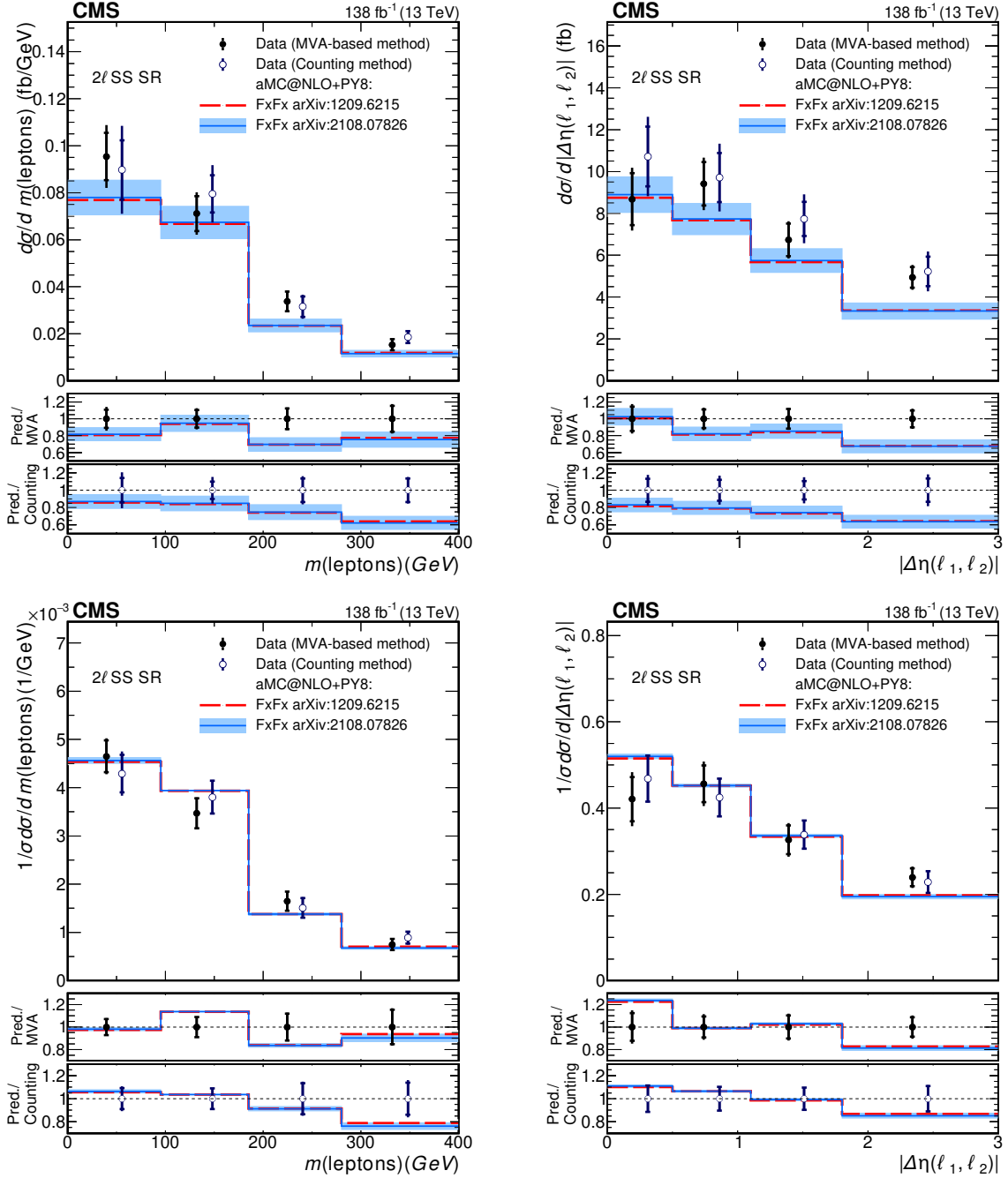


**Figure 27.** Absolute (upper row) and normalized (lower row) differential cross section measured as a function of the invariant mass of the leptons (left) and the  $|\Delta\eta(\ell_1, \ell_2)|$ , using the MVA-based and the counting method. The upper panels show the results of the two measurements together with the theoretical predictions. The blue band shows the uncertainty of the prediction from ref. [17]. Each two lower panels shows the ratio between the predictions and each of the measurements. The vertical lines on the unfolded data points represent the total experimental uncertainty of the unfolded cross section, while the horizontal bars show the statistical component of the uncertainty.

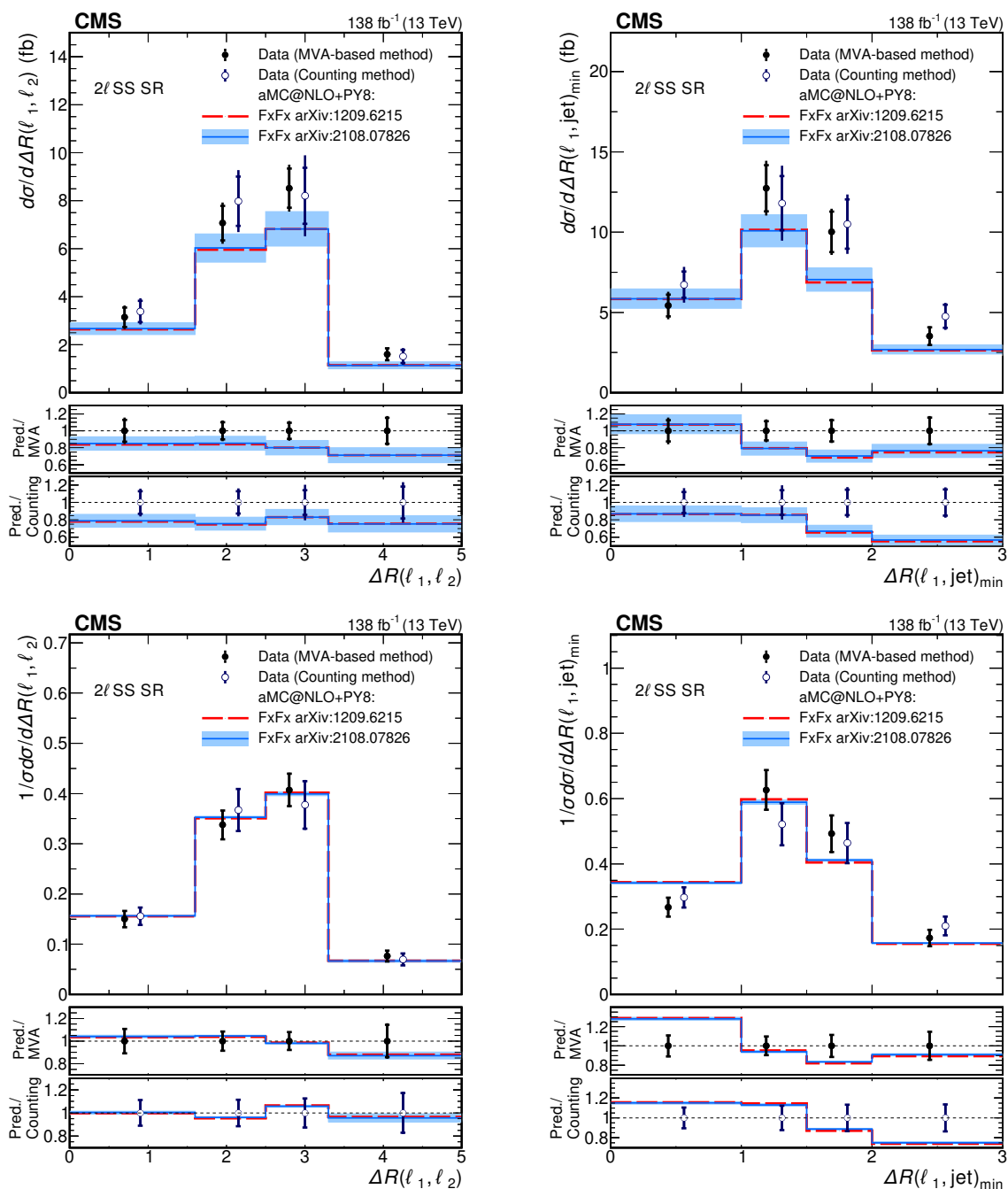


**Figure 28.** Absolute (upper row) and normalized (lower row) differential cross section measured as a function of the  $\Delta R(\ell_1, \ell_2)$  and the  $\Delta R(\ell_1, jet)_{\min}$ , using the MVA-based and the counting method. The upper panels show the results of the two measurements together with the theoretical predictions. The blue band shows the uncertainty of the prediction from ref. [17]. Each two lower panels shows the ratio between the predictions and each of the measurements. The vertical lines on the unfolded data points represent the total experimental uncertainty of the unfolded cross section, while the horizontal bars show the statistical component of the uncertainty.

**Data Availability Statement.** Release and preservation of data used by the CMS Collaboration as the basis for publications is guided by the [CMS data preservation, re-use, and open access policy](#).

**Code Availability Statement.** The CMS core software is publicly available on [GitHub](#).

**Open Access.** This article is distributed under the terms of the Creative Commons Attribution License ([CC-BY4.0](#)), which permits any use, distribution and reproduction in any medium, provided the original author(s) and source are credited.

## References

- [1] LHC HIGGS CROSS SECTION WORKING GROUP collaboration, *Handbook of LHC Higgs Cross Sections: 4. Deciphering the Nature of the Higgs Sector*, *CERN Yellow Rep. Monogr.* **2** (2017) 1 [[arXiv:1610.07922](#)] [[INSPIRE](#)].
- [2] L. Buonocore et al., *Precise Predictions for the Associated Production of a W Boson with a Top-Antitop Quark Pair at the LHC*, *Phys. Rev. Lett.* **131** (2023) 231901 [[arXiv:2306.16311](#)] [[INSPIRE](#)].
- [3] J.A. Dror, M. Farina, E. Salvioni and J. Serra, *Strong  $tW$  Scattering at the LHC*, *JHEP* **01** (2016) 071 [[arXiv:1511.03674](#)] [[INSPIRE](#)].
- [4] R. Frederix, D. Pagani and M. Zaro, *Large NLO corrections in  $t\bar{t}W^\pm$  and  $t\bar{t}t\bar{t}$  hadroproduction from supposedly subleading EW contributions*, *JHEP* **02** (2018) 031 [[arXiv:1711.02116](#)] [[INSPIRE](#)].
- [5] J.H. Kühn and G. Rodrigo, *Charge asymmetry in hadroproduction of heavy quarks*, *Phys. Rev. Lett.* **81** (1998) 49 [[hep-ph/9802268](#)] [[INSPIRE](#)].
- [6] J.H. Kühn and G. Rodrigo, *Charge asymmetry of heavy quarks at hadron colliders*, *Phys. Rev. D* **59** (1999) 054017 [[hep-ph/9807420](#)] [[INSPIRE](#)].
- [7] F. Maltoni, M.L. Mangano, I. Tsinikos and M. Zaro, *Top-quark charge asymmetry and polarization in  $t\bar{t}W^\pm$  production at the LHC*, *Phys. Lett. B* **736** (2014) 252 [[arXiv:1406.3262](#)] [[INSPIRE](#)].
- [8] CMS collaboration, *Search for physics beyond the standard model in top quark production with additional leptons in the context of effective field theory*, *JHEP* **12** (2023) 068 [[arXiv:2307.15761](#)] [[INSPIRE](#)].
- [9] CMS collaboration, *Observation of four top quark production in proton-proton collisions at  $\sqrt{s} = 13$  TeV*, *Phys. Lett. B* **847** (2023) 138290 [[arXiv:2305.13439](#)] [[INSPIRE](#)].
- [10] ATLAS collaboration, *Observation of four-top-quark production in the multilepton final state with the ATLAS detector*, *Eur. Phys. J. C* **83** (2023) 496 [*Erratum* *ibid.* **84** (2024) 156] [[arXiv:2303.15061](#)] [[INSPIRE](#)].
- [11] CMS collaboration, *Measurement of the Higgs boson production rate in association with top quarks in final states with electrons, muons, and hadronically decaying tau leptons at  $\sqrt{s} = 13$  TeV*, *Eur. Phys. J. C* **81** (2021) 378 [[arXiv:2011.03652](#)] [[INSPIRE](#)].
- [12] A. Kulesza et al., *Associated production of a top quark pair with a heavy electroweak gauge boson at NLO+NNLL accuracy*, *Eur. Phys. J. C* **79** (2019) 249 [[arXiv:1812.08622](#)] [[INSPIRE](#)].

- [13] A. Broggio et al., *Top-quark pair hadroproduction in association with a heavy boson at NLO+NNLL including EW corrections*, *JHEP* **08** (2019) 039 [[arXiv:1907.04343](#)] [[INSPIRE](#)].
- [14] A. Kulesza et al., *Associated top quark pair production with a heavy boson: differential cross sections at NLO+NNLL accuracy*, *Eur. Phys. J. C* **80** (2020) 428 [[arXiv:2001.03031](#)] [[INSPIRE](#)].
- [15] G. Bevilacqua et al., *The simplest of them all:  $t\bar{t}W^\pm$  at NLO accuracy in QCD*, *JHEP* **08** (2020) 043 [[arXiv:2005.09427](#)] [[INSPIRE](#)].
- [16] G. Bevilacqua et al., *NLO QCD corrections to off-shell  $t\bar{t}W^\pm$  production at the LHC: correlations and asymmetries*, *Eur. Phys. J. C* **81** (2021) 675 [[arXiv:2012.01363](#)] [[INSPIRE](#)].
- [17] R. Frederix and I. Tsinikos, *On improving NLO merging for  $t\bar{t}W$  production*, *JHEP* **11** (2021) 029 [[arXiv:2108.07826](#)] [[INSPIRE](#)].
- [18] F. Febres Cordero, M. Kraus and L. Reina, *Top-quark pair production in association with a  $W^\pm$  gauge boson in the POWHEG-BOX*, *Phys. Rev. D* **103** (2021) 094014 [[arXiv:2101.11808](#)] [[INSPIRE](#)].
- [19] L. Ferencz et al., *Study of  $t\bar{t}b\bar{b}$  and  $t\bar{t}W$  background modelling for  $t\bar{t}H$  analyses*, [arXiv:2301.11670](#) [[INSPIRE](#)].
- [20] ATLAS collaboration, *Measurement of the total and differential cross-sections of  $t\bar{t}W$  production in  $pp$  collisions at  $\sqrt{s} = 13$  TeV with the ATLAS detector*, *JHEP* **05** (2024) 131 [*Erratum ibid.* **11** (2025) 127] [[arXiv:2401.05299](#)] [[INSPIRE](#)].
- [21] CMS collaboration, *Measurement of the cross section of top quark-antiquark pair production in association with a  $W$  boson in proton-proton collisions at  $\sqrt{s} = 13$  TeV*, *JHEP* **07** (2023) 219 [[arXiv:2208.06485](#)] [[INSPIRE](#)].
- [22] ATLAS collaboration, *Search for leptonic charge asymmetry in  $t\bar{t}W$  production in final states with three leptons at  $\sqrt{s} = 13$  TeV*, *JHEP* **07** (2023) 033 [[arXiv:2301.04245](#)] [[INSPIRE](#)].
- [23] *HEPData record for this analysis*, [DOI:10.17182/hepdata.156814](#).
- [24] CMS collaboration, *The CMS Experiment at the CERN LHC*, 2008 *JINST* **3** S08004 [[INSPIRE](#)].
- [25] CMS collaboration, *Development of the CMS detector for the CERN LHC Run 3*, 2024 *JINST* **19** P05064 [[arXiv:2309.05466](#)] [[INSPIRE](#)].
- [26] CMS collaboration, *Performance of the CMS Level-1 trigger in proton-proton collisions at  $\sqrt{s} = 13$  TeV*, 2020 *JINST* **15** P10017 [[arXiv:2006.10165](#)] [[INSPIRE](#)].
- [27] CMS collaboration, *The CMS trigger system*, 2017 *JINST* **12** P01020 [[arXiv:1609.02366](#)] [[INSPIRE](#)].
- [28] CMS collaboration, *Performance of the CMS high-level trigger during LHC Run 2*, 2024 *JINST* **19** P11021 [[arXiv:2410.17038](#)] [[INSPIRE](#)].
- [29] CMS collaboration, *Particle-flow reconstruction and global event description with the CMS detector*, 2017 *JINST* **12** P10003 [[arXiv:1706.04965](#)] [[INSPIRE](#)].
- [30] D. Contardo et al., *Technical Proposal for the Phase-II Upgrade of the CMS Detector*, CERN-LHCC-2015-010 (2015) [[DOI:10.17181/CERN.VU8I.D59J](#)] [[INSPIRE](#)].
- [31] CMS collaboration, *Electron and photon reconstruction and identification with the CMS experiment at the CERN LHC*, 2021 *JINST* **16** P05014 [[arXiv:2012.06888](#)] [[INSPIRE](#)].
- [32] CMS collaboration, *Performance of the CMS electromagnetic calorimeter in  $pp$  collisions at  $\sqrt{s} = 13$  TeV*, 2024 *JINST* **19** P09004 [[arXiv:2403.15518](#)] [[INSPIRE](#)].

- [33] CMS collaboration, *Performance of the CMS muon detector and muon reconstruction with proton-proton collisions at  $\sqrt{s} = 13$  TeV*, 2018 *JINST* **13** P06015 [[arXiv:1804.04528](#)] [[INSPIRE](#)].
- [34] M. Cacciari, G.P. Salam and G. Soyez, *The anti- $k_t$  jet clustering algorithm*, *JHEP* **04** (2008) 063 [[arXiv:0802.1189](#)] [[INSPIRE](#)].
- [35] M. Cacciari, G.P. Salam and G. Soyez, *FastJet User Manual*, *Eur. Phys. J. C* **72** (2012) 1896 [[arXiv:1111.6097](#)] [[INSPIRE](#)].
- [36] CMS collaboration, *Pileup mitigation at CMS in 13 TeV data*, 2020 *JINST* **15** P09018 [[arXiv:2003.00503](#)] [[INSPIRE](#)].
- [37] CMS collaboration, *Jet energy scale and resolution in the CMS experiment in pp collisions at 8 TeV*, 2017 *JINST* **12** P02014 [[arXiv:1607.03663](#)] [[INSPIRE](#)].
- [38] CMS collaboration, *Performance of missing transverse momentum reconstruction in proton-proton collisions at  $\sqrt{s} = 13$  TeV using the CMS detector*, 2019 *JINST* **14** P07004 [[arXiv:1903.06078](#)] [[INSPIRE](#)].
- [39] CMS collaboration, *Identification of heavy-flavour jets with the CMS detector in pp collisions at 13 TeV*, 2018 *JINST* **13** P05011 [[arXiv:1712.07158](#)] [[INSPIRE](#)].
- [40] E. Bols et al., *Jet Flavour Classification Using DeepJet*, 2020 *JINST* **15** P12012 [[arXiv:2008.10519](#)] [[INSPIRE](#)].
- [41] CMS collaboration, *Performance of the DeepJet b tagging algorithm using 41.9/fb of data from proton-proton collisions at 13 TeV with Phase 1 CMS detector*, *CMS-DP-2018-058* (2018).
- [42] NNPDF collaboration, *Parton distributions from high-precision collider data*, *Eur. Phys. J. C* **77** (2017) 663 [[arXiv:1706.00428](#)] [[INSPIRE](#)].
- [43] T. Sjöstrand et al., *An introduction to PYTHIA 8.2*, *Comput. Phys. Commun.* **191** (2015) 159 [[arXiv:1410.3012](#)] [[INSPIRE](#)].
- [44] CMS collaboration, *CMS PYTHIA8 colour reconnection tunes based on underlying-event data*, *Eur. Phys. J. C* **83** (2023) 587 [[arXiv:2205.02905](#)] [[INSPIRE](#)].
- [45] J. Alwall et al., *Comparative study of various algorithms for the merging of parton showers and matrix elements in hadronic collisions*, *Eur. Phys. J. C* **53** (2008) 473 [[arXiv:0706.2569](#)] [[INSPIRE](#)].
- [46] R. Frederix and S. Frixione, *Merging meets matching in MC@NLO*, *JHEP* **12** (2012) 061 [[arXiv:1209.6215](#)] [[INSPIRE](#)].
- [47] J. Alwall et al., *The automated computation of tree-level and next-to-leading order differential cross sections, and their matching to parton shower simulations*, *JHEP* **07** (2014) 079 [[arXiv:1405.0301](#)] [[INSPIRE](#)].
- [48] GEANT4 collaboration, *GEANT4 — A Simulation Toolkit*, *Nucl. Instrum. Meth. A* **506** (2003) 250 [[INSPIRE](#)].
- [49] D. Barducci et al., *Interpreting top-quark LHC measurements in the standard-model effective field theory*, [arXiv:1802.07237](#) [[INSPIRE](#)].
- [50] O. Mattelaer, *On the maximal use of Monte Carlo samples: re-weighting events at NLO accuracy*, *Eur. Phys. J. C* **76** (2016) 674 [[arXiv:1607.00763](#)] [[INSPIRE](#)].
- [51] S. Frixione et al., *Automated simulations beyond the Standard Model: supersymmetry*, *JHEP* **12** (2019) 008 [[arXiv:1907.04898](#)] [[INSPIRE](#)].

- [52] P. Nason, *A new method for combining NLO QCD with shower Monte Carlo algorithms*, *JHEP* **11** (2004) 040 [[hep-ph/0409146](#)] [[INSPIRE](#)].
- [53] S. Frixione, P. Nason and C. Oleari, *Matching NLO QCD computations with Parton Shower simulations: the POWHEG method*, *JHEP* **11** (2007) 070 [[arXiv:0709.2092](#)] [[INSPIRE](#)].
- [54] S. Alioli, P. Nason, C. Oleari and E. Re, *A general framework for implementing NLO calculations in shower Monte Carlo programs: the POWHEG BOX*, *JHEP* **06** (2010) 043 [[arXiv:1002.2581](#)] [[INSPIRE](#)].
- [55] S. Alioli, P. Nason, C. Oleari and E. Re, *NLO single-top production matched with shower in POWHEG: s- and t-channel contributions*, *JHEP* **09** (2009) 111 [*Erratum ibid.* **02** (2010) 011] [[arXiv:0907.4076](#)] [[INSPIRE](#)].
- [56] S. Frixione, P. Nason and G. Ridolfi, *A Positive-weight next-to-leading-order Monte Carlo for heavy flavour hadroproduction*, *JHEP* **09** (2007) 126 [[arXiv:0707.3088](#)] [[INSPIRE](#)].
- [57] CMS collaboration, *Measurement of the inclusive and differential  $t\bar{t}\gamma$  cross sections in the dilepton channel and effective field theory interpretation in proton-proton collisions at  $\sqrt{s} = 13$  TeV*, *JHEP* **05** (2022) 091 [[arXiv:2201.07301](#)] [[INSPIRE](#)].
- [58] CMS collaboration, *Measurements of Inclusive W and Z Cross Sections in pp Collisions at  $\sqrt{s} = 7$  TeV*, *JHEP* **01** (2011) 080 [[arXiv:1012.2466](#)] [[INSPIRE](#)].
- [59] K. Rehermann and B. Tweedie, *Efficient Identification of Boosted Semileptonic Top Quarks at the LHC*, *JHEP* **03** (2011) 059 [[arXiv:1007.2221](#)] [[INSPIRE](#)].
- [60] CMS collaboration, *Performance of electron reconstruction and selection with the CMS detector in proton-proton collisions at  $\sqrt{s} = 8$  TeV*, 2015 *JINST* **10** P06005 [[arXiv:1502.02701](#)] [[INSPIRE](#)].
- [61] CMS collaboration, *Muon identification using multivariate techniques in the CMS experiment in proton-proton collisions at  $\sqrt{s} = 13$  TeV*, 2024 *JINST* **19** P02031 [[arXiv:2310.03844](#)] [[INSPIRE](#)].
- [62] PARTICLE DATA GROUP collaboration, *Review of particle physics*, *Phys. Rev. D* **110** (2024) 030001 [[INSPIRE](#)].
- [63] CMS collaboration, *Inclusive and differential cross section measurements of single top quark production in association with a Z boson in proton-proton collisions at  $\sqrt{s} = 13$  TeV*, *JHEP* **02** (2022) 107 [[arXiv:2111.02860](#)] [[INSPIRE](#)].
- [64] CMS collaboration, *Precision luminosity measurement in proton-proton collisions at  $\sqrt{s} = 13$  TeV in 2015 and 2016 at CMS*, *Eur. Phys. J. C* **81** (2021) 800 [[arXiv:2104.01927](#)] [[INSPIRE](#)].
- [65] CMS collaboration, *CMS luminosity measurement for the 2017 data-taking period at  $\sqrt{s} = 13$  TeV*, *CMS-PAS-LUM-17-004* (2018) [[INSPIRE](#)].
- [66] CMS collaboration, *CMS luminosity measurement for the 2018 data-taking period at  $\sqrt{s} = 13$  TeV*, *CMS-PAS-LUM-18-002* (2019) [[INSPIRE](#)].
- [67] CMS collaboration, *Performance of the CMS muon trigger system in proton-proton collisions at  $\sqrt{s} = 13$  TeV*, 2021 *JINST* **16** P07001 [[arXiv:2102.04790](#)] [[INSPIRE](#)].
- [68] CMS collaboration, *Measurement of top quark pair production in association with a Z boson in proton-proton collisions at  $\sqrt{s} = 13$  TeV*, *JHEP* **03** (2020) 056 [[arXiv:1907.11270](#)] [[INSPIRE](#)].
- [69] CMS collaboration, *Measurements of the  $pp \rightarrow WZ$  inclusive and differential production cross section and constraints on charged anomalous triple gauge couplings at  $\sqrt{s} = 13$  TeV*, *JHEP* **04** (2019) 122 [[arXiv:1901.03428](#)] [[INSPIRE](#)].

- [70] CMS collaboration, *Measurements of the  $pp \rightarrow ZZ$  production cross section and the  $Z \rightarrow 4\ell$  branching fraction, and constraints on anomalous triple gauge couplings at  $\sqrt{s} = 13$  TeV*, *Eur. Phys. J. C* **78** (2018) 165 [Erratum *ibid.* **78** (2018) 515] [[arXiv:1709.08601](#)] [[INSPIRE](#)].
- [71] CMS collaboration, *Measurement of the inclusive and differential  $t\bar{t}\gamma$  cross sections in the single-lepton channel and EFT interpretation at  $\sqrt{s} = 13$  TeV*, *JHEP* **12** (2021) 180 [[arXiv:2107.01508](#)] [[INSPIRE](#)].
- [72] CMS collaboration, *Measurement of the cross section for electroweak production of a Z boson, a photon and two jets in proton-proton collisions at  $\sqrt{s} = 13$  TeV and constraints on anomalous quartic couplings*, *JHEP* **06** (2020) 076 [[arXiv:2002.09902](#)] [[INSPIRE](#)].
- [73] S. Catani et al., *Higgs Boson Production in Association with a Top-Antitop Quark Pair in Next-to-Next-to-Leading Order QCD*, *Phys. Rev. Lett.* **130** (2023) 111902 [[arXiv:2210.07846](#)] [[INSPIRE](#)].
- [74] J. Butterworth et al., *PDF4LHC recommendations for LHC Run II*, *J. Phys. G* **43** (2016) 023001 [[arXiv:1510.03865](#)] [[INSPIRE](#)].
- [75] CMS collaboration, *Object definitions for top quark analyses at the particle level*, *CMS-NOTE-2017-004* (2017).
- [76] CMS collaboration, *The CMS Statistical Analysis and Combination Tool: Combine*, *Comput. Softw. Big Sci.* **8** (2024) 19 [[arXiv:2404.06614](#)] [[INSPIRE](#)].
- [77] T. Chen and C. Guestrin, *XGBoost: A Scalable Tree Boosting System*, [arXiv:1603.02754](#) [[DOI:10.1145/2939672.2939785](#)] [[INSPIRE](#)].
- [78] A. Paszke et al., *PyTorch: An Imperative Style, High-Performance Deep Learning Library*, [arXiv:1912.01703](#) [[INSPIRE](#)].

## The CMS collaboration

A. Hayrapetyan<sup>1</sup>, V. Makarenko<sup>1</sup>, A. Tumasyan<sup>1,a</sup>, W. Adam<sup>2</sup>, J.W. Andrejkovic<sup>2</sup>,  
 L. Benato<sup>2</sup>, T. Bergauer<sup>2</sup>, M. Dragicevic<sup>2</sup>, C. Giordano<sup>2</sup>, P.S. Hussain<sup>2</sup>, M. Jeitler<sup>2,b</sup>,  
 N. Krammer<sup>2</sup>, A. Li<sup>2</sup>, D. Liko<sup>2</sup>, I. Mikulec<sup>2</sup>, J. Schieck<sup>2,b</sup>, D. Schwarz<sup>2</sup>,  
 R. Schöfbeck<sup>2,b</sup>, M. Shooshtari<sup>2</sup>, M. Sonawane<sup>2</sup>, W. Waltenberger<sup>2</sup>, C.-E. Wulz<sup>2,b</sup>,  
 T. Janssen<sup>3</sup>, H. Kwon<sup>3</sup>, D. Ocampo Henao<sup>3</sup>, T. Van Laer<sup>3</sup>, P. Van Mechelen<sup>3</sup>,  
 J. Bierkens<sup>4</sup>, N. Breugelmans<sup>4</sup>, J. D’Hondt<sup>4</sup>, S. Dansana<sup>4</sup>, A. De Moor<sup>4</sup>, M. Delcourt<sup>4</sup>,  
 F. Heyen<sup>4</sup>, Y. Hong<sup>4</sup>, P. Kashko<sup>4</sup>, S. Lowette<sup>4</sup>, I. Makarenko<sup>4</sup>, D. Müller<sup>4</sup>, J. Song<sup>4</sup>,  
 S. Tavernier<sup>4</sup>, M. Tytgat<sup>4,c</sup>, G.P. Van Onsem<sup>4</sup>, S. Van Putte<sup>4</sup>, D. Vannerom<sup>4</sup>, B. Bilin<sup>5</sup>,  
 B. Clerbaux<sup>5</sup>, A.K. Das<sup>5</sup>, I. De Bruyn<sup>5</sup>, G. De Lentdecker<sup>5</sup>, H. Evard<sup>5</sup>, L. Favart<sup>5</sup>,  
 P. Gianneios<sup>5</sup>, A. Khalilzadeh<sup>5</sup>, F.A. Khan<sup>5</sup>, A. Malara<sup>5</sup>, M.A. Shahzad<sup>5</sup>, L. Thomas<sup>5</sup>,  
 M. Vanden Bemden<sup>5</sup>, C. Vander Velde<sup>5</sup>, P. Vanlaer<sup>5</sup>, F. Zhang<sup>5</sup>, M. De Coen<sup>6</sup>,  
 D. Dobur<sup>6</sup>, G. Gokbulut<sup>6</sup>, J. Knolle<sup>6</sup>, L. Lambrecht<sup>6</sup>, D. Marecx<sup>6</sup>, K. Skovpen<sup>6</sup>,  
 N. Van Den Bossche<sup>6</sup>, J. van der Linden<sup>6</sup>, J. Vandenbroeck<sup>6</sup>, L. Wezenbeek<sup>6</sup>, S. Bein<sup>7</sup>,  
 A. Benecke<sup>7</sup>, A. Bethani<sup>7</sup>, G. Bruno<sup>7</sup>, A. Cappati<sup>7</sup>, J. De Favereau De Jeneret<sup>7</sup>,  
 C. Delaere<sup>7</sup>, A. Giammanco<sup>7</sup>, A.O. Guzel<sup>7</sup>, V. Lemaitre<sup>7</sup>, J. Lidrych<sup>7</sup>, P. Malek<sup>7</sup>,  
 P. Mastrapasqua<sup>7</sup>, S. Turckapar<sup>7</sup>, G.A. Alves<sup>8</sup>, M. Barroso Ferreira Filho<sup>8</sup>, E. Coelho<sup>8</sup>,  
 C. Hensel<sup>8</sup>, T. Menezes De Oliveira<sup>8</sup>, C. Mora Herrera<sup>8,d</sup>, P. Rebello Teles<sup>8</sup>, M. Soeiro<sup>8</sup>,  
 E.J. Tonelli Manganote<sup>8,e</sup>, A. Vilela Pereira<sup>8,d</sup>, W.L. Aldá Júnior<sup>9</sup>,  
 H. Brandao Malbouisson<sup>9</sup>, W. Carvalho<sup>9</sup>, J. Chinellato<sup>9,f</sup>, M. Costa Reis<sup>9</sup>,  
 E.M. Da Costa<sup>9</sup>, G.G. Da Silveira<sup>9,g</sup>, D. De Jesus Damiao<sup>9</sup>, S. Fonseca De Souza<sup>9</sup>,  
 R. Gomes De Souza<sup>9</sup>, S. S. Jesus<sup>9</sup>, T. Laux Kuhn<sup>9,g</sup>, M. Macedo<sup>9</sup>, K. Mota Amarilo<sup>9</sup>,  
 L. Mundim<sup>9</sup>, H. Nogima<sup>9</sup>, J.P. Pinheiro<sup>9</sup>, A. Santoro<sup>9</sup>, A. Sznajder<sup>9</sup>, M. Thiel<sup>9</sup>,  
 F. Torres Da Silva De Araujo<sup>9,h</sup>, C.A. Bernardes<sup>10,g</sup>, E.M. Gregores<sup>10</sup>, B. Lopes Da Costa<sup>10</sup>,  
 I. Maietto Silverio<sup>10</sup>, P.G. Mercadante<sup>10</sup>, S.F. Novaes<sup>10</sup>, B. Orzari<sup>10</sup>, Sandra S. Padula<sup>10</sup>,  
 V. Scheurer<sup>10</sup>, T.R. Fernandez Perez Tomei<sup>10</sup>, A. Aleksandrov<sup>11</sup>, G. Antchev<sup>11</sup>, P. Danev<sup>11</sup>,  
 R. Hadjiiska<sup>11</sup>, P. Iaydjiev<sup>11</sup>, M. Misheva<sup>11</sup>, M. Shopova<sup>11</sup>, G. Sultanov<sup>11</sup>,  
 A. Dimitrov<sup>12</sup>, L. Litov<sup>12</sup>, B. Pavlov<sup>12</sup>, P. Petkov<sup>12</sup>, A. Petrov<sup>12</sup>, S. Keshri<sup>13</sup>,  
 D. Laroze<sup>13</sup>, S. Thakur<sup>13</sup>, W. Brooks<sup>14</sup>, T. Cheng<sup>15</sup>, T. Javaid<sup>15</sup>, L. Wang<sup>15</sup>,  
 L. Yuan<sup>15</sup>, Z. Hu<sup>16</sup>, Z. Liang<sup>16</sup>, J. Liu<sup>16</sup>, X. Wang<sup>16</sup>, G.M. Chen<sup>17,i</sup>, H.S. Chen<sup>17,i</sup>,  
 M. Chen<sup>17,i</sup>, Y. Chen<sup>17</sup>, Q. Hou<sup>17</sup>, X. Hou<sup>17</sup>, F. Iemmi<sup>17</sup>, C.H. Jiang<sup>17</sup>, A. Kapoor<sup>17,j</sup>,  
 H. Liao<sup>17</sup>, G. Liu<sup>17</sup>, Z.-A. Liu<sup>17,k</sup>, J.N. Song<sup>17,k</sup>, S. Song<sup>17</sup>, J. Tao<sup>17</sup>, C. Wang<sup>17,i</sup>,  
 J. Wang<sup>17</sup>, H. Zhang<sup>17</sup>, J. Zhao<sup>17</sup>, A. Agapitos<sup>18</sup>, Y. Ban<sup>18</sup>,  
 A. Carvalho Antunes De Oliveira<sup>18</sup>, S. Deng<sup>18</sup>, B. Guo<sup>18</sup>, Q. Guo<sup>18</sup>, C. Jiang<sup>18</sup>, A. Levin<sup>18</sup>,  
 C. Li<sup>18</sup>, Q. Li<sup>18</sup>, Y. Mao<sup>18</sup>, S. Qian<sup>18</sup>, S.J. Qian<sup>18</sup>, X. Qin<sup>18</sup>, X. Sun<sup>18</sup>, D. Wang<sup>18</sup>,  
 J. Wang<sup>18</sup>, H. Yang<sup>18</sup>, M. Zhang<sup>18</sup>, Y. Zhao<sup>18</sup>, C. Zhou<sup>18</sup>, S. Yang<sup>19</sup>, Z. You<sup>20</sup>, K. Jaffel<sup>21</sup>,  
 N. Lu<sup>21</sup>, G. Bauer<sup>22,l</sup>, B. Li<sup>22,m</sup>, H. Wang<sup>22</sup>, K. Yi<sup>22,n</sup>, J. Zhang<sup>22</sup>, Y. Li<sup>23</sup>, Z. Lin<sup>24</sup>,  
 C. Lu<sup>24</sup>, M. Xiao<sup>24,o</sup>, C. Avila<sup>25</sup>, D.A. Barbosa Trujillo<sup>25</sup>, A. Cabrera<sup>25</sup>, C. Florez<sup>25</sup>,  
 J. Fraga<sup>25</sup>, J.A. Reyes Vega<sup>25</sup>, C. Rendón<sup>26</sup>, M. Rodriguez<sup>26</sup>, A.A. Ruales Barbosa<sup>26</sup>,  
 J.D. Ruiz Alvarez<sup>26</sup>, N. Godinovic<sup>27</sup>, D. Lelas<sup>27</sup>, A. Sculac<sup>27</sup>, M. Kovac<sup>28</sup>, A. Petkovic<sup>28</sup>,  
 T. Sculac<sup>28</sup>, P. Bargassa<sup>29</sup>, V. Brigljevic<sup>29</sup>, B.K. Chitroda<sup>29</sup>, D. Ferencek<sup>29</sup>, K. Jakovcic<sup>29</sup>,  
 A. Starodumov<sup>29</sup>, T. Susa<sup>29</sup>, A. Attikis<sup>30</sup>, K. Christoforou<sup>30</sup>, A. Hadjiagapiou<sup>30</sup>,  
 C. Leonidou<sup>30</sup>, C. Nicolaou<sup>30</sup>, L. Paizanos<sup>30</sup>, F. Ptochos<sup>30</sup>, P.A. Razis<sup>30</sup>, H. Rykaczewski<sup>30</sup>,

H. Saka <sup>30</sup>, A. Stepennov <sup>30</sup>, M. Finger <sup>31,†</sup>, M. Finger Jr. <sup>31</sup>, A. Kveton <sup>31</sup>, E. Ayala <sup>32</sup>, E. Carrera Jarrin <sup>33</sup>, Y. Assran <sup>34,p,q</sup>, B. El-mahdy <sup>34,r</sup>, A. Hussein <sup>35</sup>, H. Mohammed <sup>35</sup>, M. Abdullah Al-Mashad <sup>35</sup>, K. Ehataht <sup>36</sup>, M. Kadastik <sup>36</sup>, T. Lange <sup>36</sup>, C. Nielsen <sup>36</sup>, J. Pata <sup>36</sup>, M. Raidal <sup>36</sup>, N. Seeba <sup>36</sup>, L. Tani <sup>36</sup>, A. Milieva <sup>37</sup>, K. Osterberg <sup>37</sup>, M. Voutilainen <sup>37</sup>, N. Bin Norjoharuddeen <sup>38</sup>, E. Brücken <sup>38</sup>, F. Garcia <sup>38</sup>, P. Inkaew <sup>38</sup>, K.T.S. Kallonen <sup>38</sup>, R. Kumar Verma <sup>38</sup>, T. Lampén <sup>38</sup>, K. Lassila-Perini <sup>38</sup>, B. Lehtela <sup>38</sup>, S. Lehti <sup>38</sup>, T. Lindén <sup>38</sup>, N.R. Mancilla Xinto <sup>38</sup>, M. Myllymäki <sup>38</sup>, M.m. Rantanen <sup>38</sup>, S. Saariokari <sup>38</sup>, N.T. Toikka <sup>38</sup>, J. Tuominiemi <sup>38</sup>, H. Kirschenmann <sup>39</sup>, P. Luukka <sup>39</sup>, H. Petrow <sup>39</sup>, M. Besancon <sup>40</sup>, F. Couderc <sup>40</sup>, M. DeJardin <sup>40</sup>, D. Denegri <sup>40</sup>, P. Devoue <sup>40</sup>, J.L. Faure <sup>40</sup>, F. Ferri <sup>40</sup>, S. Ganjour <sup>40</sup>, P. Gras <sup>40</sup>, G. Hamel de Monchenault <sup>40</sup>, M. Kumar <sup>40</sup>, V. Lohezic <sup>40</sup>, J. Malcles <sup>40</sup>, F. Orlandi <sup>40</sup>, L. Portales <sup>40</sup>, S. Ronchi <sup>40</sup>, M.Ö. Sahin <sup>40</sup>, A. Savoy-Navarro <sup>40,s</sup>, P. Simkina <sup>40</sup>, M. Titov <sup>40</sup>, M. Tornago <sup>40</sup>, F. Beaudette <sup>41</sup>, G. Boldrini <sup>41</sup>, P. Busson <sup>41</sup>, C. Charlot <sup>41</sup>, M. Chiusi <sup>41</sup>, T.D. Cuisset <sup>41</sup>, F. Damas <sup>41</sup>, O. Davignon <sup>41</sup>, A. De Wit <sup>41</sup>, T. Debnath <sup>41</sup>, I.T. Ehle <sup>41</sup>, B.A. Fontana Santos Alves <sup>41</sup>, S. Ghosh <sup>41</sup>, A. Gilbert <sup>41</sup>, R. Granier de Cassagnac <sup>41</sup>, L. Kalipoliti <sup>41</sup>, M. Manoni <sup>41</sup>, M. Nguyen <sup>41</sup>, S. Obratsov <sup>41</sup>, C. Ochando <sup>41</sup>, R. Salerno <sup>41</sup>, J.B. Sauvan <sup>41</sup>, Y. Sirois <sup>41</sup>, G. Sokmen <sup>41</sup>, L. Urda Gómez <sup>41</sup>, A. Zabi <sup>41</sup>, A. Zghiche <sup>41</sup>, J.-L. Agram <sup>42,t</sup>, J. Andrea <sup>42</sup>, D. Bloch <sup>42</sup>, J.-M. Brom <sup>42</sup>, E.C. Chabert <sup>42</sup>, C. Collard <sup>42</sup>, G. Coulon <sup>42</sup>, S. Falke <sup>42</sup>, U. Goerlach <sup>42</sup>, R. Haeblerle <sup>42</sup>, A.-C. Le Bihan <sup>42</sup>, M. Meena <sup>42</sup>, O. Poncet <sup>42</sup>, G. Saha <sup>42</sup>, P. Vaucelle <sup>42</sup>, A. Di Florio <sup>43</sup>, D. Amram <sup>44</sup>, S. Beauceron <sup>44</sup>, B. Blancon <sup>44</sup>, G. Boudoul <sup>44</sup>, N. Chanon <sup>44</sup>, D. Contardo <sup>44</sup>, P. Depasse <sup>44</sup>, C. Dozen <sup>44,u</sup>, H. El Mamouni <sup>44</sup>, J. Fay <sup>44</sup>, S. Gascon <sup>44</sup>, M. Gouzevitch <sup>44</sup>, C. Greenberg <sup>44</sup>, G. Grenier <sup>44</sup>, B. Ille <sup>44</sup>, E. Jourd’huy <sup>44</sup>, I.B. Laktineh <sup>44</sup>, M. Lethuillier <sup>44</sup>, B. Massoteau <sup>44</sup>, L. Mirabito <sup>44</sup>, A. Purohit <sup>44</sup>, M. Vander Donckt <sup>44</sup>, J. Xiao <sup>44</sup>, A. Khvedelidze <sup>45,v</sup>, I. Lomidze <sup>45</sup>, Z. Tsamalaidze <sup>45,v</sup>, V. Botta <sup>46</sup>, S. Consuegra Rodríguez <sup>46</sup>, L. Feld <sup>46</sup>, K. Klein <sup>46</sup>, M. Lipinski <sup>46</sup>, D. Meuser <sup>46</sup>, P. Nattland <sup>46</sup>, V. Oppenländer <sup>46</sup>, A. Pauls <sup>46</sup>, D. Pérez Adán <sup>46</sup>, N. Röwert <sup>46</sup>, M. Teroerde <sup>46</sup>, C. Daumann <sup>47</sup>, S. Diekmann <sup>47</sup>, A. Dodonova <sup>47</sup>, N. Eich <sup>47</sup>, D. Eliseev <sup>47</sup>, F. Engelke <sup>47</sup>, J. Erdmann <sup>47</sup>, M. Erdmann <sup>47</sup>, B. Fischer <sup>47</sup>, T. Hebbeker <sup>47</sup>, K. Hoepfner <sup>47</sup>, F. Ivone <sup>47</sup>, A. Jung <sup>47</sup>, N. Kumar <sup>47</sup>, M.y. Lee <sup>47</sup>, F. Mausolf <sup>47</sup>, M. Merschmeyer <sup>47</sup>, A. Meyer <sup>47</sup>, F. Nowotny <sup>47</sup>, A. Pozdnyakov <sup>47</sup>, W. Redjeb <sup>47</sup>, H. Reithler <sup>47</sup>, U. Sarkar <sup>47</sup>, V. Sarkisovi <sup>47</sup>, A. Schmidt <sup>47</sup>, C. Seth <sup>47</sup>, A. Sharma <sup>47</sup>, J.L. Spah <sup>47</sup>, V. Vaulin <sup>47</sup>, S. Zaleski <sup>47</sup>, M.R. Beckers <sup>48</sup>, C. Dziwok <sup>48</sup>, G. Flügge <sup>48</sup>, N. Hoeflich <sup>48</sup>, T. Kress <sup>48</sup>, A. Nowack <sup>48</sup>, O. Pooth <sup>48</sup>, A. Stahl <sup>48</sup>, A. Zotz <sup>48</sup>, H. Aarup Petersen <sup>49</sup>, A. Abel <sup>49</sup>, M. Aldaya Martin <sup>49</sup>, J. Alimena <sup>49</sup>, S. Amoroso <sup>49</sup>, Y. An <sup>49</sup>, I. Andreev <sup>49</sup>, J. Bach <sup>49</sup>, S. Baxter <sup>49</sup>, M. Bayatmakou <sup>49</sup>, H. Becerril Gonzalez <sup>49</sup>, O. Behnke <sup>49</sup>, A. Belvedere <sup>49</sup>, F. Blekman <sup>49,w</sup>, K. Borrás <sup>49,x</sup>, A. Campbell <sup>49</sup>, S. Chatterjee <sup>49</sup>, L.X. Coll Saravia <sup>49</sup>, G. Eckerlin <sup>49</sup>, D. Eckstein <sup>49</sup>, E. Gallo <sup>49,w</sup>, A. Geiser <sup>49</sup>, V. Guglielmi <sup>49</sup>, M. Guthoff <sup>49</sup>, A. Hinzmann <sup>49</sup>, L. Jeppe <sup>49</sup>, M. Kasemann <sup>49</sup>, C. Kleinwort <sup>49</sup>, R. Kogler <sup>49</sup>, M. Komm <sup>49</sup>, D. Krücker <sup>49</sup>, W. Lange <sup>49</sup>, D. Leyva Pernia <sup>49</sup>, K.-Y. Lin <sup>49</sup>, K. Lipka <sup>49,y</sup>, W. Lohmann <sup>49,z</sup>, J. Malvaso <sup>49</sup>, R. Mankel <sup>49</sup>, I.-A. Melzer-Pellmann <sup>49</sup>, M. Mendizabal Morentin <sup>49</sup>, A.B. Meyer <sup>49</sup>, G. Milella <sup>49</sup>, K. Moral Figueroa <sup>49</sup>, A. Mussgiller <sup>49</sup>, L.P. Nair <sup>49</sup>, J. Niedziela <sup>49</sup>, A. Nürnberg <sup>49</sup>, J. Park <sup>49</sup>, E. Ranken <sup>49</sup>, A. Raspereza <sup>49</sup>, D. Rastorguev <sup>49</sup>, L. Rygaard <sup>49</sup>,

M. Scham [ID](#)<sup>49,aa,ab</sup>, S. Schnake [ID](#)<sup>49,x</sup>, C. Schwanenberger [ID](#)<sup>49,w</sup>, P. Schütze [ID](#)<sup>49</sup>, D. Selivanova [ID](#)<sup>49</sup>,  
 K. Sharko [ID](#)<sup>49</sup>, M. Shchedrolosiev [ID](#)<sup>49</sup>, D. Stafford [ID](#)<sup>49</sup>, M. Torkian <sup>49</sup>, F. Vazzoler [ID](#)<sup>49</sup>,  
 A. Ventura Barroso [ID](#)<sup>49</sup>, R. Walsh [ID](#)<sup>49</sup>, D. Wang [ID](#)<sup>49</sup>, Q. Wang [ID](#)<sup>49</sup>, K. Wichmann <sup>49</sup>, L. Wiens [ID](#)<sup>49,x</sup>,  
 C. Wissing [ID](#)<sup>49</sup>, Y. Yang [ID](#)<sup>49</sup>, S. Zakharov <sup>49</sup>, A. Zimmermann Castro Santos [ID](#)<sup>49</sup>, A. Albrecht [ID](#)<sup>50</sup>,  
 A.R. Alves Andrade [ID](#)<sup>50</sup>, M. Antonello [ID](#)<sup>50</sup>, S. Bollweg <sup>50</sup>, M. Bonanomi [ID](#)<sup>50</sup>, K. El Morabit [ID](#)<sup>50</sup>,  
 Y. Fischer [ID](#)<sup>50</sup>, M. Frahm <sup>50</sup>, E. Garutti [ID](#)<sup>50</sup>, A. Grohsjean [ID](#)<sup>50</sup>, J. Haller [ID](#)<sup>50</sup>, D. Hundhausen <sup>50</sup>,  
 H.R. Jabusch [ID](#)<sup>50</sup>, G. Kasieczka [ID](#)<sup>50</sup>, P. Keicher [ID](#)<sup>50</sup>, R. Klanner [ID](#)<sup>50</sup>, W. Korcari [ID](#)<sup>50</sup>, T. Kramer [ID](#)<sup>50</sup>,  
 C.c. Kuo <sup>50</sup>, V. Kutzner [ID](#)<sup>50</sup>, F. Labe [ID](#)<sup>50</sup>, J. Lange [ID](#)<sup>50</sup>, A. Lobanov [ID](#)<sup>50</sup>, L. Moureaux [ID](#)<sup>50</sup>,  
 M. Mrowietz <sup>50</sup>, A. Nigamova [ID](#)<sup>50</sup>, K. Nikolopoulos [ID](#)<sup>50</sup>, Y. Nissan <sup>50</sup>, A. Paasch [ID](#)<sup>50</sup>,  
 K.J. Pena Rodriguez [ID](#)<sup>50</sup>, N. Prouvost <sup>50</sup>, T. Quadfasel [ID](#)<sup>50</sup>, B. Raciti [ID](#)<sup>50</sup>, M. Rieger [ID](#)<sup>50</sup>,  
 D. Savoie [ID](#)<sup>50</sup>, J. Schindler [ID](#)<sup>50</sup>, P. Schleper [ID](#)<sup>50</sup>, M. Schröder [ID](#)<sup>50</sup>, J. Schwandt [ID](#)<sup>50</sup>,  
 M. Sommerhalder [ID](#)<sup>50</sup>, H. Stadie [ID](#)<sup>50</sup>, G. Steinbrück [ID](#)<sup>50</sup>, A. Tews <sup>50</sup>, R. Ward [ID](#)<sup>50</sup>, B. Wiederspan <sup>50</sup>,  
 M. Wolf [ID](#)<sup>50</sup>, S. Brommer [ID](#)<sup>51</sup>, E. Butz [ID](#)<sup>51</sup>, Y.M. Chen [ID](#)<sup>51</sup>, T. Chwalek [ID](#)<sup>51</sup>, A. Dierlamm [ID](#)<sup>51</sup>,  
 G.G. Dincer [ID](#)<sup>51</sup>, U. Elicabuk <sup>51</sup>, N. Faltermann [ID](#)<sup>51</sup>, M. Giffels [ID](#)<sup>51</sup>, A. Gottmann [ID](#)<sup>51</sup>,  
 F. Hartmann [ID](#)<sup>51,ac</sup>, R. Hofsaess [ID](#)<sup>51</sup>, M. Horzela [ID](#)<sup>51</sup>, U. Husemann [ID](#)<sup>51</sup>, J. Kieseler [ID](#)<sup>51</sup>,  
 M. Klute [ID](#)<sup>51</sup>, R. Kunnilan Muhammed Rafeek <sup>51</sup>, O. Lavoryk [ID](#)<sup>51</sup>, J.M. Lawhorn [ID](#)<sup>51</sup>,  
 A. Lintuluoto [ID](#)<sup>51</sup>, S. Maier [ID](#)<sup>51</sup>, M. Mormile [ID](#)<sup>51</sup>, Th. Müller [ID](#)<sup>51</sup>, E. Pfeffer [ID](#)<sup>51</sup>, M. Presilla [ID](#)<sup>51</sup>,  
 G. Quast [ID](#)<sup>51</sup>, K. Rabbertz [ID](#)<sup>51</sup>, B. Regnery [ID](#)<sup>51</sup>, R. Schmieder <sup>51</sup>, N. Shadskiy [ID](#)<sup>51</sup>, I. Shvetsov [ID](#)<sup>51</sup>,  
 H.J. Simonis [ID](#)<sup>51</sup>, L. Sowa [ID](#)<sup>51</sup>, L. Stockmeier <sup>51</sup>, K. Tauqeer <sup>51</sup>, M. Toms [ID](#)<sup>51</sup>, B. Topko [ID](#)<sup>51</sup>,  
 N. Trevisani [ID](#)<sup>51</sup>, C. Verstege [ID](#)<sup>51</sup>, T. Voigtländer [ID](#)<sup>51</sup>, R.F. Von Cube [ID](#)<sup>51</sup>, J. Von Den Driesch <sup>51</sup>,  
 M. Wassmer [ID](#)<sup>51</sup>, R. Wolf [ID](#)<sup>51</sup>, W.D. Zeuner [ID](#)<sup>51</sup>, X. Zuo [ID](#)<sup>51</sup>, G. Anagnostou [ID](#)<sup>52</sup>, G. Daskalakis [ID](#)<sup>52</sup>,  
 A. Kyriakis [ID](#)<sup>52</sup>, A. Papadopoulos [ID](#)<sup>52,ac</sup>, A. Stakia [ID](#)<sup>52</sup>, G. Melachroinos <sup>53</sup>, Z. Painesis [ID](#)<sup>53</sup>,  
 I. Paraskevas [ID](#)<sup>53</sup>, N. Saoulidou [ID](#)<sup>53</sup>, K. Theofilatos [ID](#)<sup>53</sup>, E. Tziaferi [ID](#)<sup>53</sup>, K. Vellidis [ID](#)<sup>53</sup>,  
 I. Zisopoulos [ID](#)<sup>53</sup>, T. Chatzistavrou <sup>54</sup>, G. Karapostoli [ID](#)<sup>54</sup>, K. Kousouris [ID](#)<sup>54</sup>, E. Siamarkou <sup>54</sup>,  
 G. Tsiopolitis [ID](#)<sup>54</sup>, I. Bestintzanos <sup>55</sup>, I. Evangelou [ID](#)<sup>55</sup>, C. Foudas <sup>55</sup>, P. Katsoulis <sup>55</sup>, P. Kokkas [ID](#)<sup>55</sup>,  
 P.G. Kosmoglou Kioseoglou [ID](#)<sup>55</sup>, N. Manthos [ID](#)<sup>55</sup>, I. Papadopoulos [ID](#)<sup>55</sup>, J. Strologas [ID](#)<sup>55</sup>,  
 D. Druzhkin [ID](#)<sup>56</sup>, C. Hajdu [ID](#)<sup>56</sup>, D. Horvath [ID](#)<sup>56,ad,ae</sup>, K. Márton <sup>56</sup>, A.J. Rádl [ID](#)<sup>56,af</sup>, F. Sikler [ID](#)<sup>56</sup>,  
 V. Veszpremi [ID](#)<sup>56</sup>, M. Csanád [ID](#)<sup>57</sup>, K. Farkas [ID](#)<sup>57</sup>, A. Fehérkuti [ID](#)<sup>57,ag</sup>, M.M.A. Gadallah [ID](#)<sup>57,ah</sup>,  
 Á. Kadlecik [ID](#)<sup>57</sup>, M. León Coello [ID](#)<sup>57</sup>, G. Pásztor [ID](#)<sup>57</sup>, G.I. Veres [ID](#)<sup>57</sup>, B. Ujvari [ID](#)<sup>58</sup>, G. Zilizi [ID](#)<sup>58</sup>,  
 G. Bencze <sup>59</sup>, S. Czellar <sup>59</sup>, J. Molnar <sup>59</sup>, Z. Szillasi <sup>59</sup>, T. Csorgo [ID](#)<sup>60,ag</sup>, F. Nemes [ID](#)<sup>60,ag</sup>, T. Novak [ID](#)<sup>60</sup>,  
 I. Szanyi [ID](#)<sup>60,ai</sup>, S. Bansal [ID](#)<sup>61</sup>, S.B. Beri <sup>61</sup>, V. Bhatnagar [ID](#)<sup>61</sup>, G. Chaudhary [ID](#)<sup>61</sup>, S. Chauhan [ID](#)<sup>61</sup>,  
 N. Dhingra [ID](#)<sup>61,aj</sup>, A. Kaur [ID](#)<sup>61</sup>, A. Kaur [ID](#)<sup>61</sup>, H. Kaur [ID](#)<sup>61</sup>, M. Kaur [ID](#)<sup>61</sup>, S. Kumar [ID](#)<sup>61</sup>,  
 T. Sheokand <sup>61</sup>, J.B. Singh [ID](#)<sup>61</sup>, A. Singla [ID](#)<sup>61</sup>, A. Bhardwaj [ID](#)<sup>62</sup>, A. Chhetri [ID](#)<sup>62</sup>, B.C. Choudhary [ID](#)<sup>62</sup>,  
 A. Kumar [ID](#)<sup>62</sup>, A. Kumar [ID](#)<sup>62</sup>, M. Naimuddin [ID](#)<sup>62</sup>, S. Phor [ID](#)<sup>62</sup>, K. Ranjan [ID](#)<sup>62</sup>, M.K. Saini <sup>62</sup>,  
 S. Acharya [ID](#)<sup>63,ak</sup>, B. Gomber [ID](#)<sup>63,ak</sup>, B. Sahu [ID](#)<sup>63,ak</sup>, S. Mukherjee [ID](#)<sup>64</sup>, S. Baradia [ID](#)<sup>65</sup>,  
 S. Bhattacharya [ID](#)<sup>65</sup>, S. Das Gupta <sup>65</sup>, S. Dutta [ID](#)<sup>65</sup>, S. Dutta <sup>65</sup>, S. Sarkar <sup>65</sup>, M.M. Ameen [ID](#)<sup>66</sup>,  
 P.K. Behera [ID](#)<sup>66</sup>, S. Chatterjee [ID](#)<sup>66</sup>, G. Dash [ID](#)<sup>66</sup>, A. Dattamunsi <sup>66</sup>, P. Jana [ID](#)<sup>66</sup>, P. Kalbhor [ID](#)<sup>66</sup>,  
 S. Kamble [ID](#)<sup>66</sup>, J.R. Komaragiri [ID](#)<sup>66,al</sup>, T. Mishra [ID](#)<sup>66</sup>, P.R. Pujahari [ID](#)<sup>66</sup>, N.R. Saha [ID](#)<sup>66</sup>,  
 A.K. Sikdar [ID](#)<sup>66</sup>, R.K. Singh [ID](#)<sup>66</sup>, P. Verma [ID](#)<sup>66</sup>, S. Verma [ID](#)<sup>66</sup>, A. Vijay [ID](#)<sup>66</sup>, B.K. Sirasva <sup>67</sup>,  
 L. Bhatt <sup>68</sup>, S. Dugad [ID](#)<sup>68</sup>, G.B. Mohanty [ID](#)<sup>68</sup>, M. Shelake [ID](#)<sup>68</sup>, P. Suryadevara <sup>68</sup>, A. Bala [ID](#)<sup>69</sup>,  
 S. Banerjee [ID](#)<sup>69</sup>, S. Barman [ID](#)<sup>69,am</sup>, R.M. Chatterjee <sup>69</sup>, M. Guchait [ID](#)<sup>69</sup>, Sh. Jain [ID](#)<sup>69</sup>, A. Jaiswal <sup>69</sup>,  
 B.M. Joshi [ID](#)<sup>69</sup>, S. Kumar [ID](#)<sup>69</sup>, M. Maity <sup>69,am</sup>, G. Majumder [ID](#)<sup>69</sup>, K. Mazumdar [ID](#)<sup>69</sup>, S. Parolia [ID](#)<sup>69</sup>,  
 R. Saxena [ID](#)<sup>69</sup>, A. Thachayath [ID](#)<sup>69</sup>, S. Bahinipati [ID](#)<sup>70,an</sup>, D. Maity [ID](#)<sup>70,ao</sup>, P. Mal [ID](#)<sup>70</sup>,

K. Naskar [ID](#)<sup>70,ao</sup>, A. Nayak [ID](#)<sup>70,ao</sup>, S. Nayak<sup>70</sup>, K. Pal [ID](#)<sup>70</sup>, R. Raturi<sup>70</sup>, P. Sadangi<sup>70</sup>, S.K. Swain [ID](#)<sup>70</sup>,  
 S. Varghese [ID](#)<sup>70,ao</sup>, D. Vats [ID](#)<sup>70,ao</sup>, A. Alpana [ID](#)<sup>71</sup>, S. Dube [ID](#)<sup>71</sup>, P. Hazarika [ID](#)<sup>71</sup>, B. Kansal [ID](#)<sup>71</sup>,  
 A. Laha [ID](#)<sup>71</sup>, R. Sharma [ID](#)<sup>71</sup>, S. Sharma [ID](#)<sup>71</sup>, K.Y. Vaish [ID](#)<sup>71</sup>, S. Ghosh [ID](#)<sup>72</sup>, H. Bakhshiansohi [ID](#)<sup>73,ap</sup>,  
 A. Jafari [ID](#)<sup>73,aq</sup>, V. Sedighzadeh Dalavi [ID](#)<sup>73</sup>, M. Zeinali [ID](#)<sup>73,ar</sup>, S. Bashiri [ID](#)<sup>74</sup>, S. Chenarani [ID](#)<sup>74,as</sup>,  
 S.M. Etesami [ID](#)<sup>74</sup>, Y. Hosseini [ID](#)<sup>74</sup>, M. Khakzad [ID](#)<sup>74</sup>, E. Khazaie [ID](#)<sup>74</sup>, M. Mohammadi Najafabadi [ID](#)<sup>74</sup>,  
 S. Tizchang [ID](#)<sup>74,at</sup>, M. Felcini [ID](#)<sup>75</sup>, M. Grunewald [ID](#)<sup>75</sup>, M. Abbrescia [ID](#)<sup>76a,76b</sup>, M. Barbieri [ID](#)<sup>76a,76b</sup>,  
 M. Buonsante [ID](#)<sup>76a,76b</sup>, A. Colaleo [ID](#)<sup>76a,76b</sup>, D. Creanza [ID](#)<sup>76a,76c</sup>, B. D'Anzi [ID](#)<sup>76a,76b</sup>,  
 N. De Filippis [ID](#)<sup>76a,76c</sup>, M. De Palma [ID](#)<sup>76a,76b</sup>, W. Elmetenawee [ID](#)<sup>76a,76b,au</sup>, N. Ferrara [ID](#)<sup>76a,76c</sup>,  
 L. Fiore [ID](#)<sup>76a</sup>, L. Longo [ID](#)<sup>76a</sup>, M. Louka [ID](#)<sup>76a,76b</sup>, G. Maggi [ID](#)<sup>76a,76c</sup>, M. Maggi [ID](#)<sup>76a</sup>, I. Margjeka [ID](#)<sup>76a</sup>,  
 V. Mastrapasqua [ID](#)<sup>76a,76b</sup>, S. My [ID](#)<sup>76a,76b</sup>, F. Nenna [ID](#)<sup>76a,76b</sup>, S. Nuzzo [ID](#)<sup>76a,76b</sup>, A. Pellicchia [ID](#)<sup>76a,76b</sup>,  
 A. Pompili [ID](#)<sup>76a,76b</sup>, G. Pugliese [ID](#)<sup>76a,76c</sup>, R. Radogna [ID](#)<sup>76a,76b</sup>, D. Ramos [ID](#)<sup>76a</sup>, A. Ranieri [ID](#)<sup>76a</sup>,  
 L. Silvestris [ID](#)<sup>76a</sup>, F.M. Simone [ID](#)<sup>76a,76c</sup>, A. Stamerra [ID](#)<sup>76a,76b</sup>, Ü. Sözbilir [ID](#)<sup>76a</sup>, D. Troiano [ID](#)<sup>76a,76b</sup>,  
 R. Venditti [ID](#)<sup>76a,76b</sup>, P. Verwilligen [ID](#)<sup>76a</sup>, A. Zaza [ID](#)<sup>76a,76b</sup>, G. Abbiendi [ID](#)<sup>77a</sup>, C. Battilana [ID](#)<sup>77a,77b</sup>,  
 D. Bonacorsi [ID](#)<sup>77a,77b</sup>, P. Capiluppi [ID](#)<sup>77a,77b</sup>, F.R. Cavallo [ID](#)<sup>77a</sup>, M. Cuffiani [ID](#)<sup>77a,77b</sup>,  
 G.M. Dallavalle [ID](#)<sup>77a</sup>, T. Diotallevi [ID](#)<sup>77a,77b</sup>, F. Fabbri [ID](#)<sup>77a</sup>, A. Fanfani [ID](#)<sup>77a,77b</sup>, D. Fasanella [ID](#)<sup>77a</sup>,  
 P. Giacomelli [ID](#)<sup>77a</sup>, C. Grandi [ID](#)<sup>77a</sup>, L. Guiducci [ID](#)<sup>77a,77b</sup>, S. Lo Meo [ID](#)<sup>77a,av</sup>, M. Lorusso [ID](#)<sup>77a,77b</sup>,  
 L. Lunerti [ID](#)<sup>77a</sup>, S. Marcellini [ID](#)<sup>77a</sup>, G. Masetti [ID](#)<sup>77a</sup>, F.L. Navarria [ID](#)<sup>77a,77b</sup>, G. Paggi [ID](#)<sup>77a,77b</sup>,  
 F. Primavera [ID](#)<sup>77a,77b</sup>, A.M. Rossi [ID](#)<sup>77a,77b</sup>, S. Rossi Tisbeni [ID](#)<sup>77a,77b</sup>, T. Rovelli [ID](#)<sup>77a,77b</sup>,  
 G.P. Siroli [ID](#)<sup>77a,77b</sup>, S. Costa [ID](#)<sup>78a,78b,aw</sup>, A. Di Mattia [ID](#)<sup>78a</sup>, A. Lapertosa [ID](#)<sup>78a</sup>, R. Potenza [ID](#)<sup>78a,78b</sup>,  
 A. Tricomi [ID](#)<sup>78a,78b,aw</sup>, J. Altork [ID](#)<sup>79a,79b</sup>, P. Assiouras [ID](#)<sup>79a</sup>, G. Barbagli [ID](#)<sup>79a</sup>, G. Bardelli [ID](#)<sup>79a</sup>,  
 M. Bartolini [ID](#)<sup>79a,79b</sup>, A. Calandri [ID](#)<sup>79a,79b</sup>, B. Camaiani [ID](#)<sup>79a,79b</sup>, A. Cassese [ID](#)<sup>79a</sup>, R. Ceccarelli [ID](#)<sup>79a</sup>,  
 V. Ciulli [ID](#)<sup>79a,79b</sup>, C. Civinini [ID](#)<sup>79a</sup>, R. D'Alessandro [ID](#)<sup>79a,79b</sup>, L. Damenti [ID](#)<sup>79a,79b</sup>, E. Focardi [ID](#)<sup>79a,79b</sup>,  
 T. Kello [ID](#)<sup>79a</sup>, G. Latino [ID](#)<sup>79a,79b</sup>, P. Lenzi [ID](#)<sup>79a,79b</sup>, M. Lizzo [ID](#)<sup>79a</sup>, M. Meschini [ID](#)<sup>79a</sup>, S. Paoletti [ID](#)<sup>79a</sup>,  
 A. Papanastassiou [ID](#)<sup>79a,79b</sup>, G. Sguazzoni [ID](#)<sup>79a</sup>, L. Viliani [ID](#)<sup>79a</sup>, L. Benussi [ID](#)<sup>80</sup>, S. Colafranceschi [ID](#)<sup>80</sup>,  
 S. Meola [ID](#)<sup>80,ax</sup>, D. Piccolo [ID](#)<sup>80</sup>, M. Alves Gallo Pereira [ID](#)<sup>81a</sup>, F. Ferro [ID](#)<sup>81a</sup>, E. Robutti [ID](#)<sup>81a</sup>,  
 S. Tosi [ID](#)<sup>81a,81b</sup>, A. Benaglia [ID](#)<sup>82a</sup>, F. Brivio [ID](#)<sup>82a</sup>, V. Camagni [ID](#)<sup>82a,82b</sup>, F. Cetorelli [ID](#)<sup>82a,82b</sup>,  
 F. De Guio [ID](#)<sup>82a,82b</sup>, M.E. Dinardo [ID](#)<sup>82a,82b</sup>, P. Dini [ID](#)<sup>82a</sup>, S. Gennai [ID](#)<sup>82a</sup>, R. Gerosa [ID](#)<sup>82a,82b</sup>,  
 A. Ghezzi [ID](#)<sup>82a,82b</sup>, P. Govoni [ID](#)<sup>82a,82b</sup>, L. Guzzi [ID](#)<sup>82a</sup>, M.R. Kim [ID](#)<sup>82a</sup>, G. Lavizzari [ID](#)<sup>82a,82b</sup>,  
 M.T. Lucchini [ID](#)<sup>82a,82b</sup>, M. Malberti [ID](#)<sup>82a</sup>, S. Malvezzi [ID](#)<sup>82a</sup>, A. Massironi [ID](#)<sup>82a</sup>, D. Menasce [ID](#)<sup>82a</sup>,  
 L. Moroni [ID](#)<sup>82a</sup>, M. Paganoni [ID](#)<sup>82a,82b</sup>, S. Palluotto [ID](#)<sup>82a,82b</sup>, D. Pedrini [ID](#)<sup>82a</sup>, A. Perego [ID](#)<sup>82a,82b</sup>,  
 B.S. Pinolini [ID](#)<sup>82a</sup>, G. Pizzati [ID](#)<sup>82a,82b</sup>, S. Ragazzi [ID](#)<sup>82a,82b</sup>, T. Tabarelli de Fatis [ID](#)<sup>82a,82b</sup>,  
 S. Buontempo [ID](#)<sup>83a</sup>, A. Cagnotta [ID](#)<sup>83a,83b</sup>, C. Di Fraia [ID](#)<sup>83a,83b</sup>, F. Fabozzi [ID](#)<sup>83a,83c</sup>,  
 L. Favilla [ID](#)<sup>83a,83d</sup>, A.O.M. Iorio [ID](#)<sup>83a,83b</sup>, L. Lista [ID](#)<sup>83a,83b,ay</sup>, P. Paolucci [ID](#)<sup>83a,ac</sup>, B. Rossi [ID](#)<sup>83a</sup>,  
 P. Azzi [ID](#)<sup>84a</sup>, N. Bacchetta [ID](#)<sup>84a,az</sup>, M. Biasotto [ID](#)<sup>84a,ba</sup>, D. Bisello [ID](#)<sup>84a,84b</sup>, P. Bortignon [ID](#)<sup>84a</sup>,  
 G. Bortolato [ID](#)<sup>84a,84b</sup>, A.C.M. Bulla [ID](#)<sup>84a</sup>, R. Carlin [ID](#)<sup>84a,84b</sup>, P. Checchia [ID](#)<sup>84a</sup>, T. Dorigo [ID](#)<sup>84a,bb</sup>,  
 U. Gasparini [ID](#)<sup>84a,84b</sup>, S. Giorgetti [ID](#)<sup>84a</sup>, E. Lusiani [ID](#)<sup>84a</sup>, M. Margoni [ID](#)<sup>84a,84b</sup>,  
 A.T. Meneguzzo [ID](#)<sup>84a,84b</sup>, J. Pazzini [ID](#)<sup>84a,84b</sup>, P. Ronchese [ID](#)<sup>84a,84b</sup>, R. Rossin [ID](#)<sup>84a,84b</sup>,  
 M. Tosi [ID](#)<sup>84a,84b</sup>, A. Triossi [ID](#)<sup>84a,84b</sup>, S. Ventura [ID](#)<sup>84a</sup>, M. Zanetti [ID](#)<sup>84a,84b</sup>, P. Zotto [ID](#)<sup>84a,84b</sup>,  
 A. Zucchetta [ID](#)<sup>84a,84b</sup>, G. Zumerle [ID](#)<sup>84a,84b</sup>, A. Braghieri [ID](#)<sup>85a</sup>, S. Calzaferri [ID](#)<sup>85a</sup>,  
 P. Montagna [ID](#)<sup>85a,85b</sup>, M. Pelliccioni [ID](#)<sup>85a</sup>, V. Re [ID](#)<sup>85a</sup>, C. Riccardi [ID](#)<sup>85a,85b</sup>, P. Salvini [ID](#)<sup>85a</sup>,  
 I. Vai [ID](#)<sup>85a,85b</sup>, P. Vitulo [ID](#)<sup>85a,85b</sup>, S. Ajmal [ID](#)<sup>86a,86b</sup>, M.E. Ascioti [ID](#)<sup>86a,86b</sup>, G.M. Bilei [ID](#)<sup>86a</sup>,  
 C. Carrivale [ID](#)<sup>86a,86b</sup>, D. Ciangottini [ID](#)<sup>86a,86b</sup>, L. Della Penna [ID](#)<sup>86a,86b</sup>, L. Fanò [ID](#)<sup>86a,86b</sup>,  
 V. Mariani [ID](#)<sup>86a,86b</sup>, M. Menichelli [ID](#)<sup>86a</sup>, F. Moscatelli [ID](#)<sup>86a,bc</sup>, A. Rossi [ID](#)<sup>86a,86b</sup>,

A. Santocchia [ID](#)<sup>86a,86b</sup>, D. Spiga [ID](#)<sup>86a</sup>, T. Tedeschi [ID](#)<sup>86a,86b</sup>, C. Aimè [ID](#)<sup>87a,87b</sup>, C.A. Alexe [ID](#)<sup>87a,87c</sup>,  
 P. Asenov [ID](#)<sup>87a,87b</sup>, P. Azzurri [ID](#)<sup>87a</sup>, G. Bagliesi [ID](#)<sup>87a</sup>, R. Bhattacharya [ID](#)<sup>87a</sup>, L. Bianchini [ID](#)<sup>87a,87b</sup>,  
 T. Boccali [ID](#)<sup>87a</sup>, E. Bossini [ID](#)<sup>87a</sup>, D. Bruschini [ID](#)<sup>87a,87c</sup>, L. Calligaris [ID](#)<sup>87a,87b</sup>, R. Castaldi [ID](#)<sup>87a</sup>,  
 F. Cattafesta [ID](#)<sup>87a,87c</sup>, M.A. Ciocci [ID](#)<sup>87a,87d</sup>, M. Cipriani [ID](#)<sup>87a,87b</sup>, V. D'Amante [ID](#)<sup>87a,87d</sup>,  
 R. Dell'Orso [ID](#)<sup>87a</sup>, S. Donato [ID](#)<sup>87a,87b</sup>, R. Forti [ID](#)<sup>87a,87b</sup>, A. Giassi [ID](#)<sup>87a</sup>, F. Ligabue [ID](#)<sup>87a,87c</sup>,  
 A.C. Marini [ID](#)<sup>87a,87b</sup>, D. Matos Figueiredo [ID](#)<sup>87a</sup>, A. Messineo [ID](#)<sup>87a,87b</sup>, S. Mishra [ID](#)<sup>87a</sup>,  
 V.K. Muraleedharan Nair Bindhu [ID](#)<sup>87a,87b</sup>, S. Nandan [ID](#)<sup>87a</sup>, F. Palla [ID](#)<sup>87a</sup>, M. Riggirello [ID](#)<sup>87a,87c</sup>,  
 A. Rizzi [ID](#)<sup>87a,87b</sup>, G. Rolandi [ID](#)<sup>87a,87c</sup>, S. Roy Chowdhury [ID](#)<sup>87a,bd</sup>, T. Sarkar [ID](#)<sup>87a</sup>, A. Scribano [ID](#)<sup>87a</sup>,  
 P. Solanki [ID](#)<sup>87a,87b</sup>, P. Spagnolo [ID](#)<sup>87a</sup>, F. Tenchini [ID](#)<sup>87a,87b</sup>, R. Tenchini [ID](#)<sup>87a</sup>, G. Tonelli [ID](#)<sup>87a,87b</sup>,  
 N. Turini [ID](#)<sup>87a,87d</sup>, F. Vaselli [ID](#)<sup>87a,87c</sup>, A. Venturi [ID](#)<sup>87a</sup>, P.G. Verdini [ID](#)<sup>87a</sup>, P. Akrap [ID](#)<sup>88a,88b</sup>,  
 C. Basile [ID](#)<sup>88a,88b</sup>, S.C. Behera [ID](#)<sup>88a</sup>, F. Cavallari [ID](#)<sup>88a</sup>, L. Cunqueiro Mendez [ID](#)<sup>88a,88b</sup>,  
 F. De Ruggi [ID](#)<sup>88a,88b</sup>, D. Del Re [ID](#)<sup>88a,88b</sup>, E. Di Marco [ID](#)<sup>88a</sup>, M. Diemoz [ID](#)<sup>88a</sup>, F. Errico [ID](#)<sup>88a</sup>,  
 L. Frosina [ID](#)<sup>88a,88b</sup>, R. Gargiulo [ID](#)<sup>88a,88b</sup>, B. Harikrishnan [ID](#)<sup>88a,88b</sup>, F. Lombardi [ID](#)<sup>88a,88b</sup>,  
 E. Longo [ID](#)<sup>88a,88b</sup>, L. Martikainen [ID](#)<sup>88a,88b</sup>, J. Mijuskovic [ID](#)<sup>88a,88b</sup>, G. Organtini [ID](#)<sup>88a,88b</sup>,  
 N. Palmeri [ID](#)<sup>88a,88b</sup>, R. Paramatti [ID](#)<sup>88a,88b</sup>, C. Quaranta [ID](#)<sup>88a,88b</sup>, S. Rahatlou [ID](#)<sup>88a,88b</sup>,  
 C. Rovelli [ID](#)<sup>88a</sup>, F. Santanastasio [ID](#)<sup>88a,88b</sup>, L. Soffi [ID](#)<sup>88a</sup>, V. Vladimirov [ID](#)<sup>88a,88b</sup>, N. Amapane [ID](#)<sup>89a,89b</sup>,  
 R. Arcidiacono [ID](#)<sup>89a,89c</sup>, S. Argiro [ID](#)<sup>89a,89b</sup>, M. Arneodo [ID](#)<sup>89a,89c</sup>, N. Bartosik [ID](#)<sup>89a,89c</sup>,  
 R. Bellan [ID](#)<sup>89a,89b</sup>, A. Bellora [ID](#)<sup>89a,89b</sup>, C. Biino [ID](#)<sup>89a</sup>, C. Borca [ID](#)<sup>89a,89b</sup>, N. Cartiglia [ID](#)<sup>89a</sup>,  
 M. Costa [ID](#)<sup>89a,89b</sup>, R. Covarelli [ID](#)<sup>89a,89b</sup>, N. Demaria [ID](#)<sup>89a</sup>, L. Finco [ID](#)<sup>89a</sup>, M. Grippo [ID](#)<sup>89a,89b</sup>,  
 B. Kiani [ID](#)<sup>89a,89b</sup>, F. Legger [ID](#)<sup>89a</sup>, F. Luongo [ID](#)<sup>89a,89b</sup>, C. Mariotti [ID](#)<sup>89a</sup>, S. Maselli [ID](#)<sup>89a</sup>,  
 A. Mecca [ID](#)<sup>89a,89b</sup>, L. Menzio [ID](#)<sup>89a,89b</sup>, P. Meridiani [ID](#)<sup>89a</sup>, E. Migliore [ID](#)<sup>89a,89b</sup>, M. Monteno [ID](#)<sup>89a</sup>,  
 M.M. Obertino [ID](#)<sup>89a,89b</sup>, G. Ortona [ID](#)<sup>89a</sup>, L. Pacher [ID](#)<sup>89a,89b</sup>, N. Pastrone [ID](#)<sup>89a</sup>, M. Ruspa [ID](#)<sup>89a,89c</sup>,  
 F. Siviero [ID](#)<sup>89a,89b</sup>, V. Sola [ID](#)<sup>89a,89b</sup>, A. Solano [ID](#)<sup>89a,89b</sup>, A. Staiano [ID](#)<sup>89a</sup>, C. Tarricone [ID](#)<sup>89a,89b</sup>,  
 D. Trocino [ID](#)<sup>89a</sup>, G. Umoret [ID](#)<sup>89a,89b</sup>, E. Vlasov [ID](#)<sup>89a,89b</sup>, R. White [ID](#)<sup>89a,89b</sup>, J. Babbar [ID](#)<sup>90a,90b</sup>,  
 S. Belforte [ID](#)<sup>90a</sup>, V. Candelise [ID](#)<sup>90a,90b</sup>, M. Casarsa [ID](#)<sup>90a</sup>, F. Cossutti [ID](#)<sup>90a</sup>, K. De Leo [ID](#)<sup>90a</sup>,  
 G. Della Ricca [ID](#)<sup>90a,90b</sup>, R. Delli Gatti [ID](#)<sup>90a,90b</sup>, S. Dogra [ID](#)<sup>91</sup>, J. Hong [ID](#)<sup>91</sup>, J. Kim [ID](#)<sup>91</sup>, T. Kim [ID](#)<sup>91</sup>,  
 D. Lee [ID](#)<sup>91</sup>, H. Lee [ID](#)<sup>91</sup>, J. Lee [ID](#)<sup>91</sup>, S.W. Lee [ID](#)<sup>91</sup>, C.S. Moon [ID](#)<sup>91</sup>, Y.D. Oh [ID](#)<sup>91</sup>, S. Sekmen [ID](#)<sup>91</sup>, B. Tae [ID](#)<sup>91</sup>,  
 Y.C. Yang [ID](#)<sup>91</sup>, M.S. Kim [ID](#)<sup>92</sup>, G. Bak [ID](#)<sup>93</sup>, P. Gwak [ID](#)<sup>93</sup>, H. Kim [ID](#)<sup>93</sup>, D.H. Moon [ID](#)<sup>93</sup>, J. Seo [ID](#)<sup>93</sup>,  
 E. Asilar [ID](#)<sup>94</sup>, F. Carnevali [ID](#)<sup>94</sup>, J. Choi [ID](#)<sup>94,be</sup>, T.J. Kim [ID](#)<sup>94</sup>, Y. Ryou [ID](#)<sup>94</sup>, S. Ha [ID](#)<sup>95</sup>, S. Han [ID](#)<sup>95</sup>,  
 B. Hong [ID](#)<sup>95</sup>, K. Lee [ID](#)<sup>95</sup>, K.S. Lee [ID](#)<sup>95</sup>, S. Lee [ID](#)<sup>95</sup>, J. Yoo [ID](#)<sup>95</sup>, J. Goh [ID](#)<sup>96</sup>, J. Shin [ID](#)<sup>96</sup>, S. Yang [ID](#)<sup>96</sup>,  
 Y. Kang [ID](#)<sup>97</sup>, H. S. Kim [ID](#)<sup>97</sup>, Y. Kim [ID](#)<sup>97</sup>, S. Lee [ID](#)<sup>97</sup>, J. Almond [ID](#)<sup>98</sup>, J.H. Bhyun [ID](#)<sup>98</sup>, J. Choi [ID](#)<sup>98</sup>,  
 J. Choi [ID](#)<sup>98</sup>, W. Jun [ID](#)<sup>98</sup>, H. Kim [ID](#)<sup>98</sup>, J. Kim [ID](#)<sup>98</sup>, T. Kim [ID](#)<sup>98</sup>, Y. Kim [ID](#)<sup>98</sup>, Y.W. Kim [ID](#)<sup>98</sup>, S. Ko [ID](#)<sup>98</sup>,  
 H. Lee [ID](#)<sup>98</sup>, J. Lee [ID](#)<sup>98</sup>, J. Lee [ID](#)<sup>98</sup>, B.H. Oh [ID](#)<sup>98</sup>, S.B. Oh [ID](#)<sup>98</sup>, J. Shin [ID](#)<sup>98</sup>, U.K. Yang [ID](#)<sup>98</sup>, I. Yoon [ID](#)<sup>98</sup>,  
 W. Jang [ID](#)<sup>99</sup>, D.Y. Kang [ID](#)<sup>99</sup>, D. Kim [ID](#)<sup>99</sup>, S. Kim [ID](#)<sup>99</sup>, B. Ko [ID](#)<sup>99</sup>, J.S.H. Lee [ID](#)<sup>99</sup>, Y. Lee [ID](#)<sup>99</sup>,  
 J.A. Merlin [ID](#)<sup>99</sup>, I.C. Park [ID](#)<sup>99</sup>, Y. Roh [ID](#)<sup>99</sup>, I.J. Watson [ID](#)<sup>99</sup>, G. Cho [ID](#)<sup>100</sup>, K. Hwang [ID](#)<sup>100</sup>, B. Kim [ID](#)<sup>100</sup>,  
 S. Kim [ID](#)<sup>100</sup>, K. Lee [ID](#)<sup>100</sup>, H.D. Yoo [ID](#)<sup>100</sup>, M. Choi [ID](#)<sup>101</sup>, Y. Lee [ID](#)<sup>101</sup>, I. Yu [ID](#)<sup>101</sup>, T. Beyrouthy [ID](#)<sup>102</sup>,  
 Y. Gharbia [ID](#)<sup>102</sup>, F. Alazemi [ID](#)<sup>103</sup>, K. Dreimanis [ID](#)<sup>104</sup>, O.M. Eberlins [ID](#)<sup>104</sup>, A. Gaile [ID](#)<sup>104</sup>,  
 C. Munoz Diaz [ID](#)<sup>104</sup>, D. Osite [ID](#)<sup>104</sup>, G. Pikurs [ID](#)<sup>104</sup>, R. Plese [ID](#)<sup>104</sup>, A. Potrebko [ID](#)<sup>104</sup>, M. Seidel [ID](#)<sup>104</sup>,  
 D. Sidiropoulos Kontos [ID](#)<sup>104</sup>, N.R. Strautnieks [ID](#)<sup>105</sup>, M. Ambrozias [ID](#)<sup>106</sup>, A. Juodagalvis [ID](#)<sup>106</sup>,  
 S. Nargelas [ID](#)<sup>106</sup>, A. Rinkevicius [ID](#)<sup>106</sup>, G. Tamulaitis [ID](#)<sup>106</sup>, I. Yusuff [ID](#)<sup>107,bf</sup>, Z. Zolkapli [ID](#)<sup>107</sup>,  
 J.F. Benitez [ID](#)<sup>108</sup>, A. Castaneda Hernandez [ID](#)<sup>108</sup>, A. Cota Rodriguez [ID](#)<sup>108</sup>, L.E. Cuevas Picos [ID](#)<sup>108</sup>,  
 H.A. Encinas Acosta [ID](#)<sup>108</sup>, L.G. Gallegos Maríñez [ID](#)<sup>108</sup>, J.A. Murillo Quijada [ID](#)<sup>108</sup>, A. Sehrawat [ID](#)<sup>108</sup>,  
 L. Valencia Palomo [ID](#)<sup>108</sup>, G. Ayala [ID](#)<sup>109</sup>, H. Castilla-Valdez [ID](#)<sup>109</sup>, H. Crotte Ledesma [ID](#)<sup>109</sup>,

R. Lopez-Fernandez<sup>109</sup>, J. Mejia Guisao<sup>109</sup>, R. Reyes-Almanza<sup>109</sup>, A. Sánchez Hernández<sup>109</sup>, C. Oropeza Barrera<sup>110</sup>, D.L. Ramirez Guadarrama<sup>110</sup>, M. Ramírez García<sup>110</sup>, I. Bautista<sup>111</sup>, F.E. Neri Huerta<sup>111</sup>, I. Pedraza<sup>111</sup>, H.A. Salazar Ibarguen<sup>111</sup>, C. Uribe Estrada<sup>111</sup>, I. Bubanja<sup>112</sup>, N. Raicevic<sup>112</sup>, P.H. Butler<sup>113</sup>, A. Ahmad<sup>114</sup>, M.I. Asghar<sup>114</sup>, A. Awais<sup>114</sup>, M.I.M. Awan<sup>114</sup>, W.A. Khan<sup>114</sup>, V. Avati<sup>115</sup>, L. Forthomme<sup>115</sup>, L. Grzanka<sup>115</sup>, M. Malawski<sup>115</sup>, K. Piotrkowski<sup>115</sup>, M. Bluj<sup>116</sup>, M. Górski<sup>116</sup>, M. Kazana<sup>116</sup>, M. Szeleper<sup>116</sup>, P. Zalewski<sup>116</sup>, K. Bunkowski<sup>117</sup>, K. Doroba<sup>117</sup>, A. Kalinowski<sup>117</sup>, M. Konecki<sup>117</sup>, J. Krolkowski<sup>117</sup>, A. Muhammad<sup>117</sup>, P. Fokow<sup>118</sup>, K. Pozniak<sup>118</sup>, W. Zablotny<sup>118</sup>, M. Araujo<sup>119</sup>, D. Bastos<sup>119</sup>, C. Beirão Da Cruz E Silva<sup>119</sup>, A. Boletti<sup>119</sup>, M. Bozzo<sup>119</sup>, T. Camporesi<sup>119</sup>, G. Da Molin<sup>119</sup>, P. Faccioli<sup>119</sup>, M. Gallinaro<sup>119</sup>, J. Hollar<sup>119</sup>, N. Leonardo<sup>119</sup>, G.B. Marozzo<sup>119</sup>, A. Petrilli<sup>119</sup>, M. Pisano<sup>119</sup>, J. Seixas<sup>119</sup>, J. Varela<sup>119</sup>, J.W. Wulff<sup>119</sup>, P. Adzic<sup>120</sup>, L. Markovic<sup>120</sup>, P. Milenovic<sup>120</sup>, V. Milosevic<sup>120</sup>, D. Devetak<sup>121</sup>, M. Dordevic<sup>121</sup>, J. Milosevic<sup>121</sup>, L. Nadder<sup>121</sup>, V. Rekovic<sup>121</sup>, M. Stojanovic<sup>121</sup>, M. Alcalde Martinez<sup>122</sup>, J. Alcaraz Maestre<sup>122</sup>, J.A. Brochero Cifuentes<sup>122</sup>, M. Cepeda<sup>122</sup>, M. Cerrada<sup>122</sup>, N. Colino<sup>122</sup>, J. Cuchillo Ortega<sup>122</sup>, B. De La Cruz<sup>122</sup>, A. Delgado Peris<sup>122</sup>, A. Escalante Del Valle<sup>122</sup>, Cristina F. Bedoya<sup>122</sup>, D. Fernández Del Val<sup>122</sup>, J.P. Fernández Ramos<sup>122</sup>, J. Flix<sup>122</sup>, M.C. Fouz<sup>122</sup>, M. Gonzalez Hernandez<sup>122</sup>, O. Gonzalez Lopez<sup>122</sup>, S. Goy Lopez<sup>122</sup>, J.M. Hernandez<sup>122</sup>, M.I. Josa<sup>122</sup>, J. Llorente Merino<sup>122</sup>, Oliver M. Carretero<sup>122</sup>, C. Martin Perez<sup>122</sup>, E. Martin Viscasillas<sup>122</sup>, D. Moran<sup>122</sup>, C. M. Morcillo Perez<sup>122</sup>, R. Paz Herrera<sup>122</sup>, C. Perez Dengra<sup>122</sup>, J. Puerta Pelayo<sup>122</sup>, A. Pérez-Calero Yzquierdo<sup>122</sup>, I. Redondo<sup>122</sup>, J. Vazquez Escobar<sup>122</sup>, J.F. de Trocóniz<sup>123</sup>, B. Alvarez Gonzalez<sup>124</sup>, J. Ayllon Torresano<sup>124</sup>, A. Cardini<sup>124</sup>, J. Cuevas<sup>124</sup>, J. Del Riego Badas<sup>124</sup>, D. Estrada Acevedo<sup>124</sup>, J. Fernandez Menendez<sup>124</sup>, S. Folgueras<sup>124</sup>, I. Gonzalez Caballero<sup>124</sup>, P. Leguina<sup>124</sup>, M. Obeso Menendez<sup>124</sup>, E. Palencia Cortezon<sup>124</sup>, J. Prado Pico<sup>124</sup>, A. Soto Rodríguez<sup>124</sup>, C. Vico Villalba<sup>124</sup>, P. Vischia<sup>124</sup>, S. Blanco Fernández<sup>125</sup>, I.J. Cabrillo<sup>125</sup>, A. Calderon<sup>125</sup>, J. Duarte Campderros<sup>125</sup>, M. Fernandez<sup>125</sup>, G. Gomez<sup>125</sup>, C. Lasaoa García<sup>125</sup>, R. Lopez Ruiz<sup>125</sup>, C. Martinez Rivero<sup>125</sup>, P. Martinez Ruiz del Arbol<sup>125</sup>, F. Matorras<sup>125</sup>, P. Matorras Cuevas<sup>125</sup>, E. Navarrete Ramos<sup>125</sup>, J. Piedra Gomez<sup>125</sup>, C. Quintana San Emeterio<sup>125</sup>, L. Scodellaro<sup>125</sup>, I. Vila<sup>125</sup>, R. Vilar Cortabitarte<sup>125</sup>, J.M. Vizán Garcia<sup>125</sup>, D.D.C. Wickramaratna<sup>126</sup>, B. Kailasapathy<sup>126,bg</sup>, W.G.D. Dharmaratna<sup>127,bh</sup>, K. Liyanage<sup>127</sup>, N. Perera<sup>127</sup>, D. Abbaneo<sup>128</sup>, C. Amendola<sup>128</sup>, R. Ardino<sup>128</sup>, E. Auffray<sup>128</sup>, J. Baechler<sup>128</sup>, D. Barney<sup>128</sup>, M. Bianco<sup>128</sup>, A. Bocci<sup>128</sup>, L. Borgonovi<sup>128</sup>, C. Botta<sup>128</sup>, A. Bragagnolo<sup>128</sup>, C.E. Brown<sup>128</sup>, C. Caillol<sup>128</sup>, G. Cerminara<sup>128</sup>, P. Connor<sup>128</sup>, D. d’Enterria<sup>128</sup>, A. Dabrowski<sup>128</sup>, A. David<sup>128</sup>, A. De Roeck<sup>128</sup>, M.M. Defranchis<sup>128</sup>, M. Deile<sup>128</sup>, M. Dobson<sup>128</sup>, W. Funk<sup>128</sup>, A. Gaddi<sup>128</sup>, S. Giani<sup>128</sup>, D. Gigi<sup>128</sup>, K. Gill<sup>128</sup>, F. Glege<sup>128</sup>, M. Glowacki<sup>128</sup>, A. Gruber<sup>128</sup>, J. Hegeman<sup>128</sup>, J.K. Heikkilä<sup>128</sup>, B. Huber<sup>128</sup>, V. Innocente<sup>128</sup>, T. James<sup>128</sup>, P. Janot<sup>128</sup>, O. Kaluzinska<sup>128</sup>, O. Karacheban<sup>128,z</sup>, G. Karathanasis<sup>128</sup>, L. Lanteri<sup>128</sup>, S. Laurila<sup>128</sup>, P. Lecoq<sup>128</sup>, C. Lourenço<sup>128</sup>, A.-M. Lyon<sup>128</sup>, M. Magherini<sup>128</sup>, L. Malgeri<sup>128</sup>, M. Mannelli<sup>128</sup>, A. Mehta<sup>128</sup>, F. Meijers<sup>128</sup>, S. Mersi<sup>128</sup>, E. Meschi<sup>128</sup>, M. Migliorini<sup>128</sup>, F. Monti<sup>128</sup>, F. Moortgat<sup>128</sup>, M. Mulders<sup>128</sup>, M. Musich<sup>128</sup>, I. Neutelings<sup>128</sup>, S. Orfanelli<sup>128</sup>, F. Pantaleo<sup>128</sup>, M. Pari<sup>128</sup>,

G. Petrucciani<sup>128</sup>, A. Pfeiffer<sup>128</sup>, M. Pierini<sup>128</sup>, M. Pitt<sup>128</sup>, H. Qu<sup>128</sup>, D. Rabady<sup>128</sup>,  
 B. Ribeiro Lopes<sup>128</sup>, F. Riti<sup>128</sup>, P. Rosado<sup>128</sup>, M. Rovere<sup>128</sup>, H. Sakulin<sup>128</sup>,  
 R. Salvatico<sup>128</sup>, S. Sanchez Cruz<sup>128</sup>, S. Scarfi<sup>128</sup>, M. Selvaggi<sup>128</sup>, A. Sharma<sup>128</sup>,  
 K. Shchelina<sup>128</sup>, P. Silva<sup>128</sup>, P. Sphicas<sup>128,bi</sup>, A.G. Stahl Leiton<sup>128</sup>, A. Steen<sup>128</sup>,  
 S. Summers<sup>128</sup>, D. Treille<sup>128</sup>, P. Tropea<sup>128</sup>, E. Vernazza<sup>128</sup>, J. Wanczyk<sup>128,bj</sup>, J. Wang<sup>128</sup>,  
 S. Wuchterl<sup>128</sup>, M. Zarucki<sup>128</sup>, P. Zehetner<sup>128</sup>, P. Zejdl<sup>128</sup>, G. Zevi Della Porta<sup>128</sup>,  
 T. Bevilacqua<sup>129,bk</sup>, L. Caminada<sup>129,bk</sup>, W. Erdmann<sup>129</sup>, R. Horisberger<sup>129</sup>, Q. Ingram<sup>129</sup>,  
 H.C. Kaestli<sup>129</sup>, D. Kotlinski<sup>129</sup>, C. Lange<sup>129</sup>, U. Langenegger<sup>129</sup>, M. Missiroli<sup>129,bk</sup>,  
 L. Noehte<sup>129,bk</sup>, T. Rohe<sup>129</sup>, A. Samalan<sup>129</sup>, T.K. Aarrestad<sup>130</sup>, M. Backhaus<sup>130</sup>,  
 G. Bonomelli<sup>130</sup>, C. Cazzaniga<sup>130</sup>, K. Datta<sup>130</sup>, P. De Bryas Dexmiers D'archiacchiac<sup>130,bj</sup>,  
 A. De Cosa<sup>130</sup>, G. Dissertori<sup>130</sup>, M. Dittmar<sup>130</sup>, M. Donegà<sup>130</sup>, F. Eble<sup>130</sup>, K. Gedia<sup>130</sup>,  
 F. Glessgen<sup>130</sup>, C. Grab<sup>130</sup>, T.G. Harte<sup>130</sup>, N. Härringer<sup>130</sup>, W. Lustermann<sup>130</sup>,  
 M. Malucchi<sup>130</sup>, R.A. Manzoni<sup>130</sup>, M. Marchegiani<sup>130</sup>, L. Marchese<sup>130</sup>, A. Mascellani<sup>130,bj</sup>,  
 F. Nessi-Tedaldi<sup>130</sup>, F. Pauss<sup>130</sup>, V. Perovic<sup>130</sup>, B. Ristic<sup>130</sup>, R. Seidita<sup>130</sup>,  
 J. Steggemann<sup>130,bj</sup>, A. Tarabini<sup>130</sup>, D. Valsecchi<sup>130</sup>, R. Wallny<sup>130</sup>, C. AMSler<sup>131,bl</sup>,  
 F. Bilandzija<sup>131</sup>, P. Bärtschi<sup>131</sup>, M.F. Canelli<sup>131</sup>, G. Celotto<sup>131</sup>, K. Cormier<sup>131</sup>,  
 M. Huwiler<sup>131</sup>, W. Jin<sup>131</sup>, A. Jofrehei<sup>131</sup>, B. Kilminster<sup>131</sup>, T.H. Kwok<sup>131</sup>,  
 S. Leontsinis<sup>131</sup>, V. Lukashenko<sup>131</sup>, A. Macchiolo<sup>131</sup>, F. Meng<sup>131</sup>, J. Motta<sup>131</sup>,  
 A. Reimers<sup>131</sup>, P. Robmann<sup>131</sup>, M. Senger<sup>131</sup>, E. Shokr<sup>131</sup>, F. Stäger<sup>131</sup>,  
 R. Tramontano<sup>131</sup>, D. Bhowmik<sup>132</sup>, C.M. Kuo<sup>132</sup>, P.K. Rout<sup>132</sup>, S. Taj<sup>132</sup>, P.C. Tiwari<sup>132,al</sup>,  
 L. Ceard<sup>133</sup>, K.F. Chen<sup>133</sup>, Z.g. Chen<sup>133</sup>, A. De Iorio<sup>133</sup>, W.-S. Hou<sup>133</sup>, T.h. Hsu<sup>133</sup>,  
 Y.w. Kao<sup>133</sup>, S. Karmakar<sup>133</sup>, G. Kole<sup>133</sup>, Y.y. Li<sup>133</sup>, R.-S. Lu<sup>133</sup>, E. Paganis<sup>133</sup>,  
 X.f. Su<sup>133</sup>, J. Thomas-Wilsker<sup>133</sup>, L.s. Tsai<sup>133</sup>, D. Tsiou<sup>133</sup>, H.y. Wu<sup>133</sup>, E. Yazgan<sup>133</sup>,  
 C. Asawatangtrakuldee<sup>134</sup>, N. Srimanobhas<sup>134</sup>, Y. Maghrbi<sup>135</sup>, D. Agyel<sup>136</sup>, F. Boran<sup>136</sup>,  
 F. Dolek<sup>136</sup>, I. Dumanoglu<sup>136,bm</sup>, Y. Guler<sup>136,bn</sup>, E. Gurpinar Guler<sup>136,bn</sup>, C. Isik<sup>136</sup>,  
 O. Kara<sup>136</sup>, A. Kayis Topaksu<sup>136</sup>, Y. Komurcu<sup>136</sup>, G. Onengut<sup>136</sup>, K. Ozdemir<sup>136,bo</sup>,  
 B. Tali<sup>136,bp</sup>, U.G. Tok<sup>136</sup>, E. Uslan<sup>136</sup>, I.S. Zorbakir<sup>136</sup>, M. Yalvac<sup>137,bq</sup>, B. Akgun<sup>138</sup>,  
 I.O. Atakisi<sup>138,br</sup>, E. Gülmez<sup>138</sup>, M. Kaya<sup>138,bs</sup>, O. Kaya<sup>138,bt</sup>, M.A. Sarkisla<sup>138,bu</sup>,  
 S. Tekten<sup>138,bv</sup>, A. Cakir<sup>139</sup>, K. Cankocak<sup>139,bm,bw</sup>, S. Sen<sup>139,bx</sup>, O. Aydilek<sup>140,by</sup>,  
 B. Haciasahinoglu<sup>140</sup>, I. Hos<sup>140,bz</sup>, B. Kaynak<sup>140</sup>, S. Ozkorucuklu<sup>140</sup>, O. Potok<sup>140</sup>,  
 H. Sert<sup>140</sup>, C. Simsek<sup>140</sup>, C. Zorbilmez<sup>140</sup>, S. Cerci<sup>141</sup>, A.A. Guvenli<sup>141</sup>, B. Isildak<sup>141,ca</sup>,  
 D. Sunar Cerci<sup>141</sup>, T. Yetkin<sup>141,u</sup>, A. Boyaryntsev<sup>142</sup>, O. Dadazhanova<sup>142</sup>, B. Grynyov<sup>142</sup>,  
 L. Levchuk<sup>143</sup>, J.J. Brooke<sup>144</sup>, A. Bundock<sup>144</sup>, F. Bury<sup>144</sup>, E. Clement<sup>144</sup>, D. Cussans<sup>144</sup>,  
 D. Dharmender<sup>144</sup>, H. Flacher<sup>144</sup>, J. Goldstein<sup>144</sup>, H.F. Heath<sup>144</sup>, M.-L. Holmberg<sup>144</sup>,  
 L. Kreczko<sup>144</sup>, S. Paramesvaran<sup>144</sup>, L. Robertshaw<sup>144</sup>, M.S. Sanjrani<sup>144</sup>, J. Segal<sup>144</sup>,  
 V.J. Smith<sup>144</sup>, A.H. Ball<sup>145</sup>, K.W. Bell<sup>145</sup>, A. Belyaev<sup>145,cb</sup>, C. Brew<sup>145</sup>, R.M. Brown<sup>145</sup>,  
 D.J.A. Cockerill<sup>145</sup>, C. Cooke<sup>145</sup>, A. Elliot<sup>145</sup>, K.V. Ellis<sup>145</sup>, J. Gajownik<sup>145</sup>, K. Harder<sup>145</sup>,  
 S. Harper<sup>145</sup>, J. Linacre<sup>145</sup>, K. Manolopoulos<sup>145</sup>, M. Moallemi<sup>145</sup>, D.M. Newbold<sup>145</sup>,  
 E. Olaiya<sup>145</sup>, D. Petyt<sup>145</sup>, T. Reis<sup>145</sup>, A.R. Sahasransu<sup>145</sup>, G. Salvi<sup>145</sup>, T. Schuh<sup>145</sup>,  
 C.H. Shepherd-Themistocleous<sup>145</sup>, I.R. Tomalin<sup>145</sup>, K.C. Whalen<sup>145</sup>, T. Williams<sup>145</sup>,  
 I. Andreou<sup>146</sup>, R. Bainbridge<sup>146</sup>, P. Bloch<sup>146</sup>, O. Buchmuller<sup>146</sup>, C.A. Carrillo Montoya<sup>146</sup>,  
 D. Colling<sup>146</sup>, J.S. Dancu<sup>146</sup>, I. Das<sup>146</sup>, P. Dauncey<sup>146</sup>, G. Davies<sup>146</sup>, M. Della Negra<sup>146</sup>,  
 S. Fayer<sup>146</sup>, G. Fedi<sup>146</sup>, G. Hall<sup>146</sup>, H.R. Hoorani<sup>146</sup>, A. Howard<sup>146</sup>, G. Iles<sup>146</sup>,

C.R. Knight <sup>146</sup>, P. Krueper <sup>146</sup>, J. Langford <sup>146</sup>, K.H. Law <sup>146</sup>, E. Leutgeb <sup>146</sup>,  
 J. León Holgado <sup>146</sup>, L. Lyons <sup>146</sup>, A.-M. Magnan <sup>146</sup>, B. Maier <sup>146</sup>, S. Mallios <sup>146</sup>,  
 A. Mastronikolis <sup>146</sup>, M. Mieskolainen <sup>146</sup>, J. Nash <sup>146,cc</sup>, M. Pesaresi <sup>146</sup>, P.B. Pradeep <sup>146</sup>,  
 B.C. Radburn-Smith <sup>146</sup>, A. Richards <sup>146</sup>, A. Rose <sup>146</sup>, L. Russell <sup>146</sup>, K. Savva <sup>146</sup>, C. Seez <sup>146</sup>,  
 R. Shukla <sup>146</sup>, A. Tapper <sup>146</sup>, K. Uchida <sup>146</sup>, G.P. Uttley <sup>146</sup>, T. Virdee <sup>146,ac</sup>,  
 M. Vojinovic <sup>146</sup>, N. Wardle <sup>146</sup>, D. Winterbottom <sup>146</sup>, J.E. Cole <sup>147</sup>, A. Khan <sup>147</sup>,  
 P. Kyberd <sup>147</sup>, I.D. Reid <sup>147</sup>, S. Abdullin <sup>148</sup>, A. Brinkerhoff <sup>148</sup>, E. Collins <sup>148</sup>,  
 M.R. Darwish <sup>148</sup>, J. Dittmann <sup>148</sup>, K. Hatakeyama <sup>148</sup>, V. Hegde <sup>148</sup>, J. Hiltbrand <sup>148</sup>,  
 B. McMaster <sup>148</sup>, J. Samudio <sup>148</sup>, S. Sawant <sup>148</sup>, C. Sutantawibul <sup>148</sup>, J. Wilson <sup>148</sup>,  
 J.M. Hogan <sup>149,cd</sup>, R. Bartek <sup>150</sup>, A. Dominguez <sup>150</sup>, S. Raj <sup>150</sup>, A.E. Simsek <sup>150</sup>, S.S. Yu <sup>150</sup>,  
 B. Bam <sup>151</sup>, A. Buchot Perraguin <sup>151</sup>, S. Campbell <sup>151</sup>, R. Chudasama <sup>151</sup>, S.I. Cooper <sup>151</sup>,  
 C. Crovella <sup>151</sup>, G. Fidalgo <sup>151</sup>, S.V. Gleyzer <sup>151</sup>, A. Khukhunaishvili <sup>151</sup>, K. Matchev <sup>151</sup>,  
 E. Pearson <sup>151</sup>, C.U. Perez <sup>151</sup>, P. Rumerio <sup>151,ce</sup>, E. Usai <sup>151</sup>, R. Yi <sup>151</sup>, S. Cholak <sup>152</sup>,  
 G. De Castro <sup>152</sup>, Z. Demiragli <sup>152</sup>, C. Erice <sup>152</sup>, C. Fangmeier <sup>152</sup>, C. Fernandez Madrazo <sup>152</sup>,  
 E. Fontanesi <sup>152</sup>, J. Fulcher <sup>152</sup>, F. Golf <sup>152</sup>, S. Jeon <sup>152</sup>, J. O’Cain <sup>152</sup>, I. Reed <sup>152</sup>,  
 J. Rohlf <sup>152</sup>, K. Salyer <sup>152</sup>, D. Sperka <sup>152</sup>, D. Spitzbart <sup>152</sup>, I. Suarez <sup>152</sup>, A. Tsatsos <sup>152</sup>,  
 E. Wurtz <sup>152</sup>, A.G. Zecchinelli <sup>152</sup>, G. Barone <sup>153</sup>, G. Benelli <sup>153</sup>, D. Cutts <sup>153</sup>, S. Ellis <sup>153</sup>,  
 L. Gouskos <sup>153</sup>, M. Hadley <sup>153</sup>, U. Heintz <sup>153</sup>, K.W. Ho <sup>153</sup>, T. Kwon <sup>153</sup>, G. Landsberg <sup>153</sup>,  
 K.T. Lau <sup>153</sup>, J. Luo <sup>153</sup>, S. Mondal <sup>153</sup>, J. Roloff <sup>153</sup>, T. Russell <sup>153</sup>, S. Sagir <sup>153,cf</sup>,  
 X. Shen <sup>153</sup>, M. Stamenkovic <sup>153</sup>, N. Venkatasubramanian <sup>153</sup>, S. Abbott <sup>154</sup>, B. Barton <sup>154</sup>,  
 R. Breedon <sup>154</sup>, H. Cai <sup>154</sup>, M. Calderon De La Barca Sanchez <sup>154</sup>, M. Chertok <sup>154</sup>,  
 M. Citron <sup>154</sup>, J. Conway <sup>154</sup>, P.T. Cox <sup>154</sup>, R. Erbacher <sup>154</sup>, O. Kukral <sup>154</sup>, G. Mocellin <sup>154</sup>,  
 S. Ostrom <sup>154</sup>, W. Wei <sup>154</sup>, S. Yoo <sup>154</sup>, K. Adamidis <sup>155</sup>, M. Bachtis <sup>155</sup>, D. Campos <sup>155</sup>,  
 R. Cousins <sup>155</sup>, A. Datta <sup>155</sup>, G. Flores Avila <sup>155</sup>, J. Hauser <sup>155</sup>, M. Ignatenko <sup>155</sup>,  
 M.A. Iqbal <sup>155</sup>, T. Lam <sup>155</sup>, Y.f. Lo <sup>155</sup>, E. Manca <sup>155</sup>, A. Nunez Del Prado <sup>155</sup>,  
 D. Saltzberg <sup>155</sup>, V. Valuev <sup>155</sup>, R. Clare <sup>156</sup>, J.W. Gary <sup>156</sup>, G. Hanson <sup>156</sup>, A. Aportela <sup>157</sup>,  
 A. Arora <sup>157</sup>, J.G. Branson <sup>157</sup>, S. Cittolin <sup>157</sup>, S. Cooperstein <sup>157</sup>, D. Diaz <sup>157</sup>, J. Duarte <sup>157</sup>,  
 L. Giannini <sup>157</sup>, Y. Gu <sup>157</sup>, J. Guiang <sup>157</sup>, V. Krutelyov <sup>157</sup>, R. Lee <sup>157</sup>, J. Letts <sup>157</sup>, H. Li <sup>157</sup>,  
 M. Masciovecchio <sup>157</sup>, F. Mokhtar <sup>157</sup>, S. Mukherjee <sup>157</sup>, M. Pieri <sup>157</sup>, D. Primosch <sup>157</sup>,  
 M. Quinnan <sup>157</sup>, V. Sharma <sup>157</sup>, M. Tadel <sup>157</sup>, E. Vourliotis <sup>157</sup>, F. Würthwein <sup>157</sup>,  
 A. Yagil <sup>157</sup>, Z. Zhao <sup>157</sup>, A. Barzdukas <sup>158</sup>, L. Brennan <sup>158</sup>, C. Campagnari <sup>158</sup>,  
 S. Carron Montero <sup>158,cg</sup>, K. Downham <sup>158</sup>, C. Grieco <sup>158</sup>, M.M. Hussain <sup>158</sup>, J. Incandela <sup>158</sup>,  
 J. Kim <sup>158</sup>, M.W.K. Lai <sup>158</sup>, A.J. Li <sup>158</sup>, P. Masterson <sup>158</sup>, J. Richman <sup>158</sup>, S.N. Santpur <sup>158</sup>,  
 U. Sarica <sup>158</sup>, R. Schmitz <sup>158</sup>, F. Setti <sup>158</sup>, J. Sheplock <sup>158</sup>, D. Stuart <sup>158</sup>, T.Á. Vámi <sup>158</sup>,  
 X. Yan <sup>158</sup>, D. Zhang <sup>158</sup>, A. Albert <sup>159</sup>, S. Bhattacharya <sup>159</sup>, A. Bornheim <sup>159</sup>, O. Cerri <sup>159</sup>,  
 R. Kansal <sup>159</sup>, J. Mao <sup>159</sup>, H.B. Newman <sup>159</sup>, G. Reales Gutiérrez <sup>159</sup>, T. Sievert <sup>159</sup>,  
 M. Spiropulu <sup>159</sup>, J.R. Vlimant <sup>159</sup>, R.A. Wynne <sup>159</sup>, S. Xie <sup>159</sup>, J. Alison <sup>160</sup>, S. An <sup>160</sup>,  
 M. Cremonesi <sup>160</sup>, V. Dutta <sup>160</sup>, E.Y. Ertorer <sup>160</sup>, T. Ferguson <sup>160</sup>, T.A. Gómez Espinosa <sup>160</sup>,  
 A. Harilal <sup>160</sup>, A. Kallil Tharayil <sup>160</sup>, M. Kanemura <sup>160</sup>, C. Liu <sup>160</sup>, P. Meiring <sup>160</sup>,  
 T. Mudholkar <sup>160</sup>, S. Murthy <sup>160</sup>, P. Palit <sup>160</sup>, K. Park <sup>160</sup>, M. Paulini <sup>160</sup>, A. Roberts <sup>160</sup>,  
 A. Sanchez <sup>160</sup>, W. Terrill <sup>160</sup>, J.P. Cumalat <sup>161</sup>, W.T. Ford <sup>161</sup>, A. Hart <sup>161</sup>, A. Hassani <sup>161</sup>,  
 S. Kwan <sup>161</sup>, J. Parkes <sup>161</sup>, C. Savard <sup>161</sup>, N. Schonbeck <sup>161</sup>, K. Stenson <sup>161</sup>, K.A. Ulmer <sup>161</sup>,  
 S.R. Wagner <sup>161</sup>, N. Zipper <sup>161</sup>, D. Zuolo <sup>161</sup>, J. Alexander <sup>162</sup>, X. Chen <sup>162</sup>,

D.J. Cranshaw<sup>162</sup>, J. Dickinson<sup>162</sup>, J. Fan<sup>162</sup>, X. Fan<sup>162</sup>, J. Grassi<sup>162</sup>, S. Hogan<sup>162</sup>,  
 P. Kotamnives<sup>162</sup>, J. Monroy<sup>162</sup>, G. Niendorf<sup>162</sup>, M. Oshiro<sup>162</sup>, J.R. Patterson<sup>162</sup>,  
 M. Reid<sup>162</sup>, A. Ryd<sup>162</sup>, J. Thom<sup>162</sup>, P. Wittich<sup>162</sup>, R. Zou<sup>162</sup>, L. Zygala<sup>162</sup>,  
 M. Albrow<sup>163</sup>, M. Alyari<sup>163</sup>, O. Amram<sup>163</sup>, G. Apollinari<sup>163</sup>, A. Apresyan<sup>163</sup>,  
 L.A.T. Bauerdick<sup>163</sup>, D. Berry<sup>163</sup>, J. Berryhill<sup>163</sup>, P.C. Bhat<sup>163</sup>, K. Burkett<sup>163</sup>,  
 J.N. Butler<sup>163</sup>, A. Canepa<sup>163</sup>, G.B. Cerati<sup>163</sup>, H.W.K. Cheung<sup>163</sup>, F. Chlebana<sup>163</sup>,  
 C. Cosby<sup>163</sup>, G. Cummings<sup>163</sup>, I. Dutta<sup>163</sup>, V.D. Elvira<sup>163</sup>, J. Freeman<sup>163</sup>,  
 A. Gandrakota<sup>163</sup>, Z. Gece<sup>163</sup>, L. Gray<sup>163</sup>, D. Green<sup>163</sup>, A. Grummer<sup>163</sup>,  
 S. Grünendahl<sup>163</sup>, D. Guerrero<sup>163</sup>, O. Gutsche<sup>163</sup>, R.M. Harris<sup>163</sup>, T.C. Herwig<sup>163</sup>,  
 J. Hirschauer<sup>163</sup>, B. Jayatilaka<sup>163</sup>, S. Jindariani<sup>163</sup>, M. Johnson<sup>163</sup>, U. Joshi<sup>163</sup>,  
 T. Klijsma<sup>163</sup>, B. Klima<sup>163</sup>, K.H.M. Kwok<sup>163</sup>, S. Lammel<sup>163</sup>, C. Lee<sup>163</sup>, D. Lincoln<sup>163</sup>,  
 R. Lipton<sup>163</sup>, T. Liu<sup>163</sup>, K. Maeshima<sup>163</sup>, D. Mason<sup>163</sup>, P. McBride<sup>163</sup>, P. Merkel<sup>163</sup>,  
 S. Mrenna<sup>163</sup>, S. Nahn<sup>163</sup>, J. Ngadiuba<sup>163</sup>, D. Noonan<sup>163</sup>, S. Norberg<sup>163</sup>,  
 V. Papadimitriou<sup>163</sup>, N. Pastika<sup>163</sup>, K. Pedro<sup>163</sup>, C. Pena<sup>163, ch</sup>, C.E. Perez Lara<sup>163</sup>,  
 F. Ravera<sup>163</sup>, A. Reinsvold Hall<sup>163, ci</sup>, L. Ristori<sup>163</sup>, M. Safdari<sup>163</sup>, E. Sexton-Kennedy<sup>163</sup>,  
 N. Smith<sup>163</sup>, A. Soha<sup>163</sup>, L. Spiegel<sup>163</sup>, S. Stoynev<sup>163</sup>, J. Strait<sup>163</sup>, L. Taylor<sup>163</sup>,  
 S. Tkaczyk<sup>163</sup>, N.V. Tran<sup>163</sup>, L. Uplegger<sup>163</sup>, E.W. Vaandering<sup>163</sup>, C. Wang<sup>163</sup>, I. Zoi<sup>163</sup>,  
 C. Aruta<sup>164</sup>, P. Avery<sup>164</sup>, D. Bourilkov<sup>164</sup>, P. Chang<sup>164</sup>, V. Cherepanov<sup>164</sup>, R.D. Field<sup>164</sup>,  
 C. Huh<sup>164</sup>, E. Koenig<sup>164</sup>, M. Kolosova<sup>164</sup>, J. Konigsberg<sup>164</sup>, A. Korytov<sup>164</sup>,  
 N. Menendez<sup>164</sup>, G. Mitselmakher<sup>164</sup>, K. Mohrman<sup>164</sup>, A. Muthirakalayil Madhu<sup>164</sup>,  
 N. Rawal<sup>164</sup>, S. Rosenzweig<sup>164</sup>, V. Sulimov<sup>164</sup>, Y. Takahashi<sup>164</sup>, J. Wang<sup>164</sup>,  
 T. Adams<sup>165</sup>, A. Al Kadhim<sup>165</sup>, A. Askew<sup>165</sup>, S. Bower<sup>165</sup>, R. Hashmi<sup>165</sup>, R.S. Kim<sup>165</sup>,  
 T. Kolberg<sup>165</sup>, G. Martinez<sup>165</sup>, M. Mazza<sup>165</sup>, H. Prosper<sup>165</sup>, P.R. Prova<sup>165</sup>,  
 M. Wulansatiti<sup>165</sup>, R. Yohay<sup>165</sup>, B. Alsufyani<sup>166</sup>, S. Butalla<sup>166</sup>, S. Das<sup>166</sup>,  
 M. Hohmann<sup>166</sup>, M. Lavinsky<sup>166</sup>, E. Yanes<sup>166</sup>, M.R. Adams<sup>167</sup>, N. Barnett<sup>167</sup>, A. Baty<sup>167</sup>,  
 C. Bennett<sup>167</sup>, R. Cavanaugh<sup>167</sup>, D. S. Lemos<sup>167</sup>, R. Escobar Franco<sup>167</sup>, O. Evdokimov<sup>167</sup>,  
 C.E. Gerber<sup>167</sup>, H. Gupta<sup>167</sup>, M. Hawksworth<sup>167</sup>, A. Hingrajiya<sup>167</sup>, D.J. Hofman<sup>167</sup>,  
 J.h. Lee<sup>167</sup>, C. Mills<sup>167</sup>, S. Nanda<sup>167</sup>, G. Nigmatkulov<sup>167</sup>, B. Ozek<sup>167</sup>, T. Phan<sup>167</sup>,  
 D. Pilipovic<sup>167</sup>, R. Pradhan<sup>167</sup>, E. Prifti<sup>167</sup>, P. Roy<sup>167</sup>, T. Roy<sup>167</sup>, N. Singh<sup>167</sup>,  
 M.B. Tonjes<sup>167</sup>, N. Varelas<sup>167</sup>, M.A. Wadud<sup>167</sup>, J. Yoo<sup>167</sup>, M. Alhusseini<sup>168</sup>, D. Blend<sup>168</sup>,  
 K. Dilsiz<sup>168, cj</sup>, O.K. Köseyan<sup>168</sup>, A. Mestvirishvili<sup>168, ck</sup>, O. Neogi<sup>168</sup>, H. Ogul<sup>168, cl</sup>,  
 Y. Onel<sup>168</sup>, A. Penzo<sup>168</sup>, C. Snyder<sup>168</sup>, E. Tiras<sup>168, cm</sup>, B. Blumenfeld<sup>169</sup>, J. Davis<sup>169</sup>,  
 A.V. Gritsan<sup>169</sup>, L. Kang<sup>169</sup>, S. Kyriacou<sup>169</sup>, P. Maksimovic<sup>169</sup>, M. Roguljic<sup>169</sup>,  
 S. Sekhar<sup>169</sup>, M.V. Srivastav<sup>169</sup>, M. Swartz<sup>169</sup>, A. Abreu<sup>170</sup>, L.F. Alcerro Alcerro<sup>170</sup>,  
 J. Anguiano<sup>170</sup>, S. Arteaga Escatel<sup>170</sup>, P. Baringer<sup>170</sup>, A. Bean<sup>170</sup>, Z. Flowers<sup>170</sup>,  
 D. Grove<sup>170</sup>, J. King<sup>170</sup>, G. Krintiras<sup>170</sup>, M. Lazarovits<sup>170</sup>, C. Le Mahieu<sup>170</sup>,  
 J. Marquez<sup>170</sup>, M. Murray<sup>170</sup>, M. Nickel<sup>170</sup>, S. Popescu<sup>170, cn</sup>, C. Rogan<sup>170</sup>, C. Royon<sup>170</sup>,  
 S. Rudrabhatla<sup>170</sup>, S. Sanders<sup>170</sup>, C. Smith<sup>170</sup>, G. Wilson<sup>170</sup>, B. Allmond<sup>171</sup>, N. Islam<sup>171</sup>,  
 A. Ivanov<sup>171</sup>, K. Kaadze<sup>171</sup>, Y. Maravin<sup>171</sup>, J. Natoli<sup>171</sup>, R. Gujju Gurnadha<sup>171</sup>,  
 D. Roy<sup>171</sup>, G. Sorrentino<sup>171</sup>, A. Baden<sup>172</sup>, A. Belloni<sup>172</sup>, J. Bistany-riebman<sup>172</sup>,  
 S.C. Eno<sup>172</sup>, N.J. Hadley<sup>172</sup>, S. Jabeen<sup>172</sup>, R.G. Kellogg<sup>172</sup>, T. Koeth<sup>172</sup>, B. Kronheim<sup>172</sup>,  
 S. Lascio<sup>172</sup>, P. Major<sup>172</sup>, A.C. Mignerey<sup>172</sup>, C. Palmer<sup>172</sup>, C. Papageorgakis<sup>172</sup>,  
 M.M. Paranjpe<sup>172</sup>, E. Popova<sup>172, co</sup>, A. Shevelev<sup>172</sup>, L. Zhang<sup>172</sup>, C. Baldenegro Barrera<sup>173</sup>,

J. Bendavid<sup>173</sup>, H. Bossi<sup>173</sup>, S. Bright-Thonney<sup>173</sup>, I.A. Cali<sup>173</sup>, Y.c. Chen<sup>173</sup>,  
 P.c. Chou<sup>173</sup>, M. D'Alfonso<sup>173</sup>, J. Eysermans<sup>173</sup>, C. Freer<sup>173</sup>, G. Gomez-Ceballos<sup>173</sup>,  
 M. Goncharov<sup>173</sup>, G. Grosso<sup>173</sup>, P. Harris<sup>173</sup>, D. Hoang<sup>173</sup>, G.M. Innocenti<sup>173</sup>,  
 D. Kovalskyi<sup>173</sup>, J. Krupa<sup>173</sup>, L. Lavezzo<sup>173</sup>, Y.-J. Lee<sup>173</sup>, K. Long<sup>173</sup>, C. McGinn<sup>173</sup>,  
 A. Novak<sup>173</sup>, M.I. Park<sup>173</sup>, C. Paus<sup>173</sup>, C. Reissel<sup>173</sup>, C. Roland<sup>173</sup>, G. Roland<sup>173</sup>,  
 S. Rothman<sup>173</sup>, T.a. Sheng<sup>173</sup>, G.S.F. Stephans<sup>173</sup>, D. Walter<sup>173</sup>, Z. Wang<sup>173</sup>,  
 B. Wyslouch<sup>173</sup>, T. J. Yang<sup>173</sup>, B. Crossman<sup>174</sup>, W.J. Jackson<sup>174</sup>, C. Kapsiak<sup>174</sup>,  
 M. Krohn<sup>174</sup>, D. Mahon<sup>174</sup>, J. Mans<sup>174</sup>, B. Marzocchi<sup>174</sup>, R. Rusack<sup>174</sup>, O. Sancar<sup>174</sup>,  
 R. Saradhy<sup>174</sup>, N. Strobbe<sup>174</sup>, K. Bloom<sup>175</sup>, D.R. Claes<sup>175</sup>, G. Haza<sup>175</sup>, J. Hossain<sup>175</sup>,  
 C. Joo<sup>175</sup>, I. Kravchenko<sup>175</sup>, A. Rohilla<sup>175</sup>, J.E. Siado<sup>175</sup>, W. Tabb<sup>175</sup>, A. Vagnerini<sup>175</sup>,  
 A. Wightman<sup>175</sup>, F. Yan<sup>175</sup>, H. Bandyopadhyay<sup>176</sup>, L. Hay<sup>176</sup>, H.w. Hsia<sup>176</sup>,  
 I. Iashvili<sup>176</sup>, A. Kalogeropoulos<sup>176</sup>, A. Kharchilava<sup>176</sup>, A. Mandal<sup>176</sup>, M. Morris<sup>176</sup>,  
 D. Nguyen<sup>176</sup>, S. Rappoccio<sup>176</sup>, H. Rejeb Sfar<sup>176</sup>, A. Williams<sup>176</sup>, P. Young<sup>176</sup>, D. Yu<sup>176</sup>,  
 G. Alverson<sup>177</sup>, E. Barberis<sup>177</sup>, J. Bonilla<sup>177</sup>, B. Bylisma<sup>177</sup>, M. Campana<sup>177</sup>, J. Dervan<sup>177</sup>,  
 Y. Haddad<sup>177</sup>, Y. Han<sup>177</sup>, I. Israr<sup>177</sup>, A. Krishna<sup>177</sup>, M. Lu<sup>177</sup>, N. Manganeli<sup>177</sup>,  
 R. Mccarthy<sup>177</sup>, D.M. Morse<sup>177</sup>, T. Orimoto<sup>177</sup>, A. Parker<sup>177</sup>, L. Skinnari<sup>177</sup>,  
 C.S. Thoreson<sup>177</sup>, E. Tsai<sup>177</sup>, D. Wood<sup>177</sup>, S. Dittmer<sup>178</sup>, K.A. Hahn<sup>178</sup>, Y. Liu<sup>178</sup>,  
 M. McGinnis<sup>178</sup>, Y. Miao<sup>178</sup>, D.G. Monk<sup>178</sup>, M.H. Schmitt<sup>178</sup>, A. Taliercio<sup>178</sup>,  
 M. Velasco<sup>178</sup>, J. Wang<sup>178</sup>, G. Agarwal<sup>179</sup>, R. Band<sup>179</sup>, R. Bucci<sup>179</sup>, S. Castells<sup>179</sup>,  
 A. Das<sup>179</sup>, A. Ehnis<sup>179</sup>, R. Goldouzian<sup>179</sup>, M. Hildreth<sup>179</sup>, K. Hurtado Anampa<sup>179</sup>,  
 T. Ivanov<sup>179</sup>, C. Jessop<sup>179</sup>, A. Karneyeu<sup>179</sup>, K. Lannon<sup>179</sup>, J. Lawrence<sup>179</sup>, N. Loukas<sup>179</sup>,  
 L. Lutton<sup>179</sup>, J. Mariano<sup>179</sup>, N. Marinelli<sup>179</sup>, I. Mcalister<sup>179</sup>, T. McCauley<sup>179</sup>, C. Mcgrady<sup>179</sup>,  
 C. Moore<sup>179</sup>, Y. Musienko<sup>179,cp</sup>, H. Nelson<sup>179</sup>, M. Osherson<sup>179</sup>, A. Piccinelli<sup>179</sup>,  
 R. Ruchti<sup>179</sup>, A. Townsend<sup>179</sup>, Y. Wan<sup>179</sup>, M. Wayne<sup>179</sup>, H. Yockey<sup>179</sup>, A. Basnet<sup>180</sup>,  
 M. Carrigan<sup>180</sup>, R. De Los Santos<sup>180</sup>, L.S. Durkin<sup>180</sup>, C. Hill<sup>180</sup>, M. Joyce<sup>180</sup>,  
 M. Nunez Ornelas<sup>180</sup>, D.A. Wenzl<sup>180</sup>, B.L. Winer<sup>180</sup>, B. R. Yates<sup>180</sup>, H. Bouchamaoui<sup>181</sup>,  
 K. Coldham<sup>181</sup>, P. Das<sup>181</sup>, G. Dezoort<sup>181</sup>, P. Elmer<sup>181</sup>, A. Frankenthal<sup>181</sup>, M. Galli<sup>181</sup>,  
 B. Greenberg<sup>181</sup>, N. Haubrich<sup>181</sup>, K. Kennedy<sup>181</sup>, G. Kopp<sup>181</sup>, Y. Lai<sup>181</sup>, D. Lange<sup>181</sup>,  
 A. Loeliger<sup>181</sup>, D. Marlow<sup>181</sup>, I. Ojalvo<sup>181</sup>, J. Olsen<sup>181</sup>, F. Simpson<sup>181</sup>, D. Stickland<sup>181</sup>,  
 C. Tully<sup>181</sup>, S. Malik<sup>182</sup>, R. Sharma<sup>182</sup>, A.S. Bakshi<sup>183</sup>, S. Chandra<sup>183</sup>, R. Chawla<sup>183</sup>,  
 A. Gu<sup>183</sup>, L. Gutay<sup>183</sup>, M. Jones<sup>183</sup>, A.W. Jung<sup>183</sup>, D. Kondratyev<sup>183</sup>, M. Liu<sup>183</sup>,  
 M. Matthewman<sup>183</sup>, G. Negro<sup>183</sup>, N. Neumeister<sup>183</sup>, G. Paspalaki<sup>183</sup>, S. Piperov<sup>183</sup>,  
 J.F. Schulte<sup>183</sup>, F. Wang<sup>183</sup>, A. Wildridge<sup>183</sup>, W. Xie<sup>183</sup>, Y. Yao<sup>183</sup>, Y. Zhong<sup>183</sup>,  
 N. Parashar<sup>184</sup>, A. Pathak<sup>184</sup>, E. Shumka<sup>184</sup>, D. Acosta<sup>185</sup>, A. Agrawal<sup>185</sup>,  
 C. Arbour<sup>185</sup>, T. Carnahan<sup>185</sup>, K.M. Ecklund<sup>185</sup>, P.J. Fernández Manteca<sup>185</sup>, S. Freed<sup>185</sup>,  
 P. Gardner<sup>185</sup>, F.J.M. Geurts<sup>185</sup>, T. Huang<sup>185</sup>, I. Krommydas<sup>185</sup>, N. Lewis<sup>185</sup>, W. Li<sup>185</sup>,  
 J. Lin<sup>185</sup>, O. Miguel Colin<sup>185</sup>, B.P. Padley<sup>185</sup>, R. Redjimi<sup>185</sup>, J. Rotter<sup>185</sup>,  
 E. Yigitbasi<sup>185</sup>, Y. Zhang<sup>185</sup>, O. Bessidskaia Bylund<sup>186</sup>, A. Bodek<sup>186</sup>, P. de Barbaro<sup>186,†</sup>,  
 R. Demina<sup>186</sup>, J.L. Dulemba<sup>186</sup>, A. Garcia-Bellido<sup>186</sup>, H.S. Hare<sup>186</sup>, O. Hindrichs<sup>186</sup>,  
 N. Parmar<sup>186</sup>, P. Parygin<sup>186,co</sup>, H. Seo<sup>186</sup>, R. Taus<sup>186</sup>, B. Chiarito<sup>187</sup>, J.P. Chou<sup>187</sup>,  
 S.V. Clark<sup>187</sup>, S. Donnelly<sup>187</sup>, D. Gadkari<sup>187</sup>, Y. Gershtein<sup>187</sup>, E. Halkiadakis<sup>187</sup>,  
 C. Houghton<sup>187</sup>, D. Jaroslawski<sup>187</sup>, S. Konstantinou<sup>187</sup>, I. Laflotte<sup>187</sup>, A. Lath<sup>187</sup>,  
 J. Martins<sup>187</sup>, M. Heindl<sup>187</sup>, B. Rand<sup>187</sup>, J. Reichert<sup>187</sup>, P. Saha<sup>187</sup>, S. Salur<sup>187</sup>,

S. Schnetzer<sup>187</sup>, S. Somalwar<sup>187</sup>, R. Stone<sup>187</sup>, S.A. Thayil<sup>187</sup>, S. Thomas<sup>187</sup>, J. Vora<sup>187</sup>,  
D. Ally<sup>188</sup>, A.G. Delannoy<sup>188</sup>, S. Fiorendi<sup>188</sup>, J. Harris<sup>188</sup>, S. Higginbotham<sup>188</sup>,  
T. Holmes<sup>188</sup>, A.R. Kanuganti<sup>188</sup>, N. Karunarathna<sup>188</sup>, J. Lawless<sup>188</sup>, L. Lee<sup>188</sup>,  
E. Nibigira<sup>188</sup>, B. Skipworth<sup>188</sup>, S. Spanier<sup>188</sup>, D. Aebi<sup>189</sup>, M. Ahmad<sup>189</sup>, T. Akhter<sup>189</sup>,  
K. Androsov<sup>189</sup>, A. Bolshov<sup>189</sup>, O. Bouhali<sup>189,cq</sup>, R. Eusebi<sup>189</sup>, P. Flanagan<sup>189</sup>,  
J. Gilmore<sup>189</sup>, Y. Guo<sup>189</sup>, T. Kamon<sup>189</sup>, S. Luo<sup>189</sup>, R. Mueller<sup>189</sup>, A. Safonov<sup>189</sup>,  
N. Akchurin<sup>190</sup>, J. Damgov<sup>190</sup>, Y. Feng<sup>190</sup>, N. Gogate<sup>190</sup>, Y. Kazhykarim<sup>190</sup>,  
K. Lamichhane<sup>190</sup>, S.W. Lee<sup>190</sup>, C. Madrid<sup>190</sup>, A. Mankel<sup>190</sup>, T. Peltola<sup>190</sup>,  
I. Volobouev<sup>190</sup>, E. Appelt<sup>191</sup>, Y. Chen<sup>191</sup>, S. Greene<sup>191</sup>, A. Gurrola<sup>191</sup>, W. Johns<sup>191</sup>,  
R. Kunnawalkam Elayavalli<sup>191</sup>, A. Melo<sup>191</sup>, D. Rathjens<sup>191</sup>, F. Romeo<sup>191</sup>, P. Sheldon<sup>191</sup>,  
S. Tuo<sup>191</sup>, J. Velkovska<sup>191</sup>, J. Viinikainen<sup>191</sup>, J. Zhang<sup>191</sup>, B. Cardwell<sup>192</sup>, H. Chung<sup>192</sup>,  
B. Cox<sup>192</sup>, J. Hakala<sup>192</sup>, R. Hirosky<sup>192</sup>, M. Jose<sup>192</sup>, A. Ledovskoy<sup>192</sup>, C. Mantilla<sup>192</sup>,  
C. Neu<sup>192</sup>, C. Ramón Álvarez<sup>192</sup>, S. Bhattacharya<sup>193</sup>, P.E. Karchin<sup>193</sup>, A. Aravind<sup>194</sup>,  
S. Banerjee<sup>194</sup>, K. Black<sup>194</sup>, T. Bose<sup>194</sup>, E. Chavez<sup>194</sup>, S. Dasu<sup>194</sup>, P. Everaerts<sup>194</sup>,  
C. Galloni<sup>194</sup>, H. He<sup>194</sup>, M. Herndon<sup>194</sup>, A. Herve<sup>194</sup>, C.K. Koraka<sup>194</sup>, S. Lomte<sup>194</sup>,  
R. Loveless<sup>194</sup>, A. Mallampalli<sup>194</sup>, A. Mohammadi<sup>194</sup>, S. Mondal<sup>194</sup>, T. Nelson<sup>194</sup>,  
G. Parida<sup>194</sup>, D. Pinna<sup>194</sup>, L. Pétré<sup>194</sup>, A. Savin<sup>194</sup>, V. Shang<sup>194</sup>, V. Sharma<sup>194</sup>,  
W.H. Smith<sup>194</sup>, D. Teague<sup>194</sup>, H.F. Tsoi<sup>194</sup>, W. Vetens<sup>194</sup>, A. Warden<sup>194</sup>, S. Afanasiev<sup>195</sup>,  
V. Alexakhin<sup>195</sup>, Yu. Andreev<sup>195</sup>, T. Aushev<sup>195</sup>, D. Budkouski<sup>195</sup>, R. Chistov<sup>195,cp</sup>,  
M. Danilov<sup>195,cp</sup>, T. Dimova<sup>195,cp</sup>, A. Ershov<sup>195,cp</sup>, S. Gninenko<sup>195</sup>, I. Gorbunov<sup>195</sup>,  
A. Gribushin<sup>195,cp</sup>, A. Kamenev<sup>195</sup>, V. Karjavine<sup>195</sup>, M. Kirsanov<sup>195</sup>, V. Klyukhin<sup>195,cp</sup>,  
O. Kodolova<sup>195,cr,co</sup>, V. Korenkov<sup>195</sup>, A. Kozyrev<sup>195,cp</sup>, N. Krasnikov<sup>195</sup>, A. Lanev<sup>195</sup>,  
A. Malakhov<sup>195</sup>, V. Matveev<sup>195,cp</sup>, A. Nikitenko<sup>195,cs,ct</sup>, V. Palichik<sup>195</sup>, V. Perelygin<sup>195</sup>,  
S. Petrushanko<sup>195,cp</sup>, S. Polikarpov<sup>195,cp</sup>, O. Radchenko<sup>195,cp</sup>, M. Savina<sup>195</sup>, V. Shalaev<sup>195</sup>,  
S. Shmatov<sup>195</sup>, S. Shulha<sup>195</sup>, Y. Skovpen<sup>195,cp</sup>, V. Smirnov<sup>195</sup>, O. Teryaev<sup>195</sup>,  
I. Tlisova<sup>195,cp</sup>, A. Toropin<sup>195</sup>, N. Voytishin<sup>195</sup>, B.S. Yuldashev<sup>195,cu,†</sup>, A. Zarubin<sup>195</sup>,  
I. Zhizhin<sup>195</sup>, E. Boos<sup>196</sup>, V. Bunichev<sup>196</sup>, M. Dubinin<sup>196,ch</sup>, L. Dudko<sup>196</sup>, K. Ivanov<sup>196</sup>,  
V. Kim<sup>196,cp</sup>, V. Murzin<sup>196</sup>, V. Oreshkin<sup>196</sup>, V. Savrin<sup>196</sup>, A. Snigirev<sup>196</sup>, D. Sosnov<sup>196</sup>

<sup>1</sup> *Yerevan Physics Institute, Yerevan, Armenia*

<sup>2</sup> *Institut für Hochenergiephysik, Vienna, Austria*

<sup>3</sup> *Universiteit Antwerpen, Antwerpen, Belgium*

<sup>4</sup> *Vrije Universiteit Brussel, Brussel, Belgium*

<sup>5</sup> *Université Libre de Bruxelles, Bruxelles, Belgium*

<sup>6</sup> *Ghent University, Ghent, Belgium*

<sup>7</sup> *Université Catholique de Louvain, Louvain-la-Neuve, Belgium*

<sup>8</sup> *Centro Brasileiro de Pesquisas Fisicas, Rio de Janeiro, Brazil*

<sup>9</sup> *Universidade do Estado do Rio de Janeiro, Rio de Janeiro, Brazil*

<sup>10</sup> *Universidade Estadual Paulista, Universidade Federal do ABC, São Paulo, Brazil*

<sup>11</sup> *Institute for Nuclear Research and Nuclear Energy, Bulgarian Academy of Sciences, Sofia, Bulgaria*

<sup>12</sup> *University of Sofia, Sofia, Bulgaria*

<sup>13</sup> *Instituto De Alta Investigación, Universidad de Tarapacá, Casilla 7 D, Arica, Chile*

<sup>14</sup> *Universidad Tecnica Federico Santa Maria, Valparaiso, Chile*

<sup>15</sup> *Beihang University, Beijing, China*

<sup>16</sup> *Department of Physics, Tsinghua University, Beijing, China*

<sup>17</sup> *Institute of High Energy Physics, Beijing, China*

<sup>18</sup> *State Key Laboratory of Nuclear Physics and Technology, Peking University, Beijing, China*

- <sup>19</sup> *State Key Laboratory of Nuclear Physics and Technology, Institute of Quantum Matter, South China Normal University, Guangzhou, China*
- <sup>20</sup> *Sun Yat-Sen University, Guangzhou, China*
- <sup>21</sup> *University of Science and Technology of China, Hefei, China*
- <sup>22</sup> *Nanjing Normal University, Nanjing, China*
- <sup>23</sup> *Institute of Modern Physics and Key Laboratory of Nuclear Physics and Ion-beam Application (MOE) – Fudan University, Shanghai, China*
- <sup>24</sup> *Zhejiang University, Hangzhou, Zhejiang, China*
- <sup>25</sup> *Universidad de Los Andes, Bogota, Colombia*
- <sup>26</sup> *Universidad de Antioquia, Medellin, Colombia*
- <sup>27</sup> *University of Split, Faculty of Electrical Engineering, Mechanical Engineering and Naval Architecture, Split, Croatia*
- <sup>28</sup> *University of Split, Faculty of Science, Split, Croatia*
- <sup>29</sup> *Institute Rudjer Boskovic, Zagreb, Croatia*
- <sup>30</sup> *University of Cyprus, Nicosia, Cyprus*
- <sup>31</sup> *Charles University, Prague, Czech Republic*
- <sup>32</sup> *Escuela Politecnica Nacional, Quito, Ecuador*
- <sup>33</sup> *Universidad San Francisco de Quito, Quito, Ecuador*
- <sup>34</sup> *Academy of Scientific Research and Technology of the Arab Republic of Egypt, Egyptian Network of High Energy Physics, Cairo, Egypt*
- <sup>35</sup> *Center for High Energy Physics (CHEP-FU), Fayoum University, El-Fayoum, Egypt*
- <sup>36</sup> *National Institute of Chemical Physics and Biophysics, Tallinn, Estonia*
- <sup>37</sup> *Department of Physics, University of Helsinki, Helsinki, Finland*
- <sup>38</sup> *Helsinki Institute of Physics, Helsinki, Finland*
- <sup>39</sup> *Lappeenranta-Lahti University of Technology, Lappeenranta, Finland*
- <sup>40</sup> *IRFU, CEA, Université Paris-Saclay, Gif-sur-Yvette, France*
- <sup>41</sup> *Laboratoire Leprince-Ringuet, CNRS/IN2P3, Ecole Polytechnique, Institut Polytechnique de Paris, Palaiseau, France*
- <sup>42</sup> *Université de Strasbourg, CNRS, IPHC UMR 7178, Strasbourg, France*
- <sup>43</sup> *Centre de Calcul de l'Institut National de Physique Nucleaire et de Physique des Particules, CNRS/IN2P3, Villeurbanne, France*
- <sup>44</sup> *Institut de Physique des 2 Infinis de Lyon (IP2I), Villeurbanne, France*
- <sup>45</sup> *Georgian Technical University, Tbilisi, Georgia*
- <sup>46</sup> *RWTH Aachen University, I. Physikalisches Institut, Aachen, Germany*
- <sup>47</sup> *RWTH Aachen University, III. Physikalisches Institut A, Aachen, Germany*
- <sup>48</sup> *RWTH Aachen University, III. Physikalisches Institut B, Aachen, Germany*
- <sup>49</sup> *Deutsches Elektronen-Synchrotron, Hamburg, Germany*
- <sup>50</sup> *University of Hamburg, Hamburg, Germany*
- <sup>51</sup> *Karlsruher Institut fuer Technologie, Karlsruhe, Germany*
- <sup>52</sup> *Institute of Nuclear and Particle Physics (INPP), NCSR Demokritos, Aghia Paraskevi, Greece*
- <sup>53</sup> *National and Kapodistrian University of Athens, Athens, Greece*
- <sup>54</sup> *National Technical University of Athens, Athens, Greece*
- <sup>55</sup> *University of Ioánnina, Ioánnina, Greece*
- <sup>56</sup> *HUN-REN Wigner Research Centre for Physics, Budapest, Hungary*
- <sup>57</sup> *MTA-ELTE Lendület CMS Particle and Nuclear Physics Group, Eötvös Loránd University, Budapest, Hungary*
- <sup>58</sup> *Faculty of Informatics, University of Debrecen, Debrecen, Hungary*
- <sup>59</sup> *HUN-REN ATOMKI – Institute of Nuclear Research, Debrecen, Hungary*
- <sup>60</sup> *Karoly Robert Campus, MATE Institute of Technology, Gyongyos, Hungary*
- <sup>61</sup> *Panjab University, Chandigarh, India*
- <sup>62</sup> *University of Delhi, Delhi, India*
- <sup>63</sup> *University of Hyderabad, Hyderabad, India*
- <sup>64</sup> *Indian Institute of Technology Kanpur, Kanpur, India*

- <sup>65</sup> *Saha Institute of Nuclear Physics, HBNI, Kolkata, India*  
<sup>66</sup> *Indian Institute of Technology Madras, Madras, India*  
<sup>67</sup> *IISER Mohali, India, Mohali, India*  
<sup>68</sup> *Tata Institute of Fundamental Research-A, Mumbai, India*  
<sup>69</sup> *Tata Institute of Fundamental Research-B, Mumbai, India*  
<sup>70</sup> *National Institute of Science Education and Research, An OCC of Homi Bhabha National Institute, Bhubaneswar, Odisha, India*  
<sup>71</sup> *Indian Institute of Science Education and Research (IISER), Pune, India*  
<sup>72</sup> *Indian Institute of Technology Hyderabad, Telangana, India*  
<sup>73</sup> *Isfahan University of Technology, Isfahan, Iran*  
<sup>74</sup> *Institute for Research in Fundamental Sciences (IPM), Tehran, Iran*  
<sup>75</sup> *University College Dublin, Dublin, Ireland*  
<sup>76a</sup> *INFN Sezione di Bari, Bari, Italy*  
<sup>76b</sup> *Università di Bari, Bari, Italy*  
<sup>76c</sup> *Politecnico di Bari, Bari, Italy*  
<sup>77a</sup> *INFN Sezione di Bologna, Bologna, Italy*  
<sup>77b</sup> *Università di Bologna, Bologna, Italy*  
<sup>78a</sup> *INFN Sezione di Catania, Catania, Italy*  
<sup>78b</sup> *Università di Catania, Catania, Italy*  
<sup>79a</sup> *INFN Sezione di Firenze, Firenze, Italy*  
<sup>79b</sup> *Università di Firenze, Firenze, Italy*  
<sup>80</sup> *INFN Laboratori Nazionali di Frascati, Frascati, Italy*  
<sup>81a</sup> *INFN Sezione di Genova, Genova, Italy*  
<sup>81b</sup> *Università di Genova, Genova, Italy*  
<sup>82a</sup> *INFN Sezione di Milano-Bicocca, Milano, Italy*  
<sup>82b</sup> *Università di Milano-Bicocca, Milano, Italy*  
<sup>83a</sup> *INFN Sezione di Napoli, Napoli, Italy*  
<sup>83b</sup> *Università di Napoli ‘Federico II’, Napoli, Italy*  
<sup>83c</sup> *Università della Basilicata, Potenza, Italy*  
<sup>83d</sup> *Scuola Superiore Meridionale (SSM), Napoli, Italy*  
<sup>84a</sup> *INFN Sezione di Padova, Padova, Italy*  
<sup>84b</sup> *Università di Padova, Padova, Italy*  
<sup>84c</sup> *Università degli Studi di Cagliari, Cagliari, Italy*  
<sup>85a</sup> *INFN Sezione di Pavia, Pavia, Italy*  
<sup>85b</sup> *Università di Pavia, Pavia, Italy*  
<sup>86a</sup> *INFN Sezione di Perugia, Perugia, Italy*  
<sup>86b</sup> *Università di Perugia, Perugia, Italy*  
<sup>87a</sup> *INFN Sezione di Pisa, Pisa, Italy*  
<sup>87b</sup> *Università di Pisa, Pisa, Italy*  
<sup>87c</sup> *Scuola Normale Superiore di Pisa, Pisa, Italy*  
<sup>87d</sup> *Università di Siena, Siena, Italy*  
<sup>88a</sup> *INFN Sezione di Roma, Roma, Italy*  
<sup>88b</sup> *Sapienza Università di Roma, Roma, Italy*  
<sup>89a</sup> *INFN Sezione di Torino, Torino, Italy*  
<sup>89b</sup> *Università di Torino, Torino, Italy*  
<sup>89c</sup> *Università del Piemonte Orientale, Novara, Italy*  
<sup>90a</sup> *INFN Sezione di Trieste, Trieste, Italy*  
<sup>90b</sup> *Università di Trieste, Trieste, Italy*  
<sup>91</sup> *Kyungpook National University, Daegu, Korea*  
<sup>92</sup> *Department of Mathematics and Physics – GWNNU, Gangneung, Korea*  
<sup>93</sup> *Chonnam National University, Institute for Universe and Elementary Particles, Kwangju, Korea*  
<sup>94</sup> *Hanyang University, Seoul, Korea*  
<sup>95</sup> *Korea University, Seoul, Korea*

- <sup>96</sup> *Kyung Hee University, Department of Physics, Seoul, Korea*  
<sup>97</sup> *Sejong University, Seoul, Korea*  
<sup>98</sup> *Seoul National University, Seoul, Korea*  
<sup>99</sup> *University of Seoul, Seoul, Korea*  
<sup>100</sup> *Yonsei University, Department of Physics, Seoul, Korea*  
<sup>101</sup> *Sungkyunkwan University, Suwon, Korea*  
<sup>102</sup> *College of Engineering and Technology, American University of the Middle East (AUM), Dasman, Kuwait*  
<sup>103</sup> *Kuwait University – College of Science – Department of Physics, Safat, Kuwait*  
<sup>104</sup> *Riga Technical University, Riga, Latvia*  
<sup>105</sup> *University of Latvia (LU), Riga, Latvia*  
<sup>106</sup> *Vilnius University, Vilnius, Lithuania*  
<sup>107</sup> *National Centre for Particle Physics, Universiti Malaya, Kuala Lumpur, Malaysia*  
<sup>108</sup> *Universidad de Sonora (UNISON), Hermosillo, Mexico*  
<sup>109</sup> *Centro de Investigacion y de Estudios Avanzados del IPN, Mexico City, Mexico*  
<sup>110</sup> *Universidad Iberoamericana, Mexico City, Mexico*  
<sup>111</sup> *Benemerita Universidad Autonoma de Puebla, Puebla, Mexico*  
<sup>112</sup> *University of Montenegro, Podgorica, Montenegro*  
<sup>113</sup> *University of Canterbury, Christchurch, New Zealand*  
<sup>114</sup> *National Centre for Physics, Quaid-I-Azam University, Islamabad, Pakistan*  
<sup>115</sup> *AGH University of Krakow, Krakow, Poland*  
<sup>116</sup> *National Centre for Nuclear Research, Swierk, Poland*  
<sup>117</sup> *Institute of Experimental Physics, Faculty of Physics, University of Warsaw, Warsaw, Poland*  
<sup>118</sup> *Warsaw University of Technology, Warsaw, Poland*  
<sup>119</sup> *Laboratório de Instrumentação e Física Experimental de Partículas, Lisboa, Portugal*  
<sup>120</sup> *Faculty of Physics, University of Belgrade, Belgrade, Serbia*  
<sup>121</sup> *VINCA Institute of Nuclear Sciences, University of Belgrade, Belgrade, Serbia*  
<sup>122</sup> *Centro de Investigaciones Energéticas Medioambientales y Tecnológicas (CIEMAT), Madrid, Spain*  
<sup>123</sup> *Universidad Autónoma de Madrid, Madrid, Spain*  
<sup>124</sup> *Universidad de Oviedo, Instituto Universitario de Ciencias y Tecnologías Espaciales de Asturias (ICTEA), Oviedo, Spain*  
<sup>125</sup> *Instituto de Física de Cantabria (IFCA), CSIC-Universidad de Cantabria, Santander, Spain*  
<sup>126</sup> *University of Colombo, Colombo, Sri Lanka*  
<sup>127</sup> *University of Ruhuna, Department of Physics, Matara, Sri Lanka*  
<sup>128</sup> *CERN, European Organization for Nuclear Research, Geneva, Switzerland*  
<sup>129</sup> *PSI Center for Neutron and Muon Sciences, Villigen, Switzerland*  
<sup>130</sup> *ETH Zurich – Institute for Particle Physics and Astrophysics (IPA), Zurich, Switzerland*  
<sup>131</sup> *Universität Zürich, Zurich, Switzerland*  
<sup>132</sup> *National Central University, Chung-Li, Taiwan*  
<sup>133</sup> *National Taiwan University (NTU), Taipei, Taiwan*  
<sup>134</sup> *High Energy Physics Research Unit, Department of Physics, Faculty of Science, Chulalongkorn University, Bangkok, Thailand*  
<sup>135</sup> *Tunis El Manar University, Tunis, Tunisia*  
<sup>136</sup> *Çukurova University, Physics Department, Science and Art Faculty, Adana, Turkey*  
<sup>137</sup> *Middle East Technical University, Physics Department, Ankara, Turkey*  
<sup>138</sup> *Bogazici University, Istanbul, Turkey*  
<sup>139</sup> *Istanbul Technical University, Istanbul, Turkey*  
<sup>140</sup> *Istanbul University, Istanbul, Turkey*  
<sup>141</sup> *Yildiz Technical University, Istanbul, Turkey*  
<sup>142</sup> *Institute for Scintillation Materials of National Academy of Science of Ukraine, Kharkiv, Ukraine*  
<sup>143</sup> *National Science Centre, Kharkiv Institute of Physics and Technology, Kharkiv, Ukraine*  
<sup>144</sup> *University of Bristol, Bristol, U.K.*  
<sup>145</sup> *Rutherford Appleton Laboratory, Didcot, U.K.*  
<sup>146</sup> *Imperial College, London, U.K.*

- 147 *Brunel University, Uxbridge, U.K.*  
 148 *Baylor University, Waco, Texas, U.S.A.*  
 149 *Bethel University, St. Paul, Minnesota, U.S.A.*  
 150 *Catholic University of America, Washington, DC, U.S.A.*  
 151 *The University of Alabama, Tuscaloosa, Alabama, U.S.A.*  
 152 *Boston University, Boston, Massachusetts, U.S.A.*  
 153 *Brown University, Providence, Rhode Island, U.S.A.*  
 154 *University of California, Davis, Davis, California, U.S.A.*  
 155 *University of California, Los Angeles, California, U.S.A.*  
 156 *University of California, Riverside, Riverside, California, U.S.A.*  
 157 *University of California, San Diego, La Jolla, California, U.S.A.*  
 158 *University of California, Santa Barbara – Department of Physics, Santa Barbara, California, U.S.A.*  
 159 *California Institute of Technology, Pasadena, California, U.S.A.*  
 160 *Carnegie Mellon University, Pittsburgh, Pennsylvania, U.S.A.*  
 161 *University of Colorado Boulder, Boulder, Colorado, U.S.A.*  
 162 *Cornell University, Ithaca, New York, U.S.A.*  
 163 *Fermi National Accelerator Laboratory, Batavia, Illinois, U.S.A.*  
 164 *University of Florida, Gainesville, Florida, U.S.A.*  
 165 *Florida State University, Tallahassee, Florida, U.S.A.*  
 166 *Florida Institute of Technology, Melbourne, Florida, U.S.A.*  
 167 *University of Illinois Chicago, Chicago, Illinois, U.S.A.*  
 168 *The University of Iowa, Iowa City, Iowa, U.S.A.*  
 169 *Johns Hopkins University, Baltimore, Maryland, U.S.A.*  
 170 *The University of Kansas, Lawrence, Kansas, U.S.A.*  
 171 *Kansas State University, Manhattan, Kansas, U.S.A.*  
 172 *University of Maryland, College Park, Maryland, U.S.A.*  
 173 *Massachusetts Institute of Technology, Cambridge, Massachusetts, U.S.A.*  
 174 *University of Minnesota, Minneapolis, Minnesota, U.S.A.*  
 175 *University of Nebraska-Lincoln, Lincoln, Nebraska, U.S.A.*  
 176 *State University of New York at Buffalo, Buffalo, New York, U.S.A.*  
 177 *Northeastern University, Boston, Massachusetts, U.S.A.*  
 178 *Northwestern University, Evanston, Illinois, U.S.A.*  
 179 *University of Notre Dame, Notre Dame, Indiana, U.S.A.*  
 180 *The Ohio State University, Columbus, Ohio, U.S.A.*  
 181 *Princeton University, Princeton, New Jersey, U.S.A.*  
 182 *University of Puerto Rico, Mayaguez, Puerto Rico, U.S.A.*  
 183 *Purdue University, West Lafayette, Indiana, U.S.A.*  
 184 *Purdue University Northwest, Hammond, Indiana, U.S.A.*  
 185 *Rice University, Houston, Texas, U.S.A.*  
 186 *University of Rochester, Rochester, New York, U.S.A.*  
 187 *Rutgers, The State University of New Jersey, Piscataway, New Jersey, U.S.A.*  
 188 *University of Tennessee, Knoxville, Tennessee, U.S.A.*  
 189 *Texas A&M University, College Station, Texas, U.S.A.*  
 190 *Texas Tech University, Lubbock, Texas, U.S.A.*  
 191 *Vanderbilt University, Nashville, Tennessee, U.S.A.*  
 192 *University of Virginia, Charlottesville, Virginia, U.S.A.*  
 193 *Wayne State University, Detroit, Michigan, U.S.A.*  
 194 *University of Wisconsin – Madison, Madison, Wisconsin, U.S.A.*  
 195 *An institute or international laboratory covered by a cooperation agreement with CERN*  
 196 *An institute formerly covered by a cooperation agreement with CERN*

<sup>a</sup> *Also at Yerevan State University, Yerevan, Armenia*

<sup>b</sup> *Also at TU Wien, Vienna, Austria*

- <sup>c</sup> Also at Ghent University, Ghent, Belgium
- <sup>d</sup> Also at Universidade do Estado do Rio de Janeiro, Rio de Janeiro, Brazil
- <sup>e</sup> Also at FACAMP – Faculdades de Campinas, Sao Paulo, Brazil
- <sup>f</sup> Also at Universidade Estadual de Campinas, Campinas, Brazil
- <sup>g</sup> Also at Federal University of Rio Grande do Sul, Porto Alegre, Brazil
- <sup>h</sup> Also at The University of the State of Amazonas, Manaus, Brazil
- <sup>i</sup> Also at University of Chinese Academy of Sciences, Beijing, China
- <sup>j</sup> Also at China Center of Advanced Science and Technology, Beijing, China
- <sup>k</sup> Also at University of Chinese Academy of Sciences, Beijing, China
- <sup>l</sup> Now at Henan Normal University, Xinxiang, China
- <sup>m</sup> Also at University of Shanghai for Science and Technology, Shanghai, China
- <sup>n</sup> Now at The University of Iowa, Iowa City, Iowa, U.S.A.
- <sup>o</sup> Also at Center for High Energy Physics, Peking University, Beijing, China
- <sup>p</sup> Also at Suez University, Suez, Egypt
- <sup>q</sup> Now at British University in Egypt, Cairo, Egypt
- <sup>r</sup> Also at Cairo University, Cairo, Egypt
- <sup>s</sup> Also at Purdue University, West Lafayette, Indiana, U.S.A.
- <sup>t</sup> Also at Université de Haute Alsace, Mulhouse, France
- <sup>u</sup> Also at Istinye University, Istanbul, Turkey
- <sup>v</sup> Also at Another institute or international laboratory covered by a cooperation agreement with CERN
- <sup>w</sup> Also at University of Hamburg, Hamburg, Germany
- <sup>x</sup> Also at RWTH Aachen University, III. Physikalisches Institut A, Aachen, Germany
- <sup>y</sup> Also at Bergische University Wuppertal (BUW), Wuppertal, Germany
- <sup>z</sup> Also at Brandenburg University of Technology, Cottbus, Germany
- <sup>aa</sup> Also at Forschungszentrum Jülich, Juelich, Germany
- <sup>ab</sup> Now at RWTH Aachen University, III. Physikalisches Institut A, Aachen, Germany
- <sup>ac</sup> Also at CERN, European Organization for Nuclear Research, Geneva, Switzerland
- <sup>ad</sup> Also at HUN-REN ATOMKI – Institute of Nuclear Research, Debrecen, Hungary
- <sup>ae</sup> Now at Universitatea Babeş-Bolyai – Facultatea de Fizica, Cluj-Napoca, Romania
- <sup>af</sup> Also at MTA-ELTE Lendület CMS Particle and Nuclear Physics Group, Eötvös Loránd University, Budapest, Hungary
- <sup>ag</sup> Also at HUN-REN Wigner Research Centre for Physics, Budapest, Hungary
- <sup>ah</sup> Also at Physics Department, Faculty of Science, Assiut University, Assiut, Egypt
- <sup>ai</sup> Also at The University of Kansas, Lawrence, Kansas, U.S.A.
- <sup>aj</sup> Also at Punjab Agricultural University, Ludhiana, India
- <sup>ak</sup> Also at University of Hyderabad, Hyderabad, India
- <sup>al</sup> Also at Indian Institute of Science (IISc), Bangalore, India
- <sup>am</sup> Also at University of Visva-Bharati, Santiniketan, India
- <sup>an</sup> Also at IIT Bhubaneswar, Bhubaneswar, India
- <sup>ao</sup> Also at Institute of Physics, Bhubaneswar, India
- <sup>ap</sup> Also at Deutsches Elektronen-Synchrotron, Hamburg, Germany
- <sup>aq</sup> Also at Isfahan University of Technology, Isfahan, Iran
- <sup>ar</sup> Also at Sharif University of Technology, Tehran, Iran
- <sup>as</sup> Also at Department of Physics, University of Science and Technology of Mazandaran, Behshahr, Iran
- <sup>at</sup> Also at Department of Physics, Faculty of Science, Arak University, ARAK, Iran
- <sup>au</sup> Also at Helwan University, Cairo, Egypt
- <sup>av</sup> Also at Italian National Agency for New Technologies, Energy and Sustainable Economic Development, Bologna, Italy
- <sup>aw</sup> Also at Centro Siciliano di Fisica Nucleare e di Struttura Della Materia, Catania, Italy
- <sup>ax</sup> Also at Università degli Studi Guglielmo Marconi, Roma, Italy
- <sup>ay</sup> Also at Scuola Superiore Meridionale, Università di Napoli ‘Federico II’, Napoli, Italy
- <sup>az</sup> Also at Fermi National Accelerator Laboratory, Batavia, Illinois, U.S.A.
- <sup>ba</sup> Also at Laboratori Nazionali di Legnaro dell’INFN, Legnaro, Italy

- <sup>bb</sup> Also at Lulea University of Technology, Lulea, Sweden
- <sup>bc</sup> Also at Consiglio Nazionale delle Ricerche – Istituto Officina dei Materiali, Perugia, Italy
- <sup>bd</sup> Also at UPES – University of Petroleum and Energy Studies, Dehradun, India
- <sup>be</sup> Also at Institut de Physique des 2 Infinis de Lyon (IP2I), Villeurbanne, France
- <sup>bf</sup> Also at Department of Applied Physics, Faculty of Science and Technology, Universiti Kebangsaan Malaysia, Bangi, Malaysia
- <sup>bg</sup> Also at Trincomalee Campus, Eastern University, Sri Lanka, Nilaveli, Sri Lanka
- <sup>bh</sup> Also at Saegis Campus, Nugegoda, Sri Lanka
- <sup>bi</sup> Also at National and Kapodistrian University of Athens, Athens, Greece
- <sup>bj</sup> Also at Ecole Polytechnique Fédérale Lausanne, Lausanne, Switzerland
- <sup>bk</sup> Also at Universität Zürich, Zurich, Switzerland
- <sup>bl</sup> Also at Stefan Meyer Institute for Subatomic Physics, Vienna, Austria
- <sup>bm</sup> Also at Near East University, Research Center of Experimental Health Science, Mersin, Turkey
- <sup>bn</sup> Also at Konya Technical University, Konya, Turkey
- <sup>bo</sup> Also at Izmir Bakircay University, Izmir, Turkey
- <sup>bp</sup> Also at Adiyaman University, Adiyaman, Turkey
- <sup>bq</sup> Also at Bozok Universitetesi Rektörlüğü, Yozgat, Turkey
- <sup>br</sup> Also at Istanbul Sabahattin Zaim University, Istanbul, Turkey
- <sup>bs</sup> Also at Marmara University, Istanbul, Turkey
- <sup>bt</sup> Also at Milli Savunma University, Istanbul, Turkey
- <sup>bu</sup> Also at Informatics and Information Security Research Center, Gebze/Kocaeli, Turkey
- <sup>bv</sup> Also at Kafkas University, Kars, Turkey
- <sup>bw</sup> Now at Istanbul Okan University, Istanbul, Turkey
- <sup>bx</sup> Also at Hacettepe University, Ankara, Turkey
- <sup>by</sup> Also at Erzincan Binali Yildirim University, Erzincan, Turkey
- <sup>bz</sup> Also at Istanbul University – Cerrahpasa, Faculty of Engineering, Istanbul, Turkey
- <sup>ca</sup> Also at Yildiz Technical University, Istanbul, Turkey
- <sup>cb</sup> Also at School of Physics and Astronomy, University of Southampton, Southampton, U.K.
- <sup>cc</sup> Also at Monash University, Faculty of Science, Clayton, Australia
- <sup>cd</sup> Also at Bethel University, St. Paul, Minnesota, U.S.A.
- <sup>ce</sup> Also at Università di Torino, Torino, Italy
- <sup>cf</sup> Also at Karamanoğlu Mehmetbey University, Karaman, Turkey
- <sup>cg</sup> Also at California Lutheran University, Thousand Oaks, California, U.S.A.
- <sup>ch</sup> Also at California Institute of Technology, Pasadena, California, U.S.A.
- <sup>ci</sup> Also at United States Naval Academy, Annapolis, Maryland, U.S.A.
- <sup>cj</sup> Also at Bingol University, Bingol, Turkey
- <sup>ck</sup> Also at Georgian Technical University, Tbilisi, Georgia
- <sup>cl</sup> Also at Sinop University, Sinop, Turkey
- <sup>cm</sup> Also at Erciyes University, Kayseri, Turkey
- <sup>cn</sup> Also at Horia Hulubei National Institute of Physics and Nuclear Engineering (IFIN-HH), Bucharest, Romania
- <sup>co</sup> Now at Another institute formerly covered by a cooperation agreement with CERN
- <sup>cp</sup> Also at Another institute formerly covered by a cooperation agreement with CERN
- <sup>cq</sup> Also at Hamad Bin Khalifa University (HBKU), Doha, Qatar
- <sup>cr</sup> Also at Yerevan Physics Institute, Yerevan, Armenia
- <sup>cs</sup> Also at Imperial College, London, U.K.
- <sup>ct</sup> Now at Yerevan Physics Institute, Yerevan, Armenia
- <sup>cu</sup> Also at Institute of Nuclear Physics of the Uzbekistan Academy of Sciences, Tashkent, Uzbekistan
- <sup>†</sup> Deceased